

*Technische Universität Graz
Dekanat für Bauingenieurwissenschaften
Institut für Wasserbau und Wasserwirtschaft*

Analysis of a hydraulic surge tank model

Master thesis

by

Ermal Daka

*Vorgelegt zur Erlangung des
akademischen Grades eines Master
der Studienrichtung Bauingenieurwesen*

Graz, September 2015

Supervisor of the thesis:
Univ.-Prof. Dipl.-Ing. Dr.techn. Gerald ZENZ

Co Supervisor Assistant:
DI.Wolfgang Richter

AFFIDAVIT

I declare that I have authored this thesis independently, that I have not used other, than the declared sources/resources, and that I have explicitly indicated all material, which has been quoted either literally or by content from the sources used. The text document uploaded to TUGRAZonline is identical to the present master's thesis dissertation.

Graz, September 2015

.....

Note of Thanks

I would like to take this opportunity to thank the people who made it possible for me to be here.

First of all, I would like to thank Univ.-Prof. Dipl.-Ing. Dr.techn. Gerald ZENZ, for all the help he provided me throughout this time, as well as for his advice and his unreserved feedback.

Additionally, special thanks go out to Di Wolfgang Richter, who has been a great support for me since the very beginning of my Master thesis.

I would like to thank my parents, sisters and my friends for their support and love, and for having to put up with me during these years.

Abstract

Water hammer is the wave caused from the process that occurs when fluid in motion changes direction suddenly. It is important to design pump systems to prevent water hammer in order to avoid potentially devastating consequences, such as damage to components and equipment and risks to personnel.

The intention of this thesis is to calculate and study the water-hammer phenomena in Hydraulic Engineering, which is a complex phenomenon in water supply projects and an important design criterion at Hydro-power plants. This thesis is oriented at water hammer phenomena inside the system pressure pipeline of Hydropower plants.

„TUG Hammer” software code is used for the calculation. A model in the Laboratory at the institute of Hydraulic engineering is built to understand the practice of phenomena. The ‘TUG_Hammer software is separated into a gui and a calculation package based on Matlab®.

Zusammenfassung

Der Druckstoß wird verursacht, wenn die Flüssigkeit plötzlich die Fließrichtung ändert. Es ist wichtig Pumpensysteme zu entwerfen um den Druckstoß und eventuell durch den Druckstoß entstehende Schaden zu vermeiden.

Das Ziel dieser Masterarbeit ist den Druckstoß zu berechnen und studieren, der ein komplexes Phänomen im Wasserkraftwerk und Wasserversorgung Projekten darstellt. Diese Masterarbeit orientiert sich an Druckstoß in den Druckrohrleitungen des Wasserkraftwerkes.

Für die Berechnung wurde die TUG Hammer Software verwendet.

Um den Druckstoß Phänomen zu studieren, wurde es im Labor des Wasserbau Institutes ein Model gebaut.

Die TUG Hammer Software entsteht aus ein Gui und einer Berechnungspaket, die sich auf Matlab basieren.

Am Ende wurden die Laborergebnisse im Detail beschrieben .

Content

Abstract.....	v
Zusammenfassung.....	vi
1. Introduction	1
1.1 Analysis of a hydraulic surge tank model.	1
1.2 Surge Tank	2
1.3 Hyrdopower types	2
2. Pressure pipelines	4
2.1 General (hydraulic basics principles).....	4
2.1.1 Pipe types and pipe connections.....	4
2.2 Parts of construction	5
2.2.1 Intake	5
2.2.2 Pressure tunnel.....	6
2.3 High-pressure tunnels.....	7
2.4 Penstock.....	8
2.5 Economic aspects.....	10
2.6 Penstock types	10
2.7 Hydraulics of pipe-flow regimes	15
2.8 Losses at the pipeline (Loss of energy due to friction).....	16
2.9 Local losses or Minor losses	18
2.10 Loss at Entrance.....	19
3. Water hammer phenomenon	22
3.1 Dynamic flow processes	22
3.2 Water hammer and column separation	23
3.3 The unsteady flow-Vapor formation	23
3.4 Water-hammer calculation	24
3.5 Pressure wave velocity	24
3.6 The Joukowsky Equation	26
3.6.1 Influence of closing time for Joukowsky pressure.....	28
3.7 Method of Characteristics	30

3.8	Surgetank	33
3.8.1	Types of surge tank.....	35
3.8.2	Mass Oscillations in surge tank	37
4.	Calculations with TUG_Hammer.....	38
4.1	TUG_hammer	39
5.	Surge tank model in laboratory	48
5.1	Pressure sensor.....	50
6.	Measurements at the laboratory surge tank.....	52
6.1	Description of the measurement process and the evaluation of the results. .	52
6.2	Evaluation of the results.....	56
6.2.1	Surge tank, closure of valve opened for 10°	56
6.2.2	Details of line graphic, closure of valve opened for 10°	57
6.2.3	2 nd Detail of line graphic, closure of valve opened for 10°	58
6.2.4	Surge tank, closure of the valve opened for 45° angle.....	59
6.2.5	Detail of line graphic, closure of valve opened for 45°	60
6.2.6	2 nd detail of line graphic, closure of valve opened for 45°	61
6.2.7	3 rd detail of line graphic, closure of valve opened for 45°	62
6.2.8	Surge tank, closure of the valve opened for 65°	63
6.2.9	Detail of line graphic, closure of valve opened for 65°	64
6.2.10	2 nd detail of line graphic, closure of valve opened for 65°	65
6.2.11	Surge tank, closure of valve entirely closed.....	66
6.2.12	Details of line graphic, closure of valve entirely closed	67
6.2.13	2 nd detail of line graphic, closure of valve entirely closed.....	68
6.2.14	Surge tank, closure of valve opened for 10°	69
6.2.15	Detail of line graphic, closure of valve opened for 10°	69
6.2.16	2 nd detail of line graphic, closure of valve opened for 10°	70
6.2.17	3 rd detail of line graph, closure of valve opened for 10°	71
6.2.18	Surge tank, closure of valve opened for 65°	72
6.2.19	Detail of line graphic, closure of valve opened for 65°	72
6.2.20	2 nd detail of line graphic, closure of valve opened for 65°	73
6.2.21	3 rd detail of line graph, closure of valve opened for 65°	74
6.2.22	Surge tank, closure of valve opened for 45°	75
6.2.23	Detail of line graphic, closure of valve opened for 45°	75

6.2.24	2 nd detail of line graphic, closure of valve opened for 45°	76
6.2.25	3 rd detail of line graphic, closure of valve opened for 45°	77
6.2.26	Surge tank, closure of valve entirely closed.....	78
6.2.27	Details of line graphic, closure of valve entirely closed	78
6.2.28	Surge tank, closure of valve opened for 10°	79
6.2.29	Detail of line graphic, closure of valve opened for 10°	80
6.2.30	2 nd detail of line graphic, closure of valve opened for 10°	81
6.2.31	Surge tank, closure of valve opened for 45°	82
6.2.32	Detail of line graphic, closure of valve opened for 45°	82
6.2.33	2 nd detail of line graphic, closure of valve opened for 45°	83
6.2.34	Surge tank, closure of valve opened for 65°	84
6.2.35	Details of line graph, closure of valve opened for 65°	84
6.3	Joukowsky pressure	85
7.	APPENDIX - Laboratory software (Lab view).....	91

CHAPTER 1

1. Introduction

1.1 Analysis of a hydraulic surge tank model.

Water hammer is an effect produced by the closing of the valves at hydropower plants. This effect can be referred to as a dynamic pressure change due to the transformation of kinetic energy into pressure energy. During this process, there is alternating pressure in the pipeline that connects the inlet of the reservoir with the turbines. In prototypes, the power water way is built by the headrace tunnel (usually concrete lined) and the pressure shaft (usually steel lined). Additionally, a Surge tank is placed at the transition from headrace to pressure shaft if the pressure tunnel reaches a certain length. This is needed to control the pressure of the water and protect the pipe system, as well as allow a reasonable response time to allow the regulation function of machine operation (Johnson, 1908).

Rapid pressure changes are a result of rapid changes in flow, which generally occur in a pipe system after pump shut-off, or at valve opening or closing. The effects of the water hammer vary, ranging from small changes in pressure and velocity, to high pressure, causing burst pipes and pump damage.

(Xylem, 2015)

This work deals with water hammer effect inside pipelines and the effect of a surge tank at the pipelines. The study continues with analysis of the connection between water hammer and surge tank as well as the effect of surge tank in decreasing the pressure height inside the pipelines. Thesis covers, the effect of closing time of the valve inside the pipeline, as well as the impact of closing time of the valves to water hammer phenomena. Topics are connected with each other because; they control the pressure inside the pipelines, when there is a need to stop the water flow inside the pipeline for different reasons.

The study of water hammer phenomenon in this master thesis is divided in two parts:

- Theoretical part: The explanation of the water hammer as a phenomenon, and parts of hydropower facilities, where the water hammer phenomenon occurs, and along with the causes.
- Experimental part: Software calculations and model at Laboratory with different “Load cases”, and excel diagrams, which serve to compare results of different “Load cases” of the study. Load cases are different discharge inside the pipeline.
- Model and different position of the valve before the surge tank.

The model is evaluated by connected measurement devices. Therefore two sensors are used to measure the pressure

The aim of this thesis is to analyze the effect of surge tank on pressure shaft during the water hammer and effect of surge tank on pressure tunnel as well

1.2 Surge Tank

The expression Surge tank in German: “Wasserschloss”, comes from the Latin term “castellum” from the time when the Romans used it as a name for distribution device for the water supply system. In Hydropower plants it is used to limit pressure fluctuations and to allow regulation. It reflects the pressure waves that are created by the water hammer phenomenon. So this happens as a result of accelerations of water that appear at pressure shaft produced from the closing of the valves at Hydropower plants.

(Giesecke & Mosonyi, 2009)

1.3 Hyrdopower types

There are three main types of hydropower facilities:

Low-head hydro power plants

Middle-head hydro power plants

High-head hydro power plants

High –head hydropower plants consist of:

1. Dam,
2. Intake,
3. Headrace tunnel (pressure tunnel),
4. Surge tank (with valve chamber),
5. Penstock, (pressure shaft),
6. Powerhouse,
7. Tailracetunnel

CHAPTER 2

2. Pressure pipelines

2.1 General (hydraulic basics principles)

2.1.1 *Pipe types and pipe connections*

In principle, the most important part of the system *pressure pipelines* is to find the shortest way to connect the dam with the surge tank and power station. This connection way is divided in two parts: the slightly inclined power water way (reservoir-surge tank), and the slope line (surge tank-power station)

Pressure pipelines have to be adapted to the topography. As a part of hydropower facility, this system depends on type of hydropower facility. Main part of the system is the distance between the reservoir and hydropower facility. High head hydropower plants are mostly built at a mountain, where the system of pressure pipelines (pressure tunnel; pressure shaft) and surge tank are necessary. In comparison with low head hydropower plants, which have a simpler system of pressure pipelines, there is no need for a surge tank at low-head hydropower plants, which are called barrages. However, if there is no need for a pressure tunnel, pressure shaft makes the connection and brings the power to the turbines. There are different types of connections, between dams and hydropower plants. Connections are linked in different ways, depending on the Topography, the foundation of the ground, and the development design.

2.2 Parts of construction

2.2.1 Intake

The intake towers are part of the Dam, used to transfer water from the reservoir into the pressure tunnel. They also are used in case of great discharges. The flow into the tower is mainly controlled by a number of small gates instead of a large one. The tower is constructed with two outer and inner walls, connected by radial walls or piers forming the load-bearing structure of the tower. The machine room and hoists are located on top of the tower, above the highest storage level. (Mosonyi, 1960)



Figure 1: Tower intake at Hoover dam, Colorado River

2.2.2 Pressure tunnel

Pressure tunnels may further be classified according to the head above the soffit of the tunnel. Figure 2 shows the head above the soffit of the tunnel

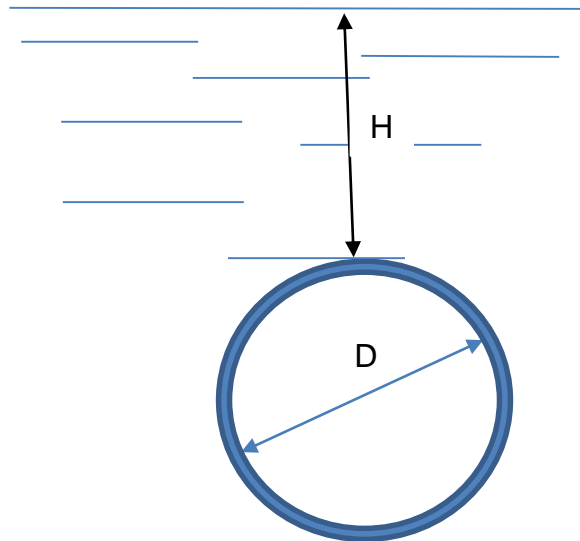


Figure 2: Head above the soffit of the tunnel

- low-pressure tunnels, with H lower than 5 mwc;
- medium-pressure tunnels, with H from 5 to 100 mwc.
- high-pressure tunnels, with H higher than 100 mwc.

Another classification of tunnels may be:

- unlined tunnels
- lined tunnel

Structural lined tunnels are safe against, the rock pressure and they offer protection against rock splitting from the tunnel roof.

Full circular linings offer protection against:

Internal water pressure to avoid water losses and to protect. If required, the rock against the aggressiveness of conveyed water. But these two types are almost similar but their differences are noticed at the detailed discussion.

Low pressure tunnels, the trimmed rock surface can be left unlined except for the visible cracks which can be fixed with concrete or cement mortar. To prevent hydraulic losses, it is better to trim smooth rock surfaces or coat them with a friction concrete layer.

Medium pressure tunnels, watertight concrete linings are usually required. In this case of tunnels, pressure of water is higher and water may leak through the smallest cracks. That is why; simple cement-mortar does not offer enough protection. Watertight concrete linings have to be applied in most cases. The part or sharing of load between concrete lining and rocks should be ensured by grouting. Grouting pipes should be placed, in most cases, at the top of the tunnel, before concrete is poured.

(Mosonyi, 1960)

2.3 High-pressure tunnels

Concrete linings and sometimes even reinforced concrete linings are not enough for the safety of tunnel. In these cases of high pressure tunnels at a lack of overburden as counter pressure, steel linings are designed for protection against full water pressure. These liners are embedded by concrete. This kind of solution is very expensive but, unquestionably, very safe and necessary at the point where the internal pressure is higher as the overburden. In order to allow proper contact between rock and concrete, on the one hand, and between steel pipe and concrete, on the other, all voids are filled by grouting with cement mortar.

(Mosonyi, 1960)

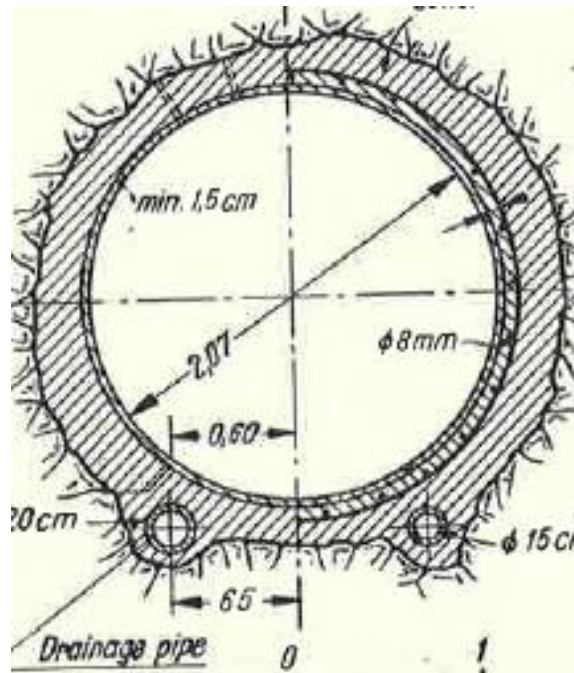


Figure 3: Concrete-lined pressure tunnel

(Mosonyi, 1960)

2.4 Penstock

The penstock is the pipe under pressure between the turbine and the first open water upstream from the turbine. The open water can be a surge tank, river, canal, free flow, tunnel or reservoir. Penstock should be hydraulically efficient and structurally safe in order, to prevent failure. Penstock can be produced from many materials, but steel is more suitable, and stronger, to prevent any kind of damage. The location and arrangement of penstocks, depends from the type of dam.

Hydraulic losses at the penstock reduce the amount and the velocity of water. The various head losses which occur between the reservoir and the turbines may be accounted as: trash rack losses, entrance losses, losses due to pipe friction, Bend losses, and losses in a valve or fittings.

(Reclamation, 1977)



Figure 4: Penstocks, Ohakuri Dam New Zealand [3]

<http://en.wikipedia.org/wiki/Penstock>

For small (low-head) concrete dams, penstocks can be formed (built) in the concrete of a dam. However, steel lining is desirable to assure water tightness. In large concrete dams, which have both transverse and longitudinal contraction joints, steel penstocks are used to provide the required water tightness in the concrete and at the contraction joints. (*Reclamation, 1977*).

2.5 Economic aspects

When a power plant has two or more turbines, the question is whether to use an individual penstock for each turbine or a single penstock with a bifurcation to serve all units. Considering only the economic aspect, a single penstock with a manifold will be cheaper to build. However, the cost of this item alone should not dictate the design. Flexibility of the operation should be given consideration because, with a single penstock system, the inspection or repair of the penstock will require shutting down the entire plant. A single penstock with a header system requires complicated branch connections and a valve to isolate each turbine. The decision as to the penstock arrangement must be made considering all factors of operation, design, and overall cost of entire installation.

(Reclamation, 1977; Reclamation, 1977)

2.6 Penstock types

- Buried penstocks are supported continuously on the soil at the bottom of a trench, backfilled after placing the pipe. The thickness of the cover over the pipe should be about 1.0 to 1.2 [m] for the protection of the pipe.

The advantages of buried pipes are the following:

- a) The soil cover protects the penstock against untoward effects of temperature variations;
- b) It protects the conveyed water against freezing;
- c) Buried pipes do not spoil the landscape;
- d) Immunity against rock slides, avalanches and falling trees;
- e) Concealment offers increased protection against damages caused by violence;
- f) Owing to the continuity of support, this solution is preferable also from the structural point of view.

Disadvantages, on the other hand are as follows:

- a) Such pipes are less accessible for inspection, faults cannot be determined readily;
- b) In case of large diameters and in rocky soil, their installation is expensive;
- c) On steep hillsides, especially if the friction coefficient of the soil is low, such pipes may have the tendency to slide;
- d) Maintenance and repair of the pipe is difficult.

(Mosonyi, 1960)

- Exposed penstocks are installed above the terrain surface and supported on piers. Consequently, there is no contact between the terrain and the pipe itself, and the support is not continuous but concentrated to the piers.

The advantages of exposed penstocks are:

- a) The possibility of continuous and adequate inspection during operation;
- b) Its installation is less expensive in case of large diameters or of rocky terrain;
- c) Safety against sliding may be ensured by properly designed anchorages;
- d) Such pipes are readily accessible and, therefore, maintenance and repair operations can be carried out easily.

Disadvantages include:

- a) Full exposure to external variations in temperature;
- b) Precautions to avoid freezing need to be taken;

- c) Owing to the spacing of supports and anchorages, significant longitudinal stresses may develop especially in pipes of large diameter designed for low internal pressures.

(Mosonyi, 1960)

As a general rule buried pipes are applied only on mildly sloping terrain where the top layers do not consist of rock. The main advantage of exposed penstocks is the possibility of continuous inspection during the operation.

Penstocks are also classified according to the material, from which they are produced:

Steel penstocks can be manufactured and erected according to several methods. The material frequently used is mild steel, although, cast steel and cast iron are also applied in some instances.

- I. For smaller diameters $d = 300-600$ [mm] pipe sections are manufactured at the works. These types are referred to commonly as seamless pipes. These pipes are usually made of steel having a tensile strength of from 55-65 [kg/m^2]. Wall thickness varies generally between 6-30 [mm]. The length of rolled or drawn pipe sections is 6-8 [m], although 12 [m] long have also been manufactured.
- II. Pipes with medium diameter $d = 2-3$ [m] are usually made of plate steel with longitudinal joints. These pipes have a tensile strength of from 34 – 45 [kg/m^2]
- III. Pipes with $d > 3$ [m] are usually delivered to the site in different sections, as half or third cylinders. Penstock with greater diameter than 3 [m] are difficult to transport.

Penstocks of reinforced concrete were successfully applied recently at installations, utilizing relatively low heads. Reinforced concrete pressure pipes have found widespread use for pipe lines of water supply systems. Reinforced concrete penstocks may be either exposed or buried. Those having diameters smaller than 1[m] are always prefabricated, while larger ones are sometimes

cast in place. Prefabricated pipes are usually manufactured with diameters between 300 and 3000 [mm], at common lengths between 3 and 7 [m]. Wall thickness ranges from 8 to 25 [cm].

(Mosonyi, 1960)

Aspects that must be calculated for materials of the pipe connection are: resistance of connection way, consequences of leakage, vibration aspects, and mounting.

Reinforced-Concrete pipes- If the ground at the site has a small drop height, then Reinforced-Concrete pipes can be used. These types are suitable for prefabrication purposes. Pipes with circle reinforcement are able to hold pressure up to 20 bars (2000kPa).

- Dimensioning of the pipe

The flow and the pressure distributions across a network are affected by the arrangement and size of pipes and the distribution of outflows. Figure 5 shows the pipe diameter. Change of diameter in one pipe length will affect the flow and pressure distribution everywhere (R.E.Featherstone, C.Nalluri, 2001).

Dimensioning of the pipe is done by determining the inner diameter and wall thickness of the pipe. The wall thickness is selected based on the required pressure rating. The inner diameter can be either determined based on allowed pressure losses or on flow velocity.

- Dimensioning based on a flow velocity

When using the dimensioning method based on a flow velocity .The inner diameter of the pipe can be determined by using the equation below .When a maximum flow rate and recommended flow velocity are known.

$$D = \sqrt{\frac{4 * Q}{\pi * v}} \quad (1)$$

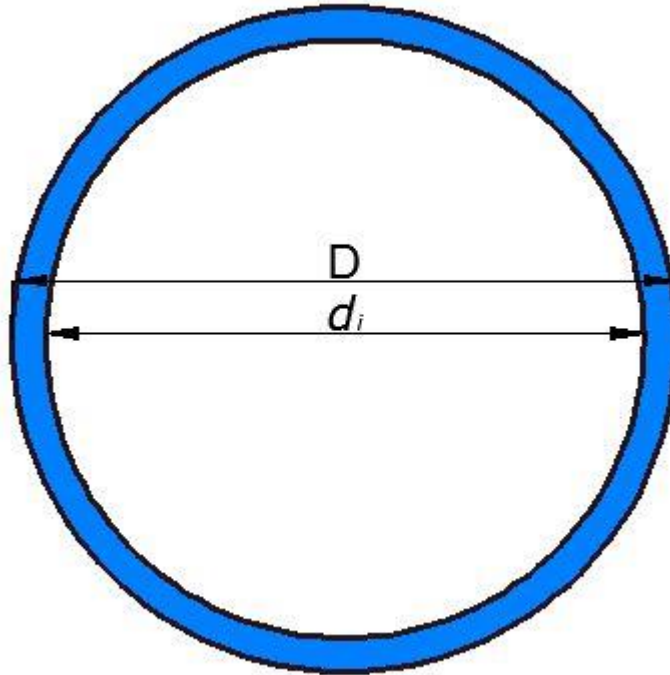


Figure 5: Outer and inner Diameter

(Idelchik, 2005)

D – Outer diameter of the pipe [m].

d_i – Inner diameter of the pipe [m].

$$Q = v * A = v * \frac{\pi * d_i^2}{4} \quad (2)$$

Q - Discharge [m³/s]

V - velocity [m/s]

A - cross section [m²]

Δ - wall thickness of the pipe [m]

2.7 Hydraulics of pipe-flow regimes

The flow regimes of water can be:

- Laminar or turbulent
- Steady or unsteady

In the laminar flow regime the fluid moves in parallel layers with no crosscurrents. In the case of circular pipe, for example, the layers are circular cylindrical tubes. In laminar flow, fluid particles move in parallel paths and this was demonstrated by Reynolds, who introduced a thread of dye into flowing water.

Turbulent flow is characterized by pulsatory cross-current velocities. One result of the crosscurrent velocities of turbulent flow is the formation of a more uniform velocity distribution over the whole flow section.

One of the most important practical differences between laminar and turbulent flow is the larger energy loss in turbulent flow. The criterion that distinguishes laminar flow from turbulent flow was also developed by Reynolds (1883) and has been named Reynolds number (Re). For circular pipe flowing full, Re is expressed as follows:

$$Re = \frac{\rho v D}{\mu} = \frac{v D}{\nu} \quad (3)$$

ρ - density [kg/m^3]

μ - Viscosity [m^2/s]

V - velocity [m/s]

D - diameter [m]

Where d is diameter of the pipe, v the average velocity, ρ the density, μ the viscosity, and ν the kinematic viscosity. For pipes, laminar flow occurs when

$Re \leq 2000$ and flow is usually turbulent when $Re \geq 4000$. For the values of Re between 2000 and 4000, flow is in transition condition.

(Horace.W.King, 1996)

Another classification of the flow depends from steadiness of the discharge. In this classification there are presented two cases as steady flow when discharge is constant with respect to time. Unsteady flow happens in pipes or open channels during and following changes in valve or gate opening. Unsteady flow is a type, which involves problems of such phenomena as water hammer in pipes, translator waves at open channels and the emptying of the tank. Another example of unsteady flow is the discharge of natural rivers, although, during periods when there is no surface runoff, the change in discharge is so slow that many problems may be solved by assuming that flow is steady.

Laminar regimes apply to $Re < 2320$ [-]

Turbulent regimes apply to $Re > 2320$ [-]

2.8 Losses at the pipeline (Loss of energy due to friction)

At this important case on field of hydraulics, one of earliest expressions, for energy loss in a pipe is a developed from Chezy in 1775:

The Chezy formula:

$$v = c * \sqrt{r * s} \quad (4)$$

c - the chezy roughness and pipe coefficient

r – hydraulic radius of the pipe [m]

v – velocity [m/s]

s – slope of the pipe [m]

There are also other empirical formulas that have been proposed. Most of these formulas were based on the assumption that the energy loss depends only on the velocity, the dimensions of pipe, and the wall roughness. The works of Hagen (1839), Poiseuille (1849), and Reynolds (1883) show that density and viscosity of the fluid also affect energy loss.

(Horace.W.King, 1996)

Darcy – Weisbach formula :

$$h_f = \lambda \frac{L}{D} * \frac{v^2}{2g} \quad (5)$$

h_f –friction losses [m]

λ -.friction [-]

L - length [m]

D - diameter [m]

V - velocity [m/s]

g - Gravitation [m/s^2]

For flow in the pipes, h_f is the energy loss per unit length of pipe. It is clear from the preceding part that for laminar flow, f is completely independent of roughness, but varies only with Reynolds number, that is, with relative strength of the viscous and inertial forces. The relation between them

$$f = \frac{64}{R} \quad (6)$$

The Manning formula: concluded that the c at Chezy's formula should vary with $r^{\frac{1}{6}}$ as follows:

$$c = \frac{r^{\frac{1}{6}}}{n} \quad (7)$$

Where n is the roughness coefficient:

$$V = \frac{r^{\frac{2}{3}} * S^{\frac{1}{2}}}{n} \quad (8)$$

(Horace.W.King, 1996)

The Darcy-Weisbach equation along with concept of variation of f and R , represents a basic approach to the solution of pipe friction losses. It is dimensionally correct, its general form can be derived analytically for laminar flow and it can be used for any fluid. The Manning formula is the only one of empirical type of energy loss equations that is still used widely. Because of the Manning equation includes the hydraulic radius; it can be applied to pipes of any shape. Its principal weakness is that it can be used only for water at normal temperatures.

(Horace.W.King, 1996)

2.9 Local losses or Minor losses

Energy losses resulting from rapid changes in the direction or magnitude of the velocity are called local losses.

Local Losses formula

$$h_l = \zeta * \frac{v^2}{2g} \quad (9)$$

ζ - single loss factor

v - velocity [m/s]

g - gravitation [m/s²]

h_l - losses [m]

2.10 Loss at Entrance

When water enters a pipe from a reservoir, the loss is expressed as

$$h_1 = \zeta_1 * \frac{v^2}{2g} \quad (10)$$

- *Loss of Head Due to Enlargement*

Borda 1733–1799 has found that the loss in pipes due to sudden enlargement may be represented by the theoretical formula:

$$h_2 = \frac{(V_1 - V_2)^2}{2g} \quad (11)$$

Where h_2 is the head loss and V_1 and V_2 are velocities in the smaller and larger pipes

- *Loss of Head Due to Contraction*

Equation for the loss in pipes due to sudden contraction is:

$$h_3 = \zeta_3 * \frac{V_2^2}{2g} \quad (12)$$

- *Loss of Head Due to Gates of Valves*

$$h_g = \zeta_g * \frac{V^2}{2g} \quad (13)$$

- *Loss of Head Due to Bends*

The local loss at bend results from distortion of the velocity distribution, thereby causing additional shear stresses within the fluid.

$$h_b = \zeta_b * \frac{V_b^2}{2g} \quad (14)$$

(Horace. W. King, 1996)

There are two types of losses at the pipeline:

- Local losses:

Losses at entrances, bends, enlargements, and contractions and other similar local losses are called minor losses, as distinguished from the friction loss in the straight sections

- Local head losses of the flow.
- Separation of flow from the wall.

- The strong turbulent agitation of the flow at the places where the configuration of the pipelines changes (entrance of fluid into the pipeline, expansion, contraction, bending).
- Branching of the flow.
- Flow through orifices.
- Grids or valves.

$$h_v = 1h_f \tag{15}$$

Friction losses(Darcy Weißbach) →[2]

(Horace.W.King, 1996)

CHAPTER 3

3. Water hammer phenomenon

3.1 Dynamic flow processes

In cases when a change of the velocity of the water inside the pipelines occurs, pressure fluctuations inside the pipes follow. If there is a delay in the flow velocity, then the transformation of kinetic energy into the pressure energy (water hammer) becomes valid (Giesek).

Therefore the water hammer phenomenon is a consequence of the force which opposes the inertial mass of the liquid and changes its direction.

Water hammer occurs as a result of operation of valves or regulatory bodies inside the pipelines. This process begins for different reasons, for example if there is a problem with the turbines, or when discharge inside pipelines has a high speed and the ventilation is inadequate. Otherwise, the pulsating discharge occurs, and there is accumulation of air in pipelines or in case of irregular working process of pumps.

The phenomenon of water hammer may be important in the design and operation of various types of hydraulic systems, such as water supply networks, irrigation systems, industrial conduits, distribution systems and waste piping, cooling circuits of thermal, and many other hydraulic installations. (Zaruba, 1993)

A sudden closure at hydro-power plants of its terminal closing mechanism, wicket gate or valve guarding the turbine, is followed by inertia effects resulting in overpressures and depressions in the penstock, which should be allowed for in the structural design of the pipe. Water moving with velocity (v) in the penstock decelerates in case of closure and the inertia force of the decelerating mass is :

$$P = -M \frac{\Delta v}{\Delta t} \quad (16)$$

M – water mass [kg/m^3]

Δv - change of velocity [m/s]

Δt – period [s]

Formula [16] describes. Where M is the water mass decelerated by Δv during the period Δt

3.2 Water hammer and column separation

Column separation refers to the breaking of liquid columns in fully filled pipelines. This may occur in a water hammer process when the pressure in a pipeline drops to the vapor pressure at specific locations such as closed ends, high points or knees. The liquid columns are separated by a vapor cavity that grows and diminishes according to the dynamics of the system. When these columns are created, they cause a rise of pressure inside the pipeline and this rise of pressure travels through the entire pipeline. The sudden shutdown of the pump or valves causes fluid transients, which may involve large pressure variations, local cavity formation, distributed cavitation (bubble flow), hydraulic and structural vibrations and excessive mass oscillations.

(A.Bergant, 2005)

3.3 The unsteady flow-Vapor formation

A quick change from steady state flow to unsteady state flow in a piping system occurs because of a change in boundary conditions. There are many kinds of boundary conditions that may introduce transients. Common ones:

1. Changes in valve settings, accidental or planned.
2. Starting or stopping of pumps.
3. Changes in power demand in turbines.
4. Action of reciprocating pumps.

5. Changing elevation of a reservoir.
6. Waves on a reservoir.
7. Turbine governor hunting.

Aside from damaging equipment attached to piping systems, water hammer may cause the pipe to fail from excessive pressure or collapse due to pressure less than atmospheric. The phenomenon of column separation may occur within a piping system when boundary conditions are such that the pressure is reduced at the upstream end of a pipe. The reduction in pressure causes a negative wave pulse to be transmitted down the pipe, thereby reducing its velocity; the fluid downstream continues at its steady velocity until the wave arrives.

(A.Bergant, 2005)

3.4 Water-hammer calculation

Water-hammer calculation is a process that needs to go through four assumptions

In the flow section, the velocity and the pressure are distributed at the same time. Pipeline is full with droppable liquid.

When compared with the pressure level, the velocity level is negligibly small.

Water-level at the reservoir from which the pipeline is supplied, stays constant throughout the time, until the Water-hammer stops.

After taking in to the consideration these assumptions for further calculations, in the following section are described other important elements of water-hammer.

(Giesecke & Mosonyi, 2009)

3.5 Pressure wave velocity

Pressure changes in the pipeline leads to the length stresses σ_l and the ring stresses σ_φ at pipe walls. Below are formulas for calculation.

$$\sigma_{\varphi} = \frac{p_i * d_i}{2 * s} \quad (17)$$

σ_{φ} . – ring strain [N/mm^2]

d_i – inner diameter [mm]

$p_{i..}$ – internal pressure [N / mm^2]

S – wall thickness [mm]

$$\varepsilon_r = \frac{\sigma_{\varphi}}{E_R} = \frac{1 * d_i * \Delta p_i}{2 * s} = \frac{2 * \pi * \Delta r_i}{2 * \pi * r_i} = \frac{2 * \pi * r_i * \Delta r_i}{2 * \pi * r_i^2} = \frac{\Delta A}{2 * A} \quad (18)$$

ε_r – Streching in Ring direction [-]

E_R – Elasticity of pipe [N/mm^2]

d_i – inner diameter [m]

By extension

$$\frac{\rho * 2}{\Delta p_i} \quad (19)$$

$$\frac{\rho}{\Delta p_i} * \frac{\Delta A}{A} = \frac{\rho * 2}{\Delta p_i} * \left(\frac{l}{E_R} * \frac{d_i * \Delta p_i}{s} \right) = \frac{\rho * d_i}{E_R * s} \quad (20)$$

The Elasticity deformation of the water in one highly rigid pipe:

$$\varepsilon_w = \frac{\Delta p_i}{E_w} \quad (21)$$

$$\varepsilon = \varepsilon_w + \varepsilon_r = \frac{\Delta p_i}{E_w} + \frac{\rho * d_i}{E_R * s} \quad (22)$$

ε – Stretching as a result of the pressure wave[-]

Speed of the sound for longitudinal wave at fluids is:

$$a_F = \sqrt{\frac{E_F}{\rho_F}} \quad [m/s] \quad (23)$$

E_F – Elasticity modul of fluid [N/mm^2]

ρ_F – Density of Fluid [N/mm^3]

$$\frac{1}{a^2} = \frac{\rho_F}{E_F} + \frac{\rho * A}{A * \Delta p_i} = \frac{1}{a_F^2} + \frac{1}{a_R^2} = \frac{1}{a_F^2} + \frac{E_F * d_i}{a_F^2 * E_R * s} = \frac{1 + \frac{E_F * d_i}{E_R * s}}{a_F^2} \quad (24)$$

$$a = \frac{a_F}{\sqrt{1 + \frac{E_F}{E_R} * \frac{d_i}{s} * k_q}} \quad (25)$$

(Giesecke & Mosonyi, 2009)

3.6 The Joukowsky Equation

In 1897 *Joukowsky* made some experiments at the Moscow drinking water supply pipes. He found out that the water hammer phenomenon is a process that is produced in pipelines due to the closing of the valves. At the moment when a valve closes, the fluid is forced to change the direction of the flow and causes deceleration of the velocity inside the pipes. Then there will be a high pressure in the pipeline that is also called the Hydraulic shock. This process is also called the *Joukowsky* pressure.

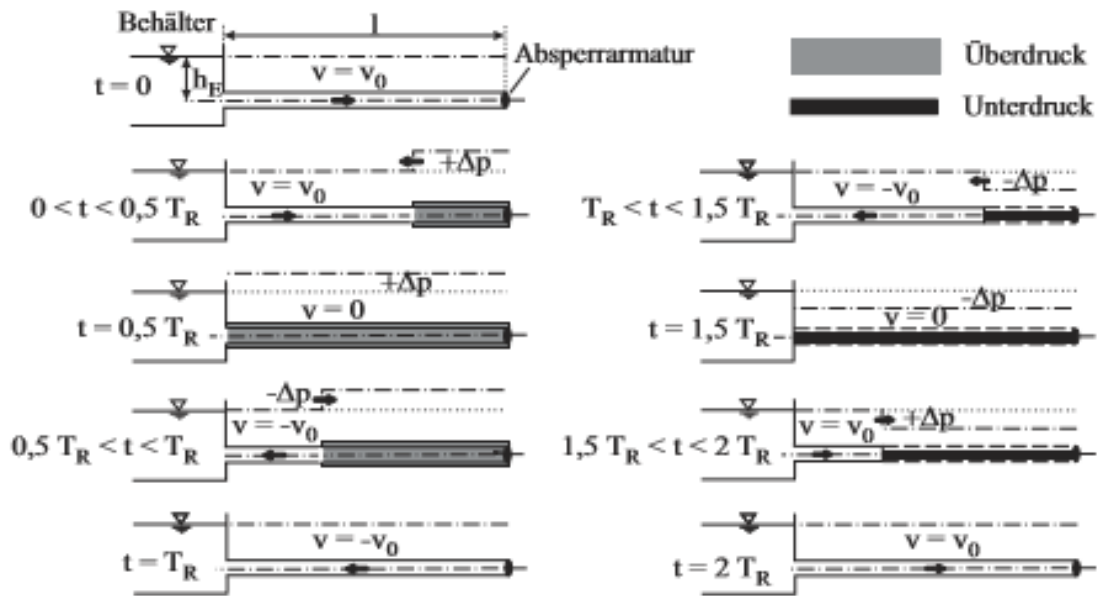


Figure 6: Joukowsky pressure and reflections time

(Giesecke & Mosonyi, 2009; Mosonyi, 1960)

To estimate pressure surge of the extreme case of sudden closing of valves A simple pipeline system with a reservoir and valves is showed in Figure 6. This figure shows the pressure curve. During a sudden closing of valve, the change of water velocity Δv creates a pressure increase

$$\Delta p_{jou} = a * \rho * \Delta v \quad (26)$$

which is called Joukowsky-pressure. The pressure surge runs as an overpressure wave with the acceleration (a) inside the pipeline up to the reservoir and back again to the source of disturbance.

Δv – flow velocity change [m/s]

ρ – density of fluid in $\left[\frac{\text{kg}}{\text{m}^3}\right]$

a – Wave propagation velocity through the fluid in the pipelin in [m/s]

Operational time T_L is a certain period that pressure waves need to travel through the whole length of the pipeline.

Operational time T_L of the pressure wave during the whole length of pipeline l is calculated with formula:

$$T_L = \frac{l}{a} \dots (s) \quad (27)$$

Reflection time T_R is a certain period, that pressure waves needs it, to arrive the entrance of reservoir.

$$T_R = 2 * T_L = 2 * \frac{l}{a} \quad (28)$$

T_R – Reflection time

T_L – Operational time

According to Joukowsky, the maximum water-hammer pressure height is calculated with following formula:

$$\max h_{a,jau} = \pm \frac{a * \Delta v}{g} \quad (29)$$

(Giesecke & Mosonyi, 2009)

3.6.1 Influence of closing time for Joukowsky pressure

The closing time t_s of a valve has a big influence on the water-hammer. Thus, when closing time t_s is smaller than Reflection time T_R , produced at closing valves independently from closing characteristics, in this case there is full Joukowsky pressure $t_s < T_R$. However, when closing time t_s is greater than Reflection time $t_s > T_R$ than the process is called pressure reduction. (Giesecke & Mosonyi, 2009).

$$\max h_a = \pm \frac{a * \Delta v}{g} * \frac{T_R}{t_s} \quad (30)$$

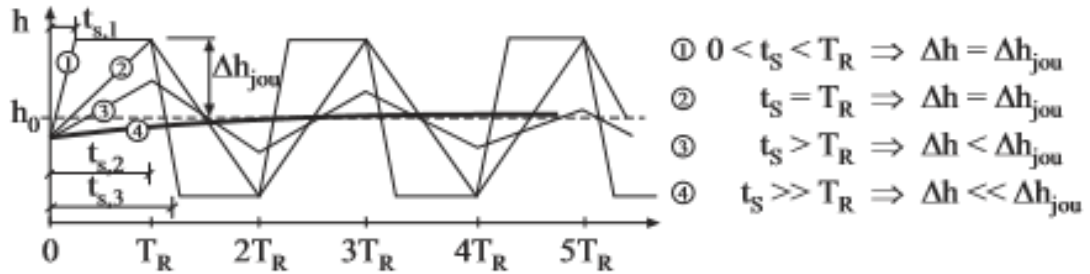


Figure 7: Report between closing time and reflection time

Figure 7 shows 4 lines, which describe the pressure height. For each line of pressure height (h_1, h_2, h_3, h_4) . Report between closing time of valves t_s and reflection time T_R of pressure wave, is different.

1. ($0 < t_s < T_R$) When closing time t_s is smaller than reflection time T_R , then the maximum pressure height is reached which is equal to Δh_{jou} , the Joukowski pressure .
2. ($t_s = T_R$) When closing time t_s is equal with reflection time T_R , the pressure also reaches like case 1 the maximum height(Δh_{jou}) but only for one point in time.
3. ($t_s > T_R$) When closing time t_s is bigger than reflection time T_R , then Δh_{jou} (joukowski pressure) is not reached.
4. ($t_s \gg T_R$) When closing time t_s is much bigger than reflection time T_R , than Δh_{jou} joukowski pressure height is also much bigger than Δh pressure height inside the pipeline.

(Giesecke & Mosonyi, 2009)

At real systems, there is no linear relationship between closing time of the valves and pressure height occurring inside the system.

3.7 Method of Characteristics

In this section the Method of characteristics (MOC) is discussed, with the continuity equation and the equation of motion as the basic equations. The method of characteristics serves with excellent conditions such accuracy, stability and programming possibility.

Multiplication of the Continuity equation and pressure wave velocity, are as follow:

$$\frac{\partial v}{\partial x} * a + \frac{1}{p_f * a} \left(v * \frac{\partial p_i}{\partial x} + \frac{\partial p_i}{\partial t} \right) = 0 \quad \left(\frac{m}{s^2} \right) \quad (31)$$

Equation of motion

$$\frac{\partial v}{\partial t} + v \frac{\partial v}{\partial x} + \frac{1}{p_f} * \frac{\partial p_i}{\partial x} + g * \frac{d_z}{d_x} + \frac{\lambda}{2d_i} * v * v = 0 \quad (32)$$

$$\begin{aligned} \frac{\partial v}{\partial t} + (v \pm a) * \frac{\partial v}{\partial x} \pm \frac{1}{p_f * a} \left((v \pm a) * \frac{\partial p_i}{\partial x} + \frac{\partial p_i}{\partial t} \right) + g \\ * \frac{d_z}{d_x} + \frac{\lambda}{2d_i} * v * v = 0 \end{aligned} \quad (33)$$

The terms $(v \pm a) = dx/d_t$ are like Charakteristik defined

$$\begin{aligned} \frac{\partial v}{\partial t} + \frac{dx}{dt} * \frac{\partial v}{\partial x} \pm \frac{1}{p_f * a} \left(\frac{dx}{dt} * \frac{\partial p_i}{\partial x} + \frac{\partial p_i}{\partial t} \right) + g * \frac{d_z}{d_x} \\ + \frac{\lambda}{2d_i} * v * v = 0 \end{aligned} \quad (34)$$

With total differential representation:

$$\frac{dv}{dt} = \frac{\partial v}{\partial t} + \frac{\partial v}{\partial x} * \frac{dx}{dt} \quad (35)$$

$$\frac{dp_i}{dt} = \frac{\partial p_i}{\partial t} + \frac{\partial p_i}{\partial x} * \frac{dx}{dt} \quad (36)$$

$$\frac{\partial v}{\partial t} \pm \frac{1}{p_f * a} * \frac{dp_i}{dt} + g * \frac{d_z}{d_x} + \frac{\lambda}{2d_i} * v * v = 0 \quad (37)$$

$$\frac{1}{p_f * a} * \frac{dp_i}{dt} = g * \left(\frac{d_h}{d_t} - \frac{d_z}{d_t} \right) \quad (38)$$

$$\frac{\partial v}{\partial t} \pm \frac{g}{a} * \left(\frac{dh}{dt} - \frac{dz}{dt} \right) + g * \frac{d_z}{d_x} + \frac{\lambda}{2d_i} * v * |v| = 0 \quad (39)$$

$$\frac{dz}{dt} = \frac{d_x}{d_t} * \frac{dx}{dt} = (v \pm a) \frac{d_z}{d_x} \quad (40)$$

$$\begin{aligned} \frac{d_v}{d_t} \pm \frac{g}{a} * \left(\frac{dh}{dt} - (v \pm a) \frac{dz}{dx} \right) + g * \frac{d_z}{d_x} + \frac{\lambda}{2d_i} * v * v \\ = 0 \end{aligned} \quad (41)$$

$$(v \pm a) \approx \pm a = \frac{d_x}{d_t} \quad (42)$$

$$\frac{d_v}{d_t} \pm \frac{g}{a} * \frac{dh}{dt} + \frac{\lambda}{2d_i} * v * v = 0 \quad (43)$$

Through an integration”

$$\left(v + \frac{g}{a} * h \right) = \int_{t_u}^{t_p} \left(- \frac{\lambda}{2d_i} * v * |v| \right) dt + Ch \quad (44)$$

$$\left(v - \frac{g}{a} * h\right) = \int_{t_R}^{t_P} \left(-\frac{\lambda}{2d_i} * v * |v|\right) dt \quad -Ch \quad (45)$$

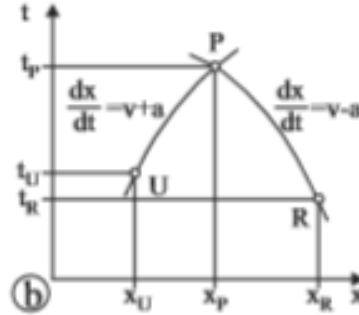


Figure 8: Graphical representation of the formulas

$$\left(v + \frac{g}{a} * h\right) = \left(v + \frac{g}{a} * h\right) + \frac{x_F - x_U}{2a} \left(-\frac{\lambda}{2d_i} * v * |v|\right) + \left(-\frac{\lambda}{2d_i} * v * |v|\right) \quad (46)$$

$$h_F = 3h_u + \frac{a}{g}(v_u - v_F) - \frac{\Delta x * \lambda}{4 * g * d_i} (V_F |V_F| + V_U |V_U|) \quad (47)$$

$$h_F = h_R + \frac{a}{g}(v_R - v_F) - \frac{\Delta x * \lambda}{4 * g * d_i} (V_F |V_F| + V_R |V_R|) \quad (48)$$

$$V_F |V_F| + V_U |V_U| = 2V_F |V_U| \quad (49)$$

$$V_F |V_F| + V_R |V_R| = 2V_F |V_R| \quad (50)$$

$$h_F = h_u + \frac{a}{g}(v_u - v_F) - \frac{\Delta x * \lambda}{4 * g * d_i} V_F |V_U| \quad (51)$$

$$h_F = h_R + \frac{a}{g}(v_R - v_F) - \frac{\Delta x * \lambda}{4 * g * d_i} V_F |V_R| \quad (52)$$

$$Q = v \cdot a \quad (53)$$

$$B = \frac{a}{g \cdot A} \quad R = \frac{\Delta x \cdot \lambda}{2 \cdot g \cdot d_i \cdot A^2} \quad (54)$$

$$h_F = h_u + B(Q_u - Q_F) - R Q_F |Q_U| \quad (55)$$

$$h_F = h_R + B(Q_R - Q_F) + R Q_F |Q_R| \quad (56)$$

$$B_U = B + R \cdot |Q_U| \quad (57)$$

$$C_U = h_U + B \cdot Q_u \quad (58)$$

$$B_R = B + R \cdot |Q_R| \quad (59)$$

$$C_R = h_R + B \cdot |Q_R| \quad (60)$$

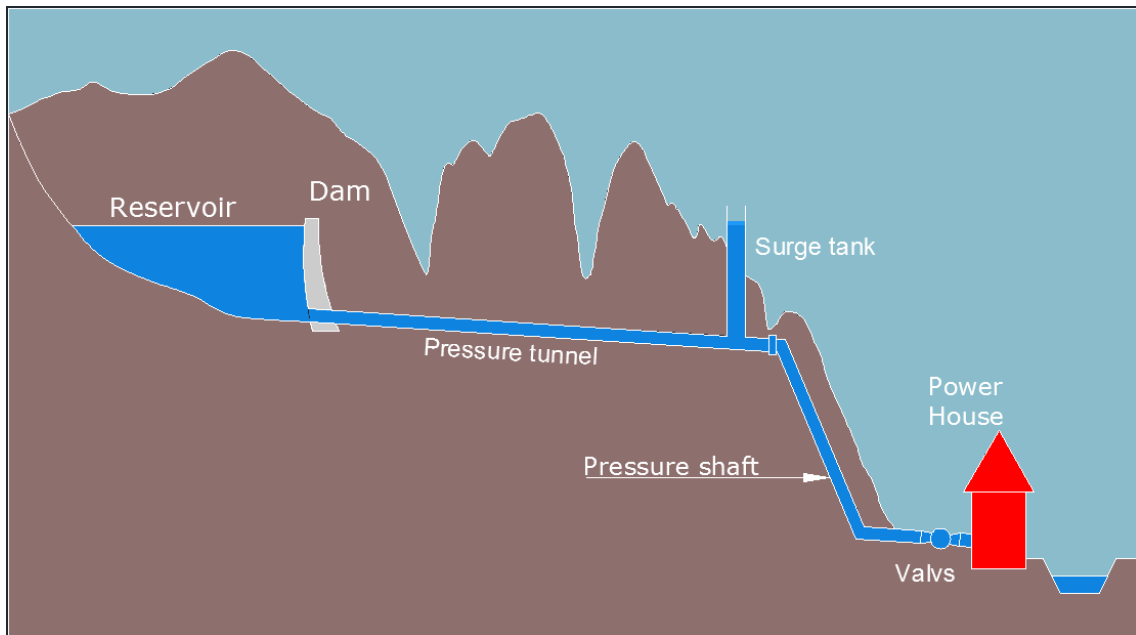
$$h_P = \frac{C_U \cdot B_R + C_R \cdot B_U}{B_U + B_R} \quad (61)$$

$$Q_F = \frac{C_U - C_R}{B_U + B_R} \quad (62)$$

(Giesecke & Mosonyi, 2009)

3.8 Surgetank

This chapter describes the necessity of surge tanks. Figure 9 shows the graphical overview of a Surge tank.



. Figure 9: High-head hydropower plant, longitudinal section surge tank

The surge tank is placed between the slightly inclined pressure tunnel and the steeply sloping penstock (pressure shaft), and is designed either as a chamber excavated in the mountain or as a tower raising high above the water level in reservoir.

For a sudden closure of the valves ahead of the turbine, the water mass that is moving in the pressure tunnel and in penstocks still contains its initial kinetic energy. This has to be dissipated. In the pressure tunnel the kinetic energy create an inflow into the surge tank. The kinetic energy in the penstock will be transferred to pressure energy. This phenomenon is called *water hammer*. Its magnitude will depend from the dimensions of the pipe, and its elastic properties. At this case, the main role is played by the surge tank, which controls the pressure wave that comes from penstocks and reduces pressure that could damage the pressure shaft and pressure tunnel. However, it should be noted that a surge tank does not neutralize the whole pressure wave. There is still a pressure wave that enters the pressure tunnel but with a lower pressure.

Another important function of surge tank is to provide water supply to the turbines in case of starting up. When the turbine valves suddenly open and the flow of

water in the penstock is suddenly initiated (respectively accelerated). The surge tank will provide during this time with water supply. By the rapid opening of the turbine, acceleration of water mass at pressure tunnel is lower, because pressure tunnel lies in an almost horizontal surface, thus the flow around the elbow would become discontinuous if no surge tank was applied. Water mass at surge tank during these kind of cases, serves as important factor in order to prevent the entering of air in penstocks.

(Mosonyi, 1960)

3.8.1 *Types of surge tank*

There is a wide variety of types of surge tank:

- According to their hydraulic design:

a) *Simple surge tank*, designed as a shafts or as basins, either of which may be provided with an overflow.

b) *Special surge tanks*, with expansions chambers, either of which may be provided with overflow, are divided in:

- Surge shaft with upper expansion chamber,
 - Surge shaft with lower expansion chamber,
 - Double-chamber surge tank.
 - Restricted-orifice type (or throttled) surge tanks:
 - Simple restricted-orifice surge tank,
 - Differential (Johnson type) surge tank,
 - Double-chamber, restricted-orifice surge tank.
- According to their location relative to the terrain, surge tanks are classified as:

1. Recessed (excavated) surge tanks, usually made accessible through a tunnel supplying, at the same time, air to surge tank.
 2. Free-standing (exposed) surge tanks designed as towers which are provided with a supporting structure in accordance with the functional principle. This structure may be from reinforced concrete or steel structure, while the penstock and the tank are connected by a vertical riser pipe.
- According to their position relative to the power-house, surge tanks may be :

Upstream (headrace) surge tank, or,

Downstream (tailrace) surge tanks.

In some instances surge tanks are applied both upstream of the penstock and downstream of the powerhouse. Interconnected surge tanks form a so-called multiple surge system. (Mosonyi, 1960)

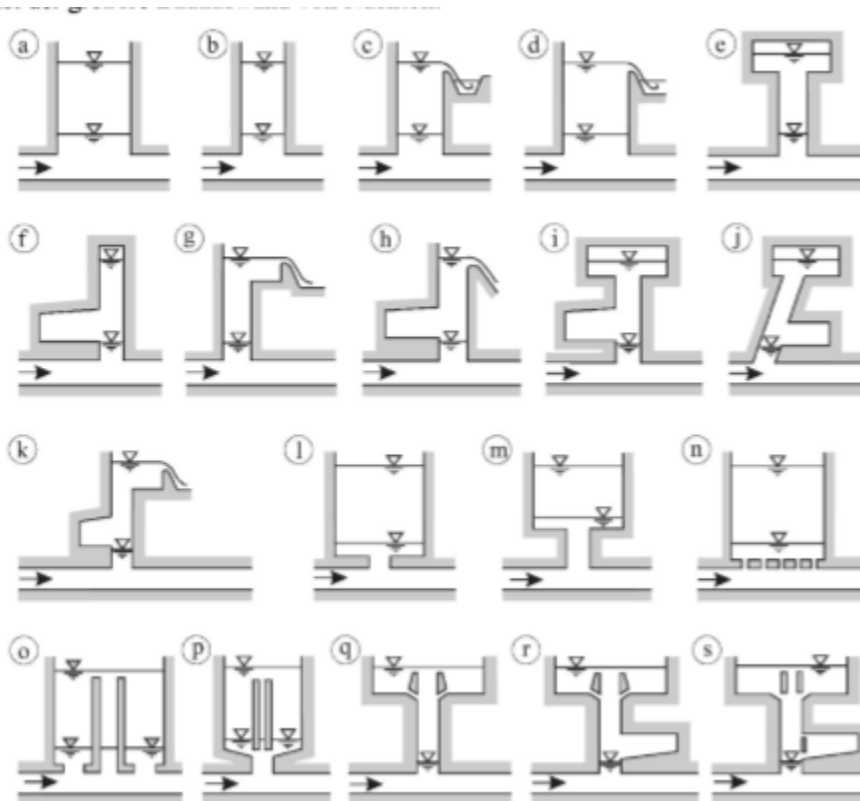


Figure 10: Surge tank types

(Giesecke & Mosonyi, 2009)

In figure 10 there are represented possible surge tank types.

3.8.2 *Mass Oscillations in surge tank*

Oscillations are movement back and forth in regular rhythm. In this case it is about movement of the mass of the water inside the system. Mass oscillations of the water surface at surge tanks happen because of the pressure waves inside the pipelines, which is caused mainly from the change in the turbine discharge. Pressure wave after traveling the length of the penstock, reaches the surge tank. Water hammer is the strongest pressure wave, which is delivered only as long as the valves are closed. Water hammer is the biggest pressure wave inside the pipelines, especially in the pressure shaft or so called penstock. This pressure wave increases the level of water, inside the surge tank and, within seconds after the closing of the valves. There is an increase and decrease of the water level in the surge tank till the pressure inside the pipelines is neutralized, and this mass of water moves back and forward between directions of the surge tank and the pressure tunnel. This process is called Mass oscillation.

CHAPTER 4

4. Calculations with TUG_Hammer

This master thesis is a study of complex hydraulic phenomena such as, water hammer behavior which occurs at the valves head of the turbines, and the mass oscillations inside the surge tank and pressure tunnel.

To study the functioning of the transient hydraulics in pipelines under the pressurized flow, the water hammer phenomena is examined at an example of a prototype hydro-power plant. This is calculated with the TUG-hammer software.

The following example was composed with a Reservoir, four pipes, and surge tank, with valves before the power plant, and a bifurcation between pipes the surge tank. Figure 11, shows the longitudinal section of the hydraulic scheme with four principal pipes and its diameters and lengths as indicated.

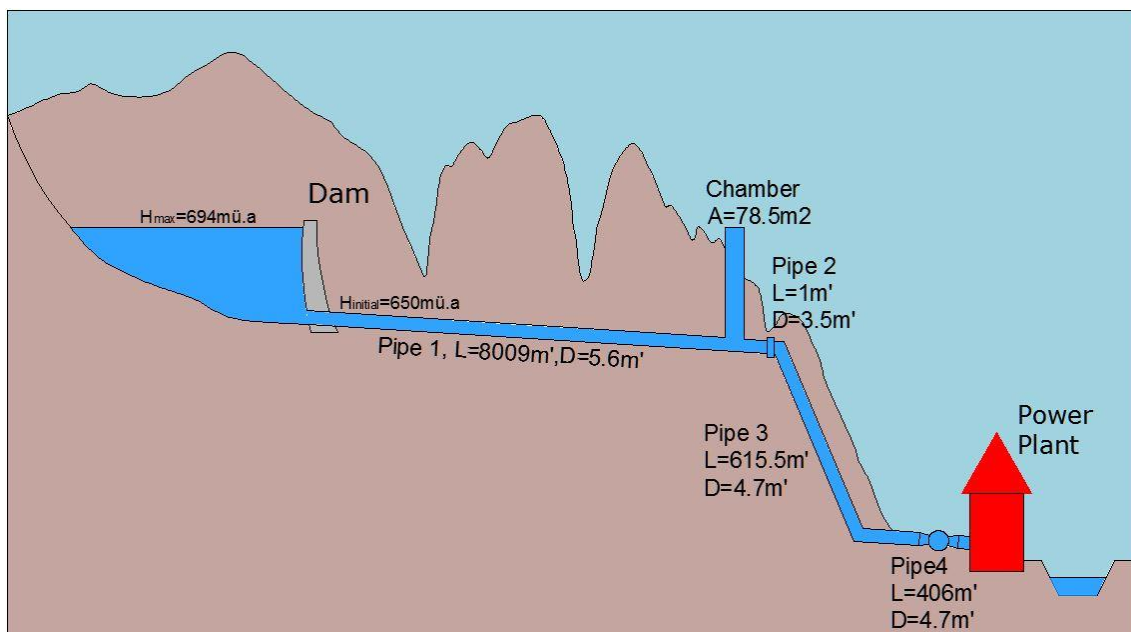


Figure 11: Sample of the investigated prototype model

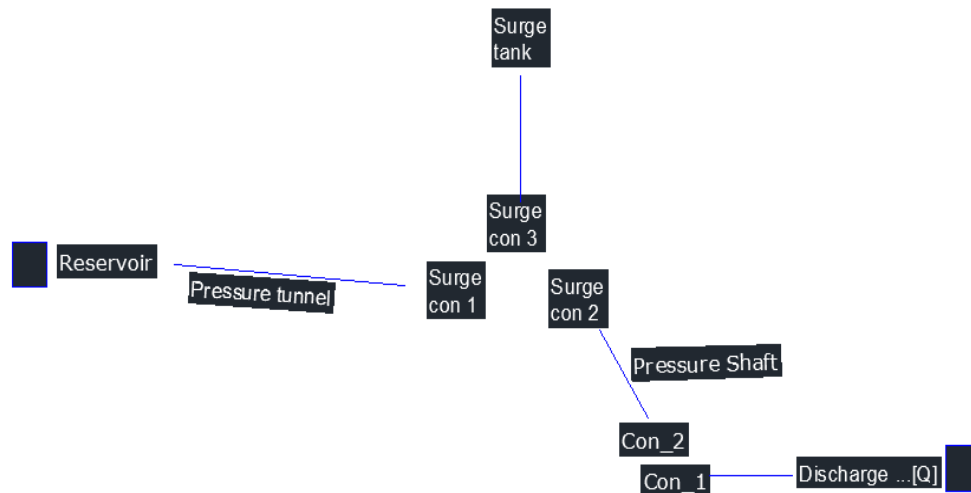


Figure 12: Description for each part of the example, elements as used for TUG Hammer

Figure 12 shows how a pipe1 is connected to the reservoir on the left side. On the right side it is connected to the Bifurcation (Surge Con_1) which creates the connection between Pipe1-Pipe2-Pipe3. Pipe2 is connected to Bifurcation (Surge Con_3) on the left side, and on the right side it is connected to the surge tank, which is followed from pressure shaft. Pressure shaft is the connection between Bifurcation and connection to pipe4. Pipe3 (Pressure shaft) on the left side is connected to Bifurcation_2 and on the right side it is connected to Connection_1. Pipe4 on the left side is connected to Connection_2, while on the right side there are turbines.

4.1 TUG_hammer

TUG_hammer - is software used for the calculation of the pressure inside the pipelines and water hammer. In the figure 13 there is presented the interface of the tool, and options that it has.

The process of calculation with this tool is as follows:

- The first step is to create the system of the pipelines, and insert the values of the parts of the system. Right part of the GUI contains system parts, while on the left side there are presented values. First step begins with inserting the pipes and filling the values of them

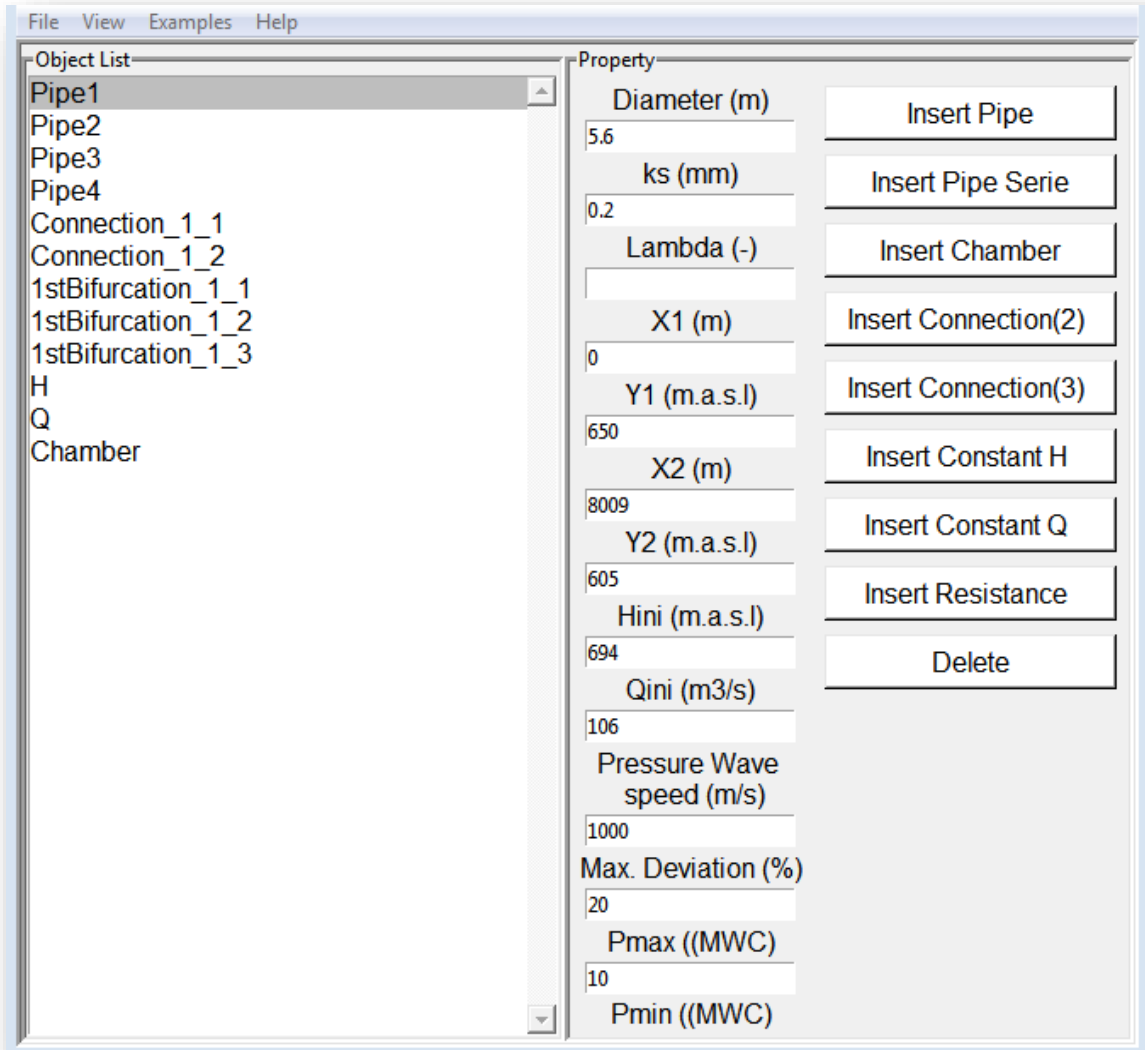


Figure 13: TUG_hammer GUI interface

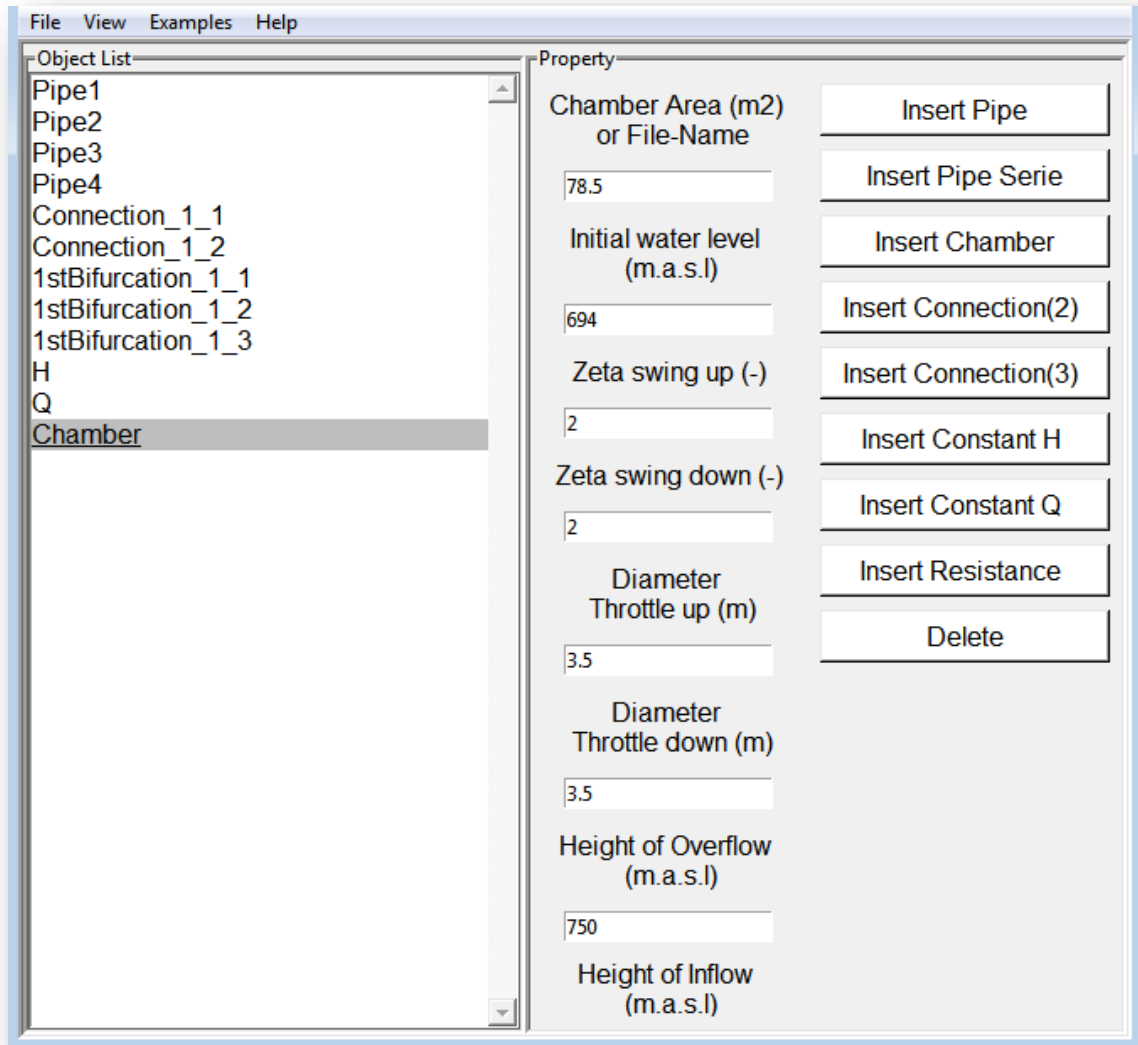


Figure 14: TUG_hammer GUI interface

- The second step as it can be seen in Figure 14 is to insert and to give values of the other parts of the system: bifurcation, surge tank, resistance, etc.

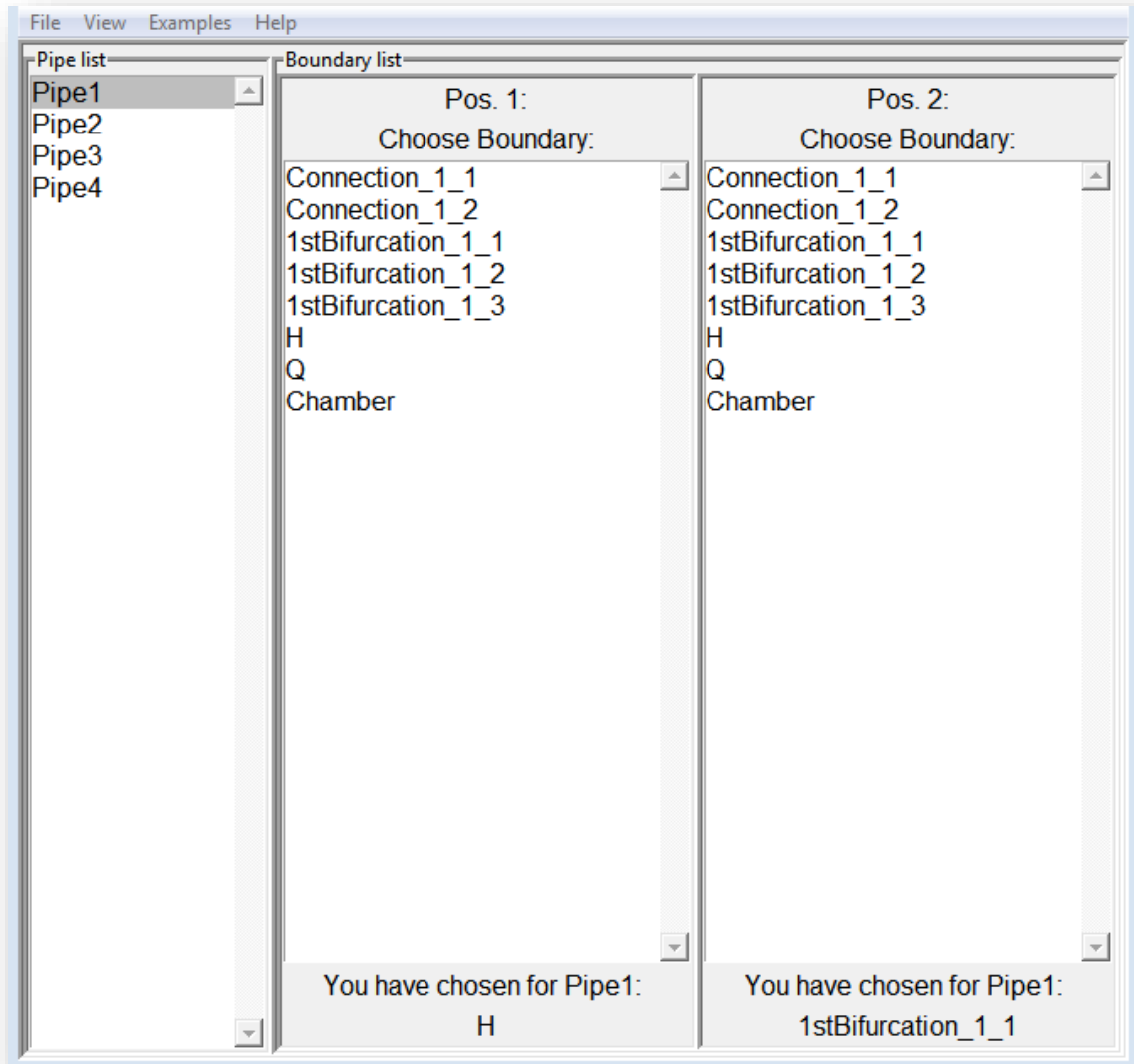
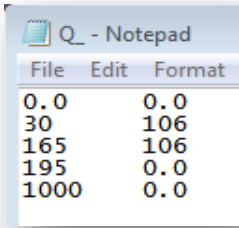


Figure 15: TUG_hammer – part connections

- The third step (Figure 15) is to make the connection between the parts inside the system. This is called the Boundary condition. We chose the pipes from the list; Pos 1 is the connection on the left side of the pipe, while Pos 2 is the connection on the right side of the pipe.

- The fourth step is discharge inside the pipelines, which is given to the Tug hammer as a text file. Figure 16 shows the text file interface that serves for file creation. The file needs two input parameters: (t) time and (Q) discharge of the water inside the system, as well the closing time of the valves.

As it can be seen in Figure 16, at time $t=0.0$ [s] discharge is $Q=0.0$ [m^3/s]. At time $t=30$ [s] discharge arrives to $Q=106$ [m^3/s], which means from time $t=0.0$ [s]- 30 [s] that is the opening time of the valves until the discharge reaches the peak. From time $t=30$ [s] - 165 [s] discharge has a same value $Q=106$ [m^3/s]; And from time $t=165$ [s]- 195 [s] is closing-time of the valves, during this time, discharge goes down to 0.0 [m^3/s];



File	Edit	Format
0.0	0.0	
30	106	
165	106	
195	0.0	
1000	0.0	

Figure 16: Notepad- values of discharge inside the pipeline.

On the left side time (t):

$T = 0$ [s]; 30 [s]; 165 [s]; 195 [s]; 1000 [s].

On the right side discharge:

$Q = 0$ [m^3/s]; 106 [m^3/s];

In this section the results are shown from this experiment:

- At time $t=0.0$ [s] there is no flow of the water inside the pipelines $Q=0.0$ [m^3/s].

- From time $t=0.0$ s till $t=30$ s valves of the system will be opened.
- From time $t=0.0$ s till $t=30$ s, discharge achieves $Q=106$ m³/s- (max design discharge of the system).
- From time $t=165$ s till $t=195$ s, closing of the valves.

Results 1:

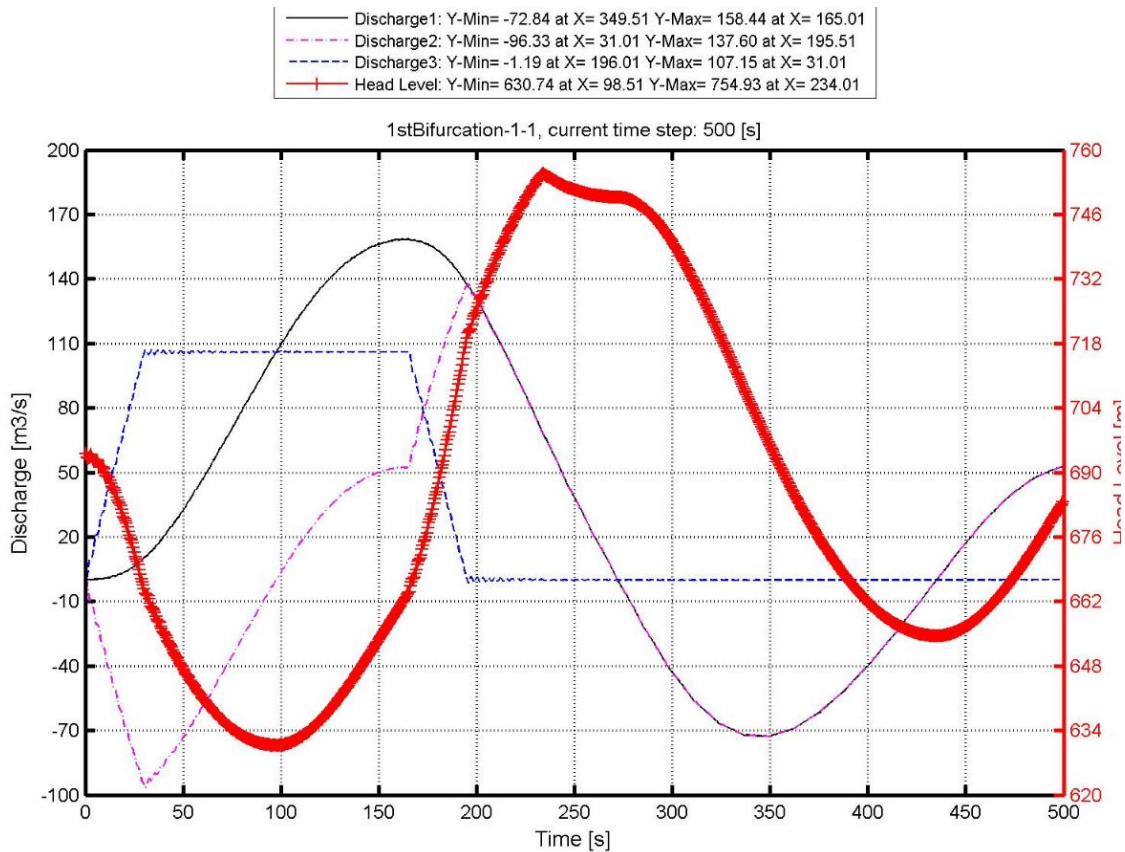


Figure 17: Evaluation of mass oscillation (a)

Figure 17, contains 4 lines showing the results from different parts of the pipe system. The diagram shows the pressure and the discharges at the location of Bifurcations, which is the connection between pressure tunnel (pipe1), pipe 2 (connection to surge tank) and pressure shaft (pipe3)

Each line is a result of a calculation at different point of parts.

- Discharge 1 (Black line) shows the discharge in pipe1 pressure tunnel. The discharge at pipe1 depends from the time on, where is the opening

and the closing of the valves. From $t=0$ s till $t=165$ s, discharge at pipe1 arrives at its peak, and the black line goes up. During time $t=165$ s – 195 s it can be noticed that, the line decreases, which means, that this is the time when the valves will be closed. It can be seen that the discharge at pipe1 changes its direction, as a result of the water hammer at the valves. This is how water hammer indicates the mass oscillation at the pressure tunnel and that is why the line continues till $Q = -70 \text{ m}^3/\text{s}$. The pressure is stable inside the pipelines and with that discharge at the pipe1 will be $Q = 0 \text{ m}^3/\text{s}$. This is what is called connection between water hammer before turbines and mass oscillations inside the pressure tunnel and surge tank.

- Blue line (Discharge 2) is the flow at the pressure shaft or pipe3 (bifurcation_3) in our case. At this part, the discharge achieves its peak from $t=0$ s – $t=30$ s. From time $t=30$ s – 165 s it is equal, and during the time $t=165$ s – $t=195$ s (closing time of the valves), discharge is $Q = 0 \text{ m}^3/\text{s}$.
- Purple line (Discharge 3) describes the flow at pipe2 (bifurcation_2) that is connected to the surge tank, during the opening time of the valves $t=0$ s – $t=30$ s. This is the flow from surge tank entering the pressure shaft. It can be seen that the discharge has a negative direction. After $t=30$ s, when flow exits pressure tunnel, flow changes its direction, which describes water entering bifurcation_2 and continues to surge tank. At the time when valves are closed there is an increase of the discharge that enters bifurcation_2 from the pressure shaft. It achieves its peak at closing time of the valves $t=165$ s – 195 s. Until the pressure waves are neutralized inside the system pipeline.
- The red line is the main line in this Diagram. It is the line that describes the flow inside the surge tank.

From time $t = 0$ [s] - 165 [s], line is going down, discharge $Q = -70 \text{ [m}^3/\text{s]}$, which goes up to $Q = 0 \text{ [m}^3/\text{s]}$. This is the flow direction going from the chamber in the direction of the pressure shaft. From time $t = 90$ [s] - 165 [s], there is a flow that comes from reservoir into the pressure tunnel and enters the surge tank as well. Between the time $t = 165$ [s] - 195 [s], which is the time of closing of valves, the

flow starts to enter the chamber from pressure shaft, and that is why the line goes up in the diagram. Because the flow comes from the other direction of the pipeline. After closing of the valves, water hammer process causes pressure waves which enter the surge tank, after this moment, mass oscillation inside the chamber surface begins; this is why the red line goes up and down till the pressure inside the pipe line is stable.

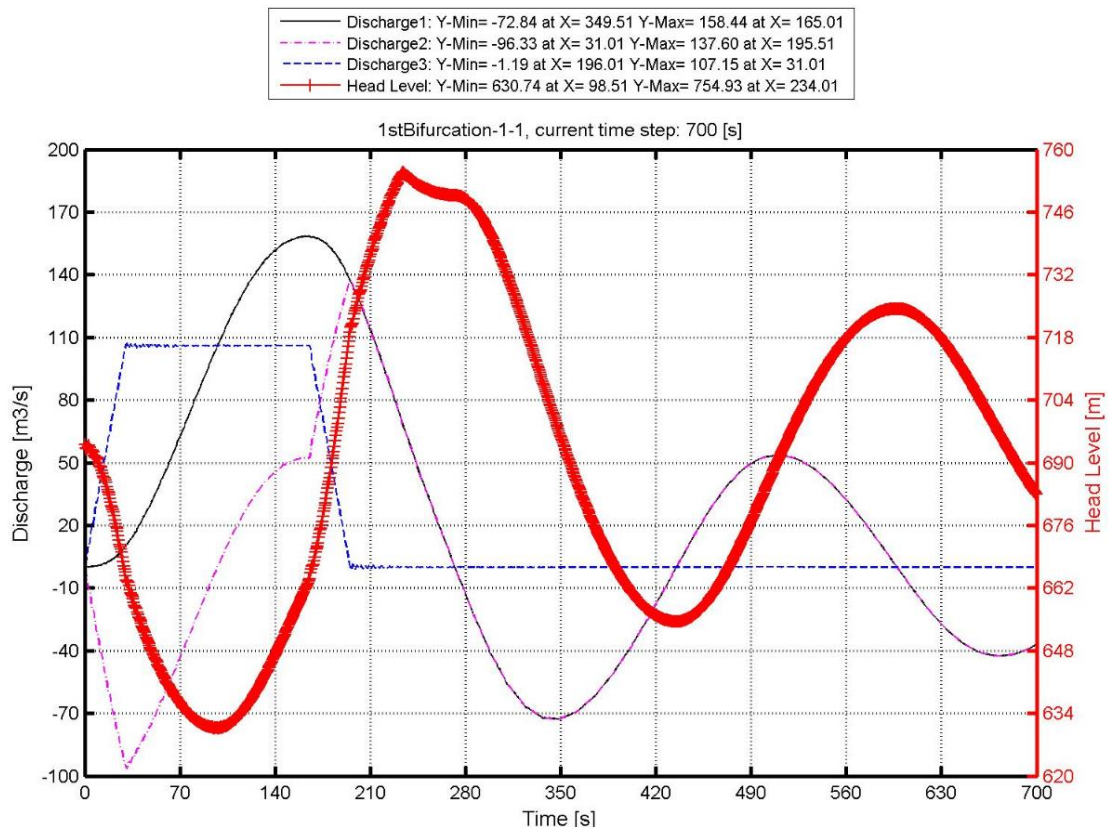


Figure 18: Evaluation mass oscillation (b)

Figure 18 shows the same mass oscillations as figure 17 but time at this figure is longer

Surge oscillations and water hammer effects are different terms but close to each other as processes inside the pipeline. These terms are often confusing since one is caused by the other. Surge is the large mass oscillation of water that sometimes takes place as a result of water hammer. As a process, when is compared to water hammer is much slower and can last for many minutes on the other side water hammer may only last for a few seconds.

An example of the difference between, these two hydrodynamic processes can be most easily seen in a hydro power plant station. Water flows down a pipeline from a large reservoir of the dam and is used to turn a turbine to work, which is connected to a generator that produces electricity. Turbines move with high speeds and require power of large quantities of water and so the velocities in the supply pipe can be very high. The demand falls and one or more of the turbines have to be shut down quickly. This is done by closing the valve on the supply pipe and this can cause water hammer. To protect a large part of the pipeline, a surge tank is located as close to the power station as possible. This is a simple shaft or a shaft with chamber arrangements with a diameter according to the Thoma criterion. The water that is no longer required for the turbine is diverted into the tank and any water hammer waves coming up from the valve closure are absorbed by the tank. Thus water hammer is confined to the pipeline between the turbine and the tank and so only this length of pipe needs to be constructed to withstand the high water hammer pressures. Gradually the tank fills with water and the flow from the reservoir slows down and eventually stops. The rushing water should not cause the tank to overflow. In such cases water may flow back and forth between the tank and the reservoir for several hours until the energy is dissipated. This slow, but large, movement of water is called a surge and although it is the result of water hammer, it is quite different in character. As seen on the diagram, this example is focused on the part of bifurcation, which is a connection between pressure tunnel-surge and tank-pressure shafts, this calculation explains more about the mass oscillation of the water that is caused by water hammer.

(Kay, 2008)

CHAPTER 5

5. Surge tank model in laboratory

The following chapter describes the calculation, which focuses on the pressure height at pressure tunnel and water hammer effect at the pressure shaft.

The surge tank model in the laboratory is composed of three main pipes connected with each other representing a model of a high-head hydropower plant. The boundary elements of the small-scale test are: a reservoir element and a surge tank element, as well as a valve representing the turbine which allow a discharge

The dimensions of pipes are:

Pipe1: $L=0.70$ [m], $D=0.40$ [m]

Pipe2: $L=2.1$ [m], $D=0.20$ [m]

Pipe3: $L=0.70$ [m], $D=0.30$ [m]

- Pipe1 is connected to Reservoir on top and on its right side is connected with Pipe2.
- Pipe2 is connected on the left side with Pipe1 and on the right side with Bifurcation. Bifurcation creates the connection between pipe2-surge tank-pipe3.
- Pipe3 is connected to Bifurcation on the top and flowmeter on the down side.

Two pressure Sensors, are installed on Pipe2 and Pipe3

- Sensor 1 is installed on Pipe 2 (Headrace tunnel), and measures the internal water pressure height
- Sensor 2 is installed at Pipe 3 (pressure shaft), and measures the pressure height (water hammer) at this pipe (pressure shaft)

For the thesis, a model at the laboratory helped, in order to understand the process of water hammer. The water hammer phenomenon was investigated by different variations of flow and closure of the surge tank connection.



Figure 19: Working lab where experiment is processed in the hydraulic laboratory

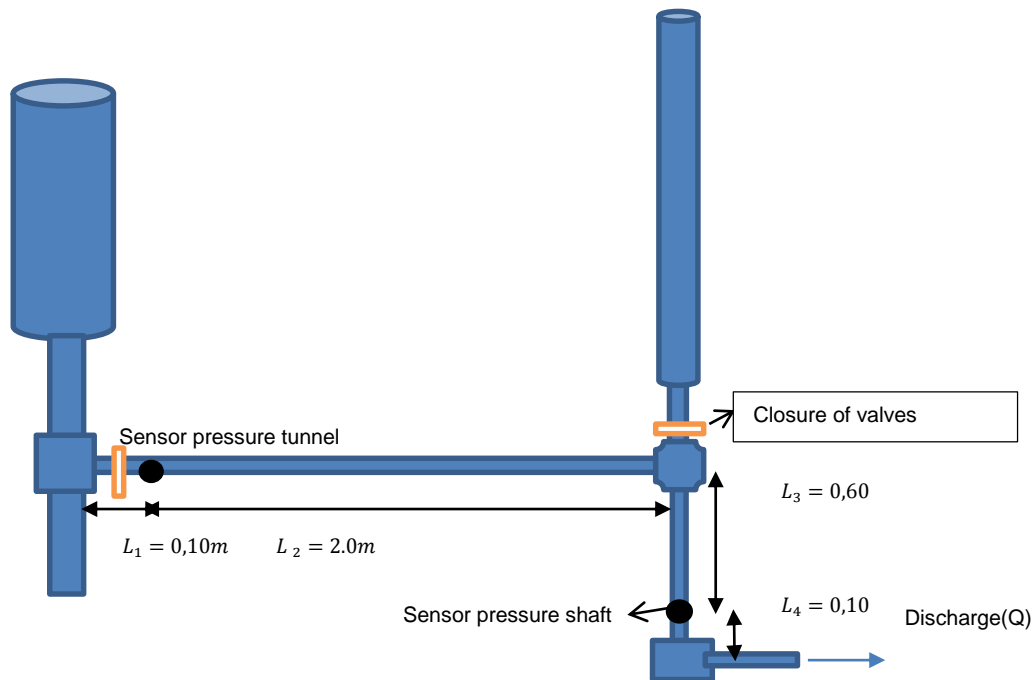


Figure 20: Scheme of the surge tank model

5.1 Pressure sensor

Pressure sensor are used to measure the pressure height at two different points of the model: Pressure tunnel (Pipe2) and pressure shaft (Pipe3).



Figure 21: Sensor

The settings of sensor are:

- Series APM-550
- Mini Pressure Transducer

- Thread M4,5,6,10,16
- Static, from “0” Hz and Dynamic
- Diaphragm :Flash mounted, S.Steel
- For aggressive Gases and Fluids
- Ranges:0-1bar to 1000bar
- Pressure ref.: Gage, Absolute
- Temperature compensation up to +220 C

CHAPTER 6

6. Measurements at the laboratory surge tank

6.1 Description of the measurement process and the evaluation of the results.

The investigation of the model at laboratory is the main part of this thesis. The model contains: pipes, surge tank, sensors, valves and a computer. The computer at laboratory reads the data from sensors which measures the pressure at the model. The pressure information is monitored by the software *Lab View®*,

- It is measured 2 or 3 times for the same Load cases of water hammer examples, with the same discharge and same closure position.
- Closure controls the entry at the surge tank. To see the impact of the pressure at the pipeline, closure position has different closure angles:
 - Closure of valve of the surge tank - positions
 - Closure of valve opened for 65°.
 - Closure of valve opened for 45°.
 - Closure of valve opened for 10°.
 - Closure of valve entirely opened.
 - Closure of valve entirely closed.
- Different discharges at the pipeline.

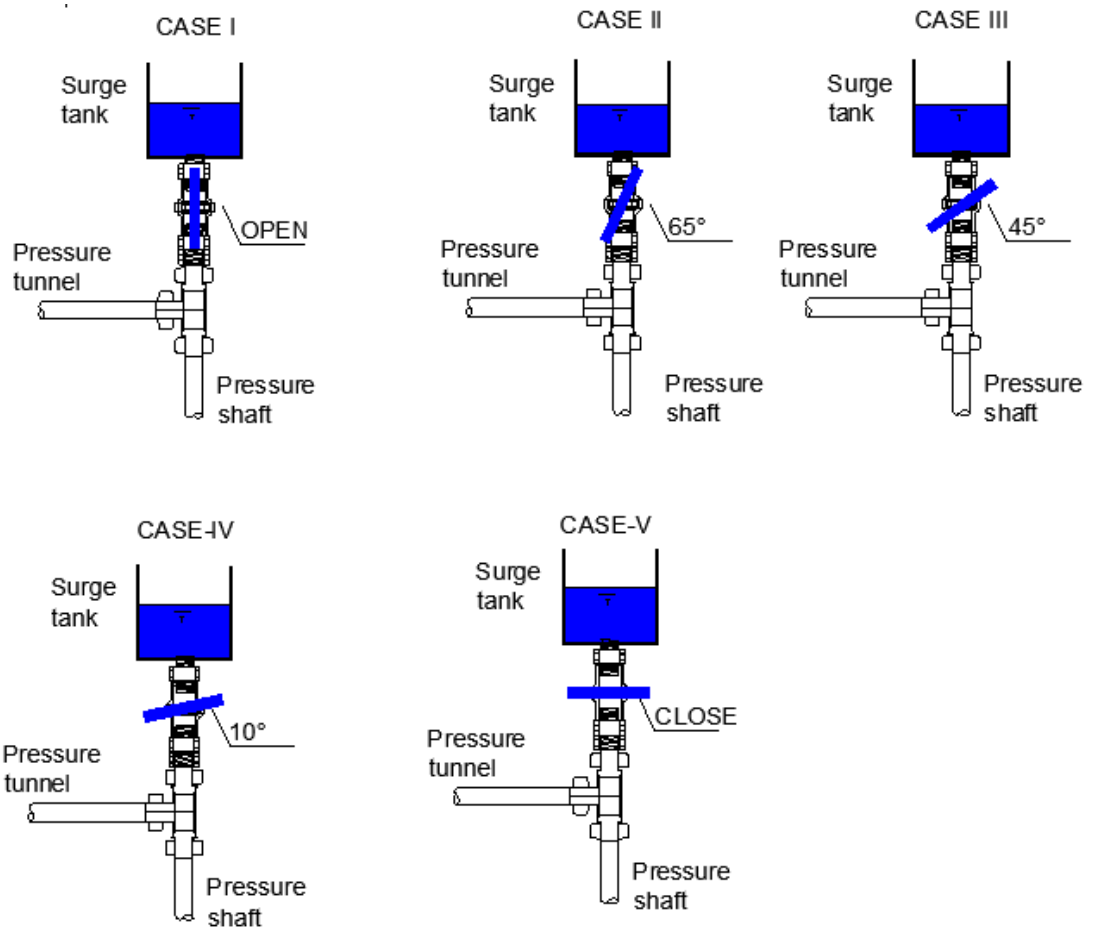


Figure 22: Closure of the valve - positions

Load Cases	Pressure tunnel ai0 [mm]		Pressure shaft ai1 [mm]	
	max	min	Max	min
Load case q= 0,5with10°_Ws1	24463.6	8402.34	86331.68	-10696.43
Load case q= 0,5with10°_Ws2	26408.12	8603.25	90388.85	-12252.7
Load case q=0.5with45°_Ws1	19597.23	8398.92	79520.28	-7764.85
Load case q=0.5with45°_Ws2	17564.18	7731.45	72549.63	-6049.33
Load case q=0.5with45°_Ws3	17444.93	7984.91	73508.72	-65451.71
Load case q=0.5with65°_Ws2	17240.67	8405.73	80866.37	-11058.63
Load case q=0.5with65°_Ws3	17639,1	8906.33	77964	-11170.55
Load case q=0.10with10°_Ws1	66429,2	1026.13	20237.17	09.26
Load case q=0.10with10°_Ws2	62717.3	1264.51	20063.45	-367.13
Load case q=0.10with45°_Ws2	5594.04	2418.96	20436.23	-3917.6
Load case q=0.10with45°_Ws3	5546.37	2459.82	19817.34	-3841.6
Load case q=0.10with65°_Ws3	5423.77	2347.44	19621.9	-5850.28
Load case q=0.25with45°_Ws1	7412.55	3644.92	38829.2	-4456.87
Load case q=0.25with45°_Ws2	7585.31	-3696	39122.35	-4167.33
Load case q=0.25with45°_Ws3	7347.85	3610.86	41984.06	-4189.05
Load case q=0.25closed_Ws1	12544.56	4680.17	46777.04	-8188.3

Load case q=0.25closed_Ws2	12813.59	4469.04	-	47580.51	-8061.63
Load case q=0.25closed_Ws3	12973.64	4387.31	-	47276.49	-8235.35
Load case q=0.25with10°_Ws1	13017.91	-4717.6	-	49719.48	-4746.41
Load case q=0.25with10°_Ws2	12742.07	4608.66	-	48467.22	-4239.72
Load case q=0.25with10°_Ws3	12942.99	4741.47	-	50179.12	-4594.4
Load case q=0.25with65°_Ws1	9908.74	-4632.5	-	46910.95	-9129.31
Load case q=0.25with65°_Ws2	9500.09	4847.04	-	45651.46	-9925.54
Load case q=0.25with65°_Ws3	9585.23	4792.55	-	46787.9	-9082.26
Load case q=0.25full opened_Ws1	6666.76	4707.42	-	41760.78	-7030.15
Load case q=0.25full opened_Ws2	12820.4	4526.93	-	47804.9	-8210.02
Load case q=0.25full opened_Ws3	12667.15	4659.74	-	48069.11	-8220.88
Load case q=0.45closed_Ws1	20240.86	5906.13	-	75256.82	-8926.63
Load case q=0.45closed_Ws2	21630.28	6583.82	-	76136.29	-8662.42

Table 1: Results from small-scale investigation at the laboratory

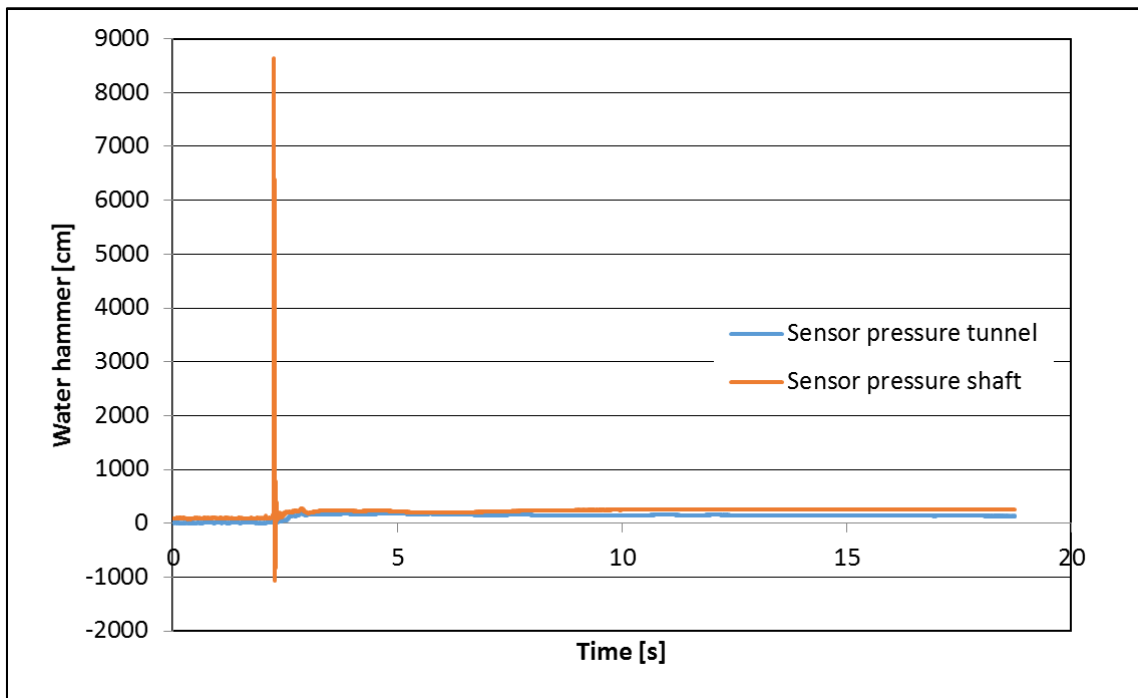
6.2 Evaluation of the results

This chapter describes the Evaluation of the results for different load cases:

- Load case, discharge $Q=0.5$ [l/s] with surge tank, closure of valve opened for 10° angle.

The greater the discharge is, the higher the pressure inside the pipelines. First measurement of the model started with discharge $Q=0.5$ [l/s] which was the Load case with the highest value of discharge, and it showed the highest pressure inside the pipelines.

6.2.1 Surge tank, closure of valve opened for 10°

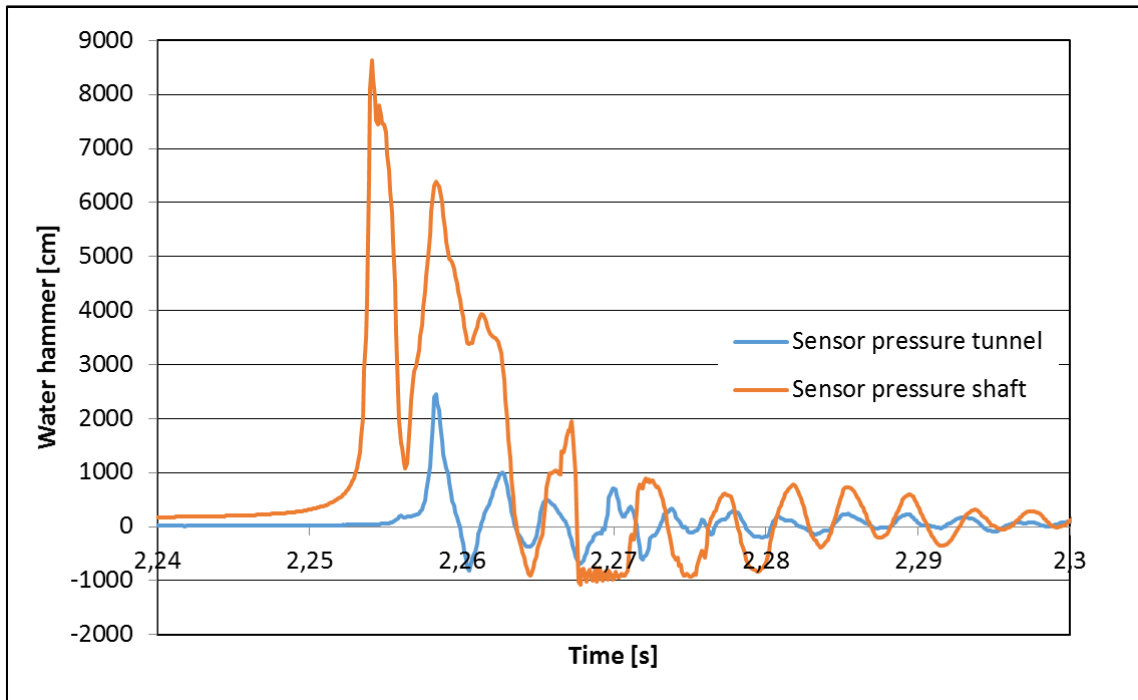


Graph 1: Load case with discharge $Q=0.5$ [l/s] and closure position of the valve, opened for 10° angle.

Graph 1 describes the amplitude of the pressure at two different points in the pipelines over a time span of 18 seconds. The blue line shows the value of the pressure height at pressure tunnel, while the orange line indicates the value of the pressure at “pressure shaft” (water hammer).

The time of the measurement is $t=18$ [s]. Thus, the time between $t=0$ [s] and 5 [s] shows how water hammer achieves its peak, due to a quick closure of the valve. This represents as a shut-off of the turbine, however, meaning that closing times of the valves are between $t=0$ [s] to 2 [s].

6.2.2 Details of line graphic, closure of valve opened for 10° .



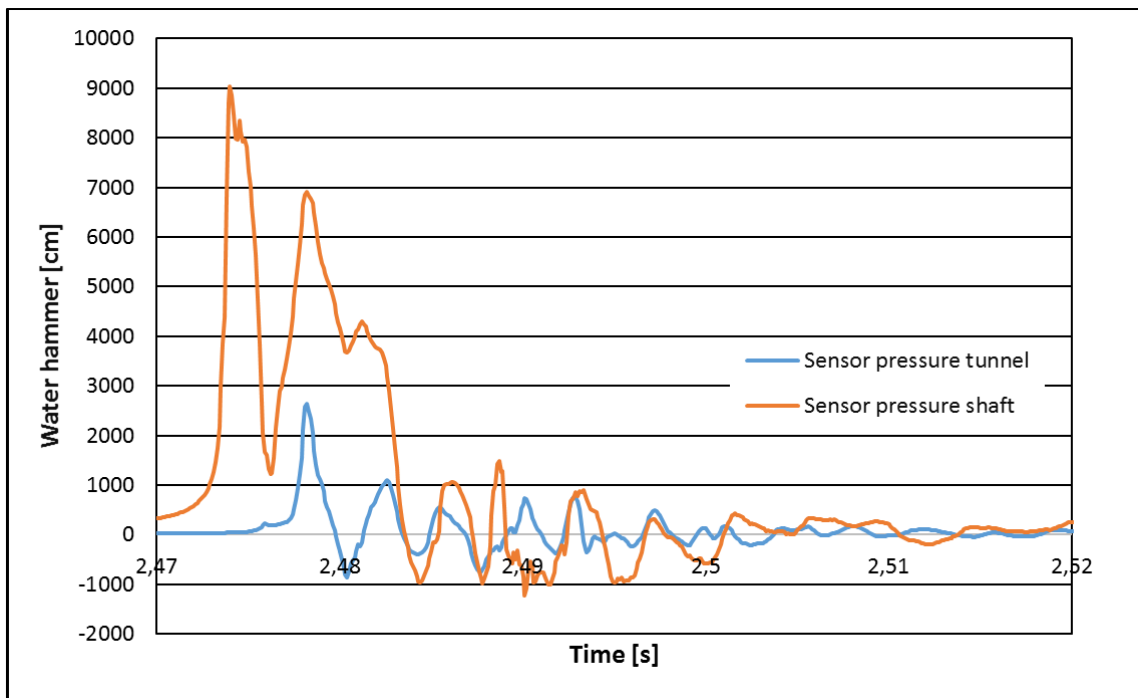
Graph 2: Load case with discharge $Q=0.5$ [l/s] and closure position of the valve, opened for 10° angle.

Graph 2 shows the details of the line graph. The orange line represents the development of the water hammer at pressure shaft part before the turbines. It is exactly at $t=2.25$ [s], when the pressure height (water hammer) begins to rise to its peak, $h=86331.68$ [mm], and this is the moment when the valves start closing. At time $t=2.3$ [s] water hammer achieves stability, which means that the process of “water hammer” lasts from $t=2.25$ [s] to 2.30 [s], or approximately 0.05 [s]. The blue line indicates the development of the pressure at the “pressure tunnel”. At this part of the pipeline, pressure height is $h=24463.6$ [mm], which is smaller than pressure height at “pressure shaft”, $h=86331.68$ [mm] $>$ $h=24463.6$ [mm]. However, pressure height achieves its peak 0.01 second later than “pressure shaft”.

Factors that impact a higher water hammer at pressure shaft are:

- Pressure shaft - connected to the valves.
- Surge tank - has a smaller impact on the pressure shaft compared to pressure tunnel.

6.2.3 2nd Detail of line graphic, closure of valve opened for 10°

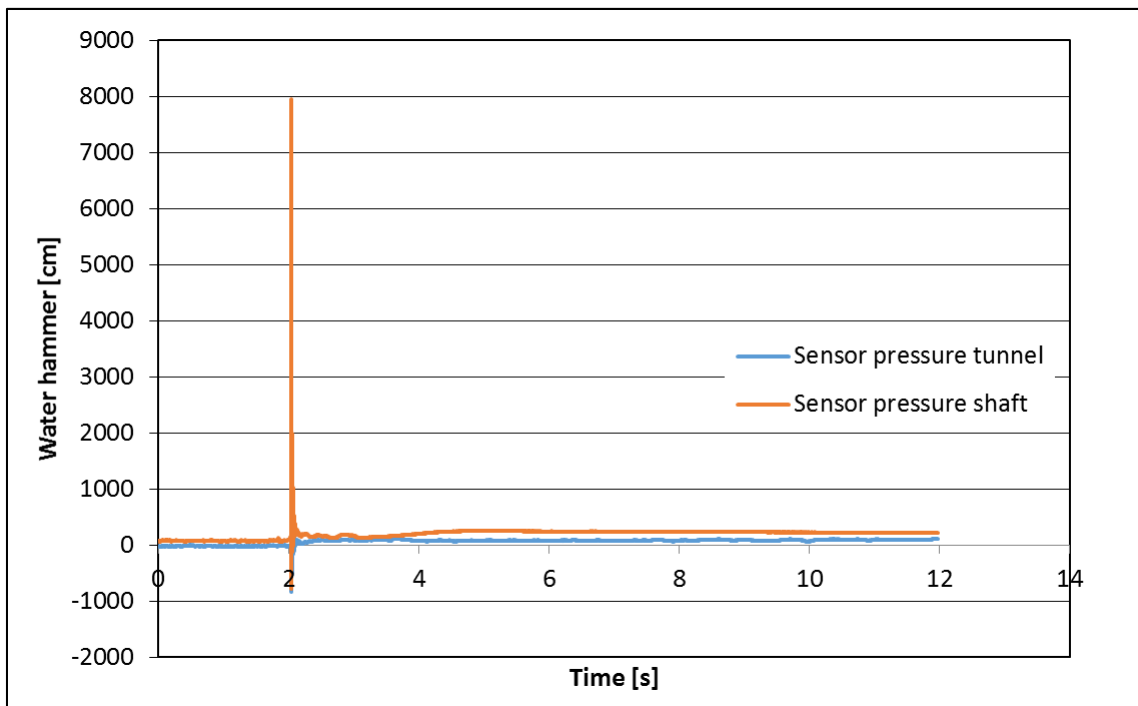


Graph 3: Load case with discharge $Q=0.5$ [l/s] and closure position of the valve, opened for 10° angle.

In the Graph 3 there is shown, a detail of line graphic with same “Load case” and with some differences compare to the Graph 2. Following the orange line, it shows that there are some differences at water hammer height, achieving a distance of $h=90388.85$ [mm]. At this “Load case” on the second measurement, water hammer is higher compare to Graph 2 first measurement $h=86331.68$ [mm] < $h= 90388.85$ [mm]. Following the blue line, the pressure height at the pressure tunnel achieves its peak at $h=26408.128$ [mm], which again is higher compared to Graph 2 $h=26408.128$ [mm] > $h=24463.6$ [mm].

These changes in the graph overall are summarized because of the discharge level being higher $Q=0.55$ [l/s] and closing time of valves being smaller. The reason why the discharge is higher is because closing time of the valves at Graph 2 begins at time $t=2.24$ [s] compare to Graph 3, where closing time of the valves begins at time $t=2.45$ [s]. That means that there is more water inside the pipelines and the pressure is higher, meaning the pressure shaft and the pressure tunnel.

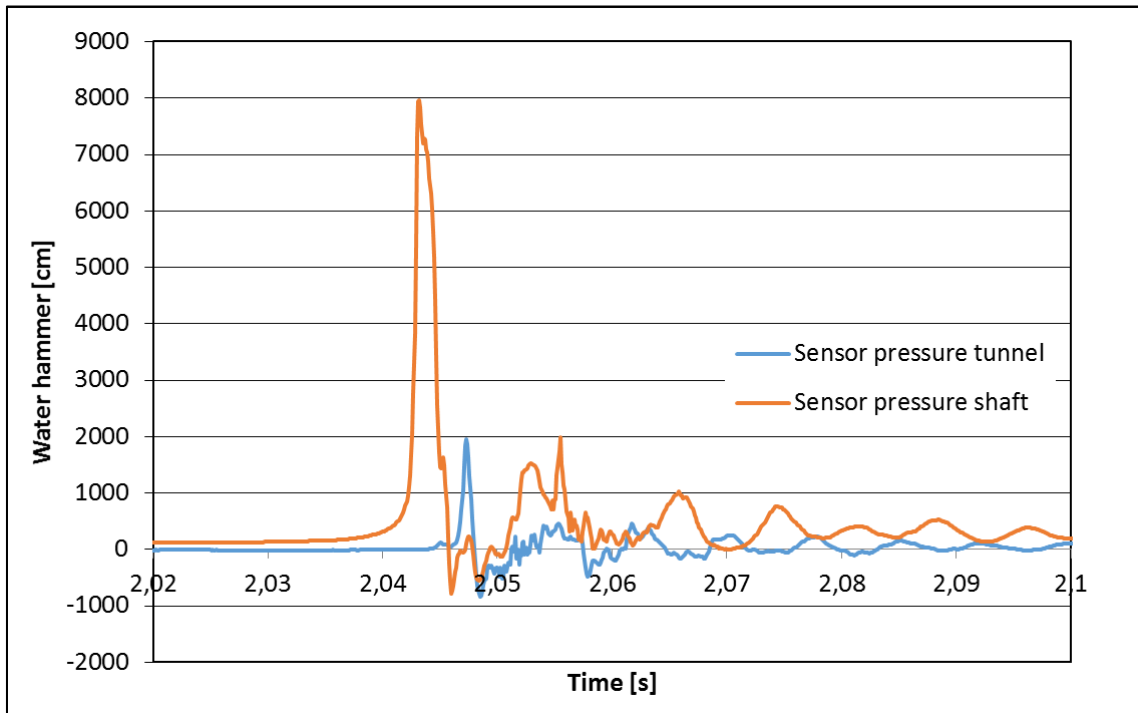
6.2.4 Surge tank, closure of the valve opened for 45° angle



Graph 4: Load case, with discharge $Q=0.5$ [l/s] and closure position of the valve, opened for 45° angle.

Graph 4 presents more than one Load cases in the same surface. While discharge (Q) is equal to 0.5 [l/s], which is the same but closed to the surge tank with different angle 45° . That means that, the entry at the surge tank is opened more and accepts more water during the water hammer. Furthermore, the pressure at the pipelines is supposed to be lower.

6.2.5 Detail of line graphic, closure of valve opened for 45°

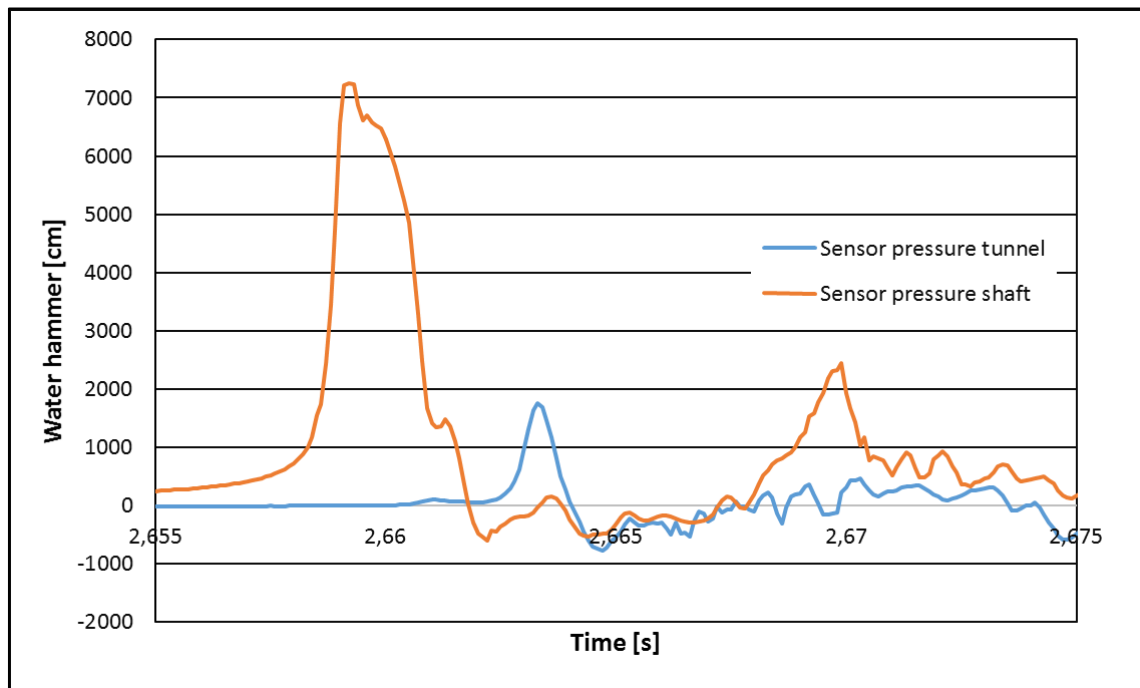


Graph 5: Load case, with discharge $Q=0.5$ [l/s] and closure position of the valve, opened for 45° angle.

Graph 5, shows the detailed version of the load case with same discharge and different closure angles. Following the orange line, there is an impact of closure of valve, in front of the surge tank. This detailed line shows, that there is also an impact of the surge tank cause at this case surge tank accepts more water and, pressure height inside the pipeline is lower. There is also shown that, water hammer at pressure shaft is $h=79520.28$ [mm] compared to the Load case with closure of valve opened for 10° showed in Graph 3 which is $h=90388.85$ [mm]. (Water hammer is lower compared to $h=79520.28$ [mm] < $h=90388.85$ [mm]). Following the blue line, there is seen an impact at the peak of the pressure height inside the pressure tunnel $h=19597.23$ [mm]). Compared to the Load case of Graph 3, where water hammer is $h=19597.23$ [mm] < $h=26408.128$ [mm].

The closing position of surge tank, when opened at Load case 45°, has an impact to lower the pressure inside the pipelines, compared to Load case 10° where the entry of the surge tank is almost closed.

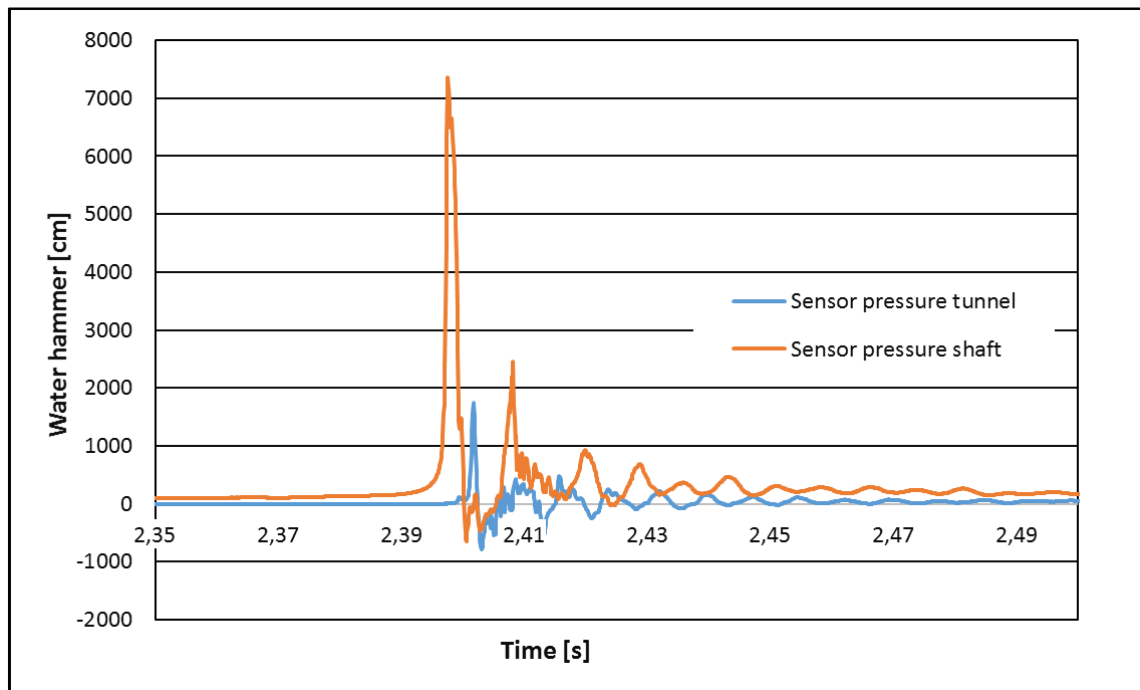
6.2.6 2nd detail of line graphic, closure of valve opened for 45°



Graph 6: Load case, with discharge $Q=0.5$ [l/s] and closure position of the valve, opened for 45° angle.

Graph 6 shows the Load case with the same discharge and same closure position as the Load case above. Pressure height at pressure tunnel part is $h=17564.188$ [mm], while the pressure height at pressure shaft is $h=72549.631$ [mm].

Load cases with the same discharge and the same closure position, have smaller differences with each other because of the small differences at the discharge points and valve closing times.

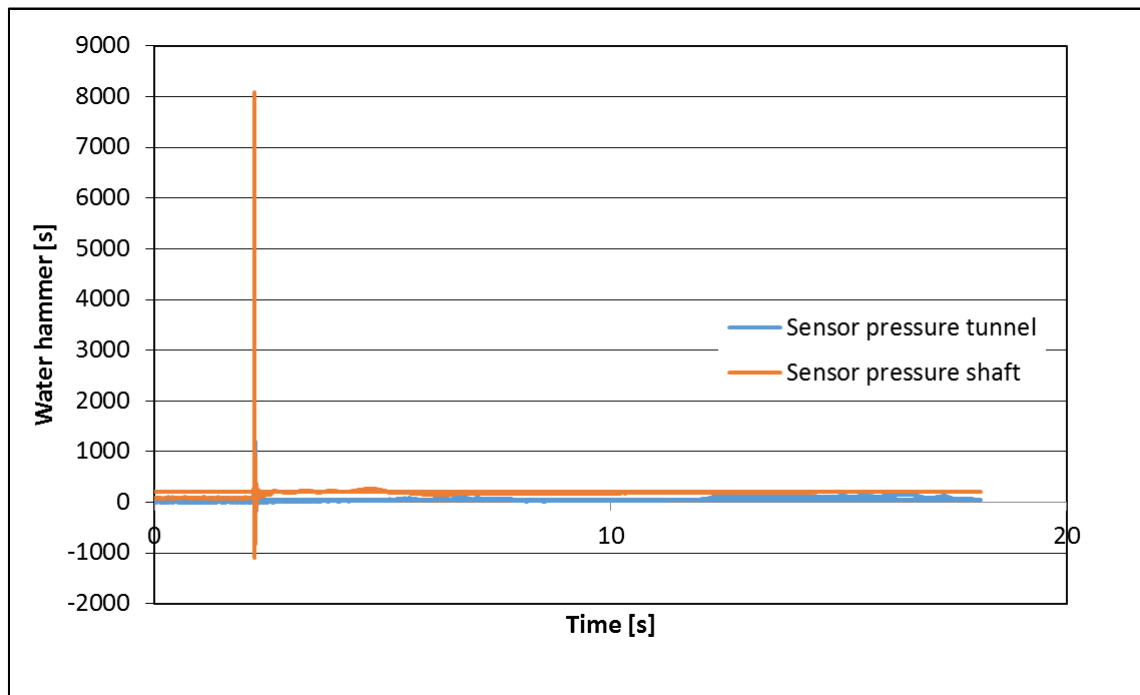
6.2.7 3rd detail of line graphic, closure of valve opened for 45° 

Graph 7: Load case, with discharge $Q=0.5$ [l/s] and closure position of the valve, opened for 45° angle.

Graph 7 shows the Load case with the same discharge $Q=0.5$ [l/s] and closure position, closure of valve opened for 45° . Pressure height at pressure tunnel part is equal to 17444.93 [mm], while pressure height at pressure shaft is equal to 73508.72 [mm].

Taking in to the consideration that, Graph 6 and Graph 7 pressure tunnel 17564.188 [mm] vs 17444.93 [mm], and pressure shaft 72549.631 [mm] vs 73508.72 [mm] values, we can conclude that there are no big differences in general.

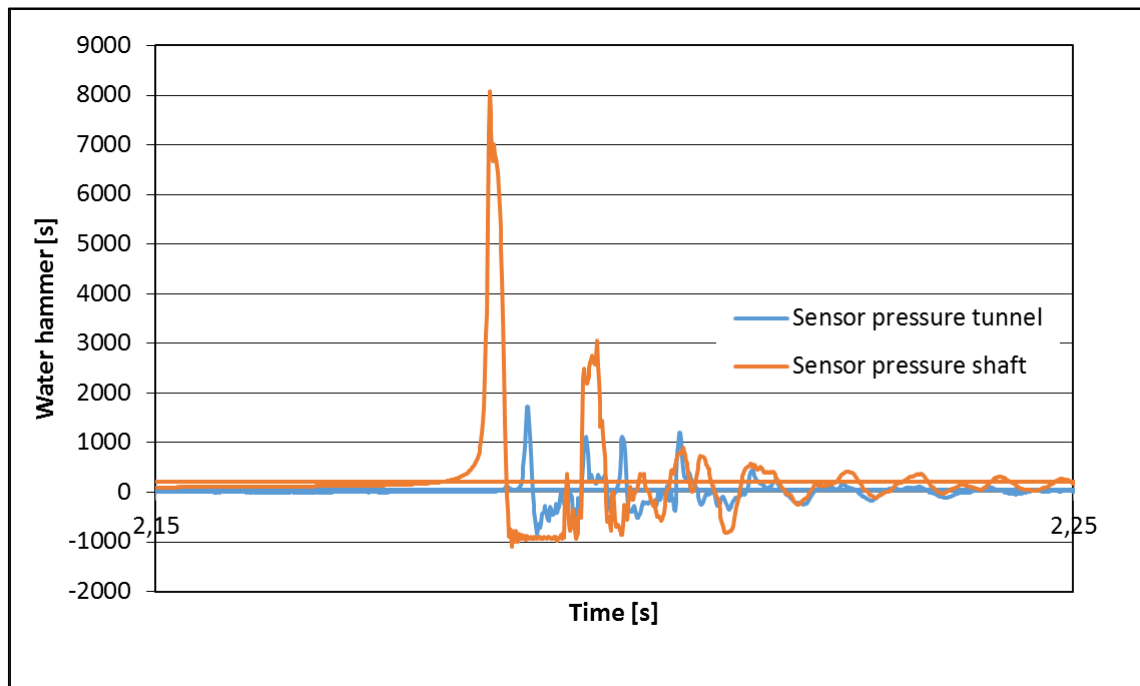
6.2.8 Surge tank, closure of the valve opened for 65°



Graph 8: Load case, with discharge $Q=0.5$ [l/s] and closure position of the valve, opened for 65° angle.

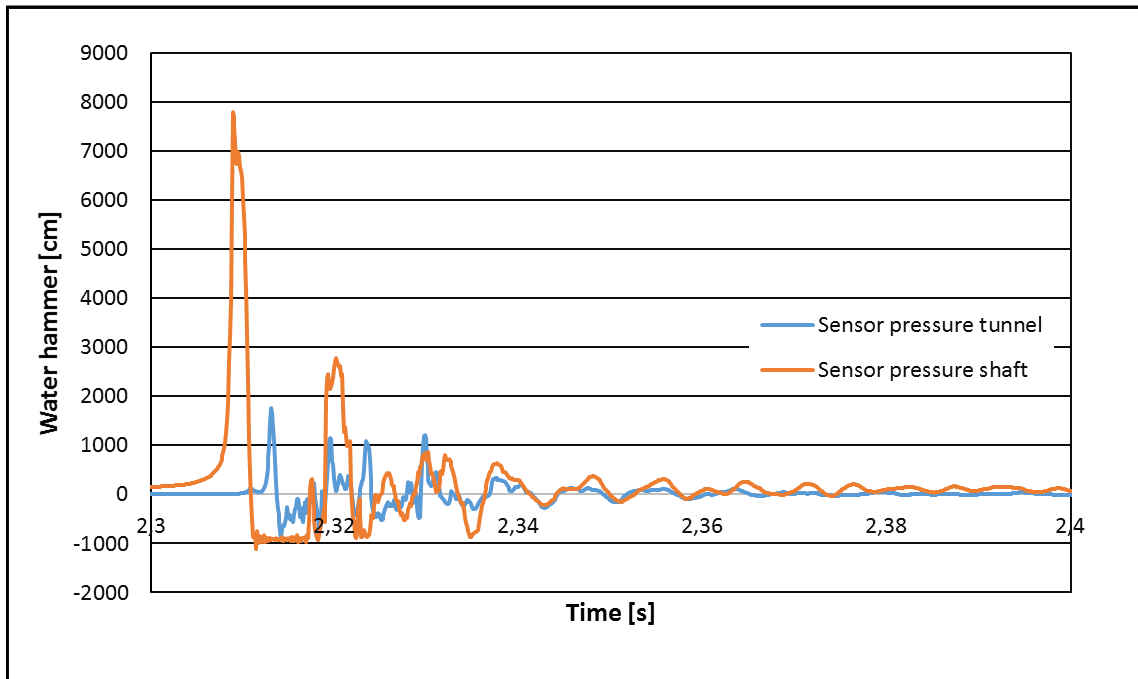
Graph 8 is the Load case with discharge $Q=0.5$ l/s and surge tank with closure position opened for 65° angle. This graph shows that the closure is almost entirely opened, while the pressure height at pressure tunnel is $h=17240.67$ [mm], and water hammer at pressure shaft is $h=80866.65$ [mm].

6.2.9 Detail of line graphic, closure of valve opened for 65°



Graph 9: Load case, with discharge $Q=0.5$ [l/s] and closure position of the valve, opened for 65° angle.

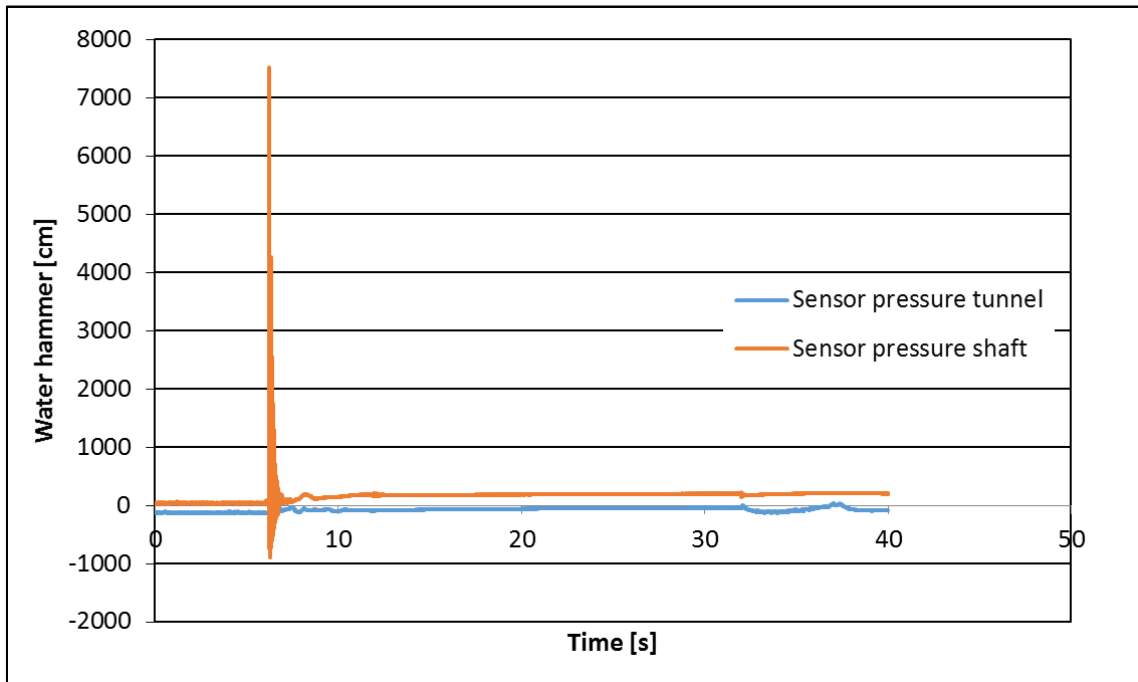
Differences between Load cases 45° and Load case 65° are small. The pressure height at the pressure shaft and pressure tunnel, have the values which are close to each other, however, the differences are visible at the peaks of pressure heights.

6.2.10 2nd detail of line graphic, closure of valve opened for 65°

Graph 10: Load case, with discharge $Q=0.5$ [l/s] and closure position of the valve, opened for 65° angle.

Graph 10 shows the Load case with discharge $Q=0.5$ [l/s] and surge tank with closure position opened for 65° angle. Pressure height at pressure tunnel is $h=17639.1$ [mm] and water hammer at pressure shaft is $h=77964$ [mm].

6.2.11 Surge tank, closure of valve entirely closed



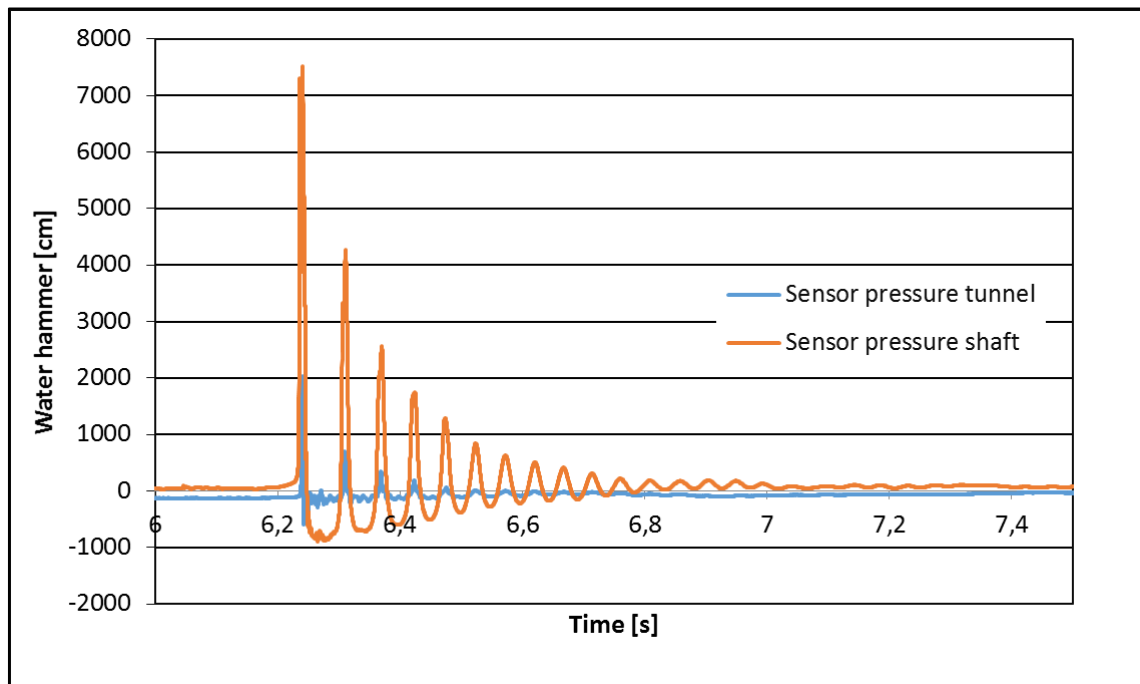
Graph 11: Load case, with discharge $Q=0.4$ [l/s], closure position of the valve, entirely closed.

Graph 11 which is about the Load case with discharge $Q=0.4$ [l/s] and surge tank closed, shows that pressure height at pressure tunnel is $h=20240.86$ [mm] and pressure height at pressure shaft is $h=75256.82$ [mm]. During these circumstances, the surge tank has an impact in the pipeline, and it can be seen in details in Graph 11.

The detailed graph is represented according to the values of the pressure height at pressure tunnel and water hammer at pressure shaft. At the pressure shaft there are no differences compared to Load cases where the surge tank was partly opened, however, there is an impact at the pressure tunnel. On this Load case, pressure height at pressure tunnel is the highest compared to the other values above - $h=20240.86$ [mm] > $h=17639.1$ [mm]

Assumption: According to the values of the water hammer at pressure shaft and pressure height at pressure tunnel, surge tank is more effective at pressure tunnel than pressure shaft.

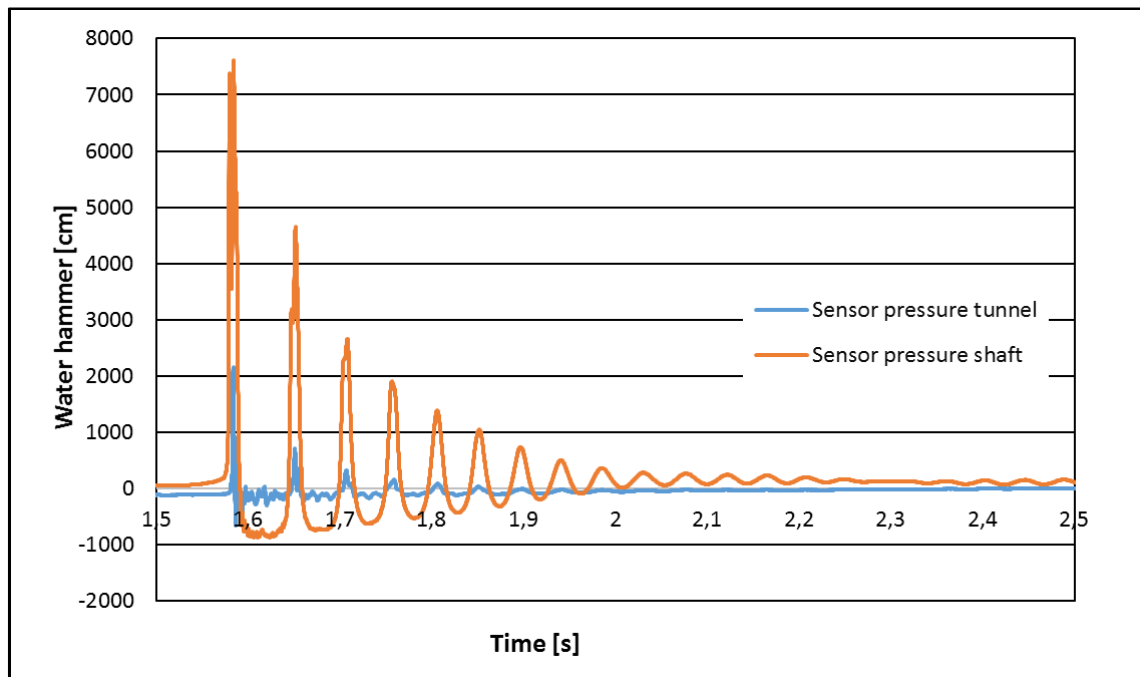
6.2.12 Details of line graphic, closure of valve entirely closed



Graph 12: Load case, with discharge $Q=0.4$ [l/s], closure position of the valve, entirely closed

In Graph 12, there are seen two color lines. The orange line shows the water hammer peak which is $h=75256.82$ [mm]. This process achieves its stability slower, compared to Load cases with surge tank partly opened. It also indicated how the water hammer lasts longer when the surge tank is closed.

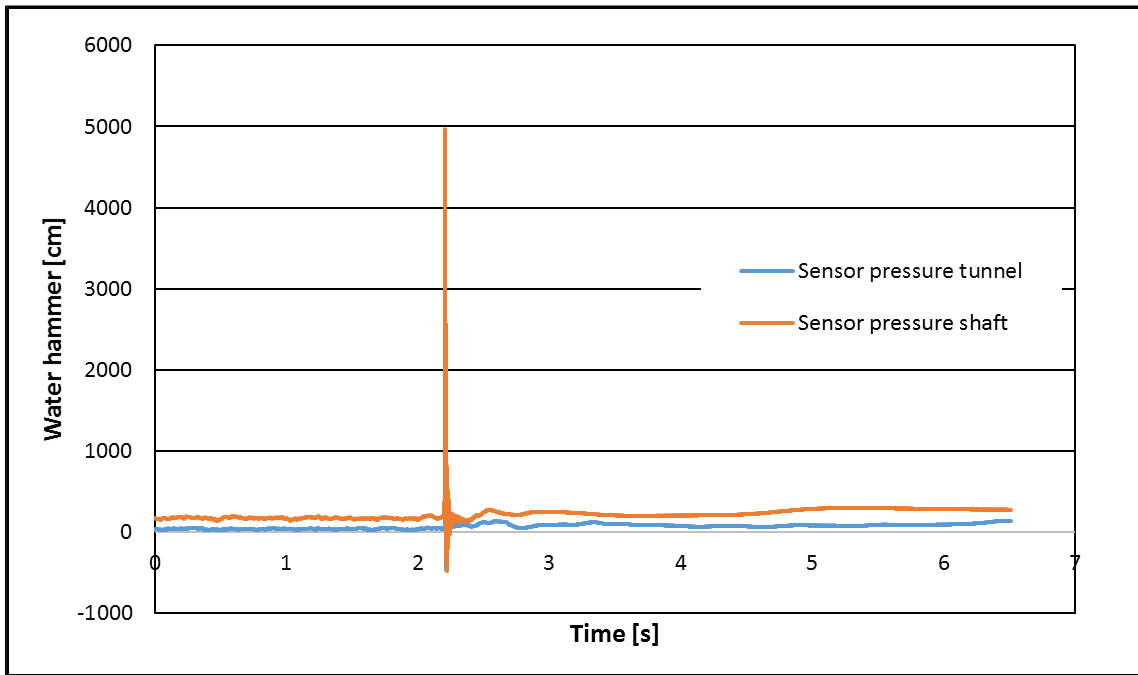
Assumption: Surge tank has no impact at water hammer height, but it has an effect at this phenomenon to achieve stability.

6.2.13 2nd detail of line graphic, closure of valve entirely closed

Graph 13: Load case, with discharge $Q=0.4$ [l/s], closure position of the valve, entirely closed.

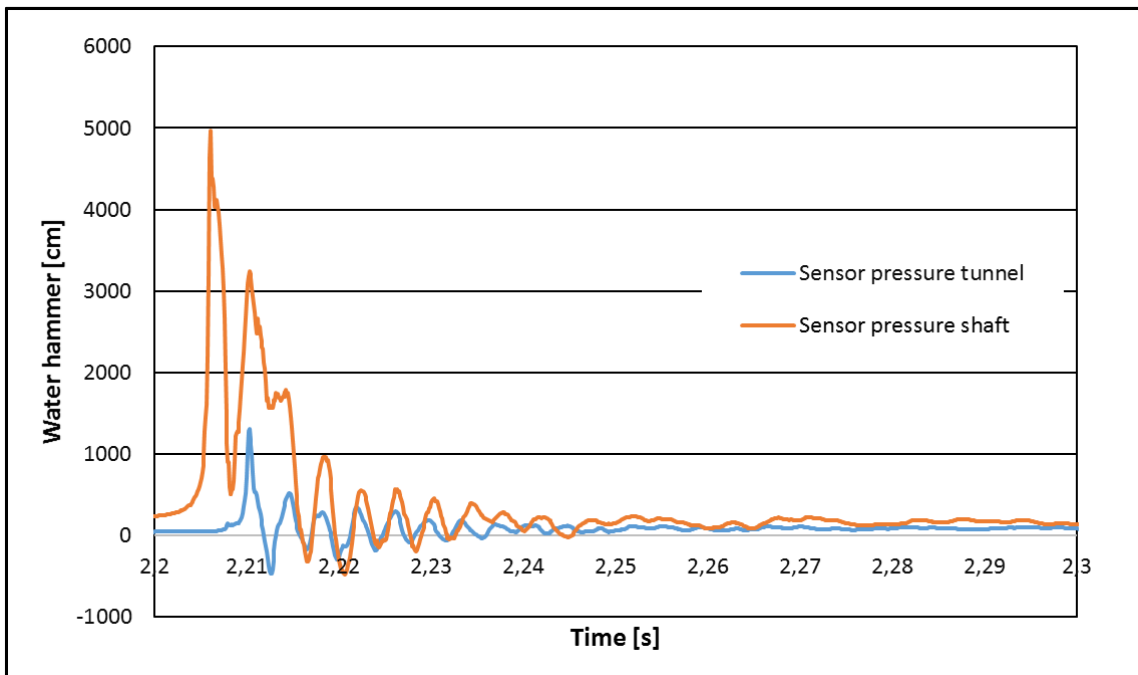
The current graph shows the second measurement of Load case with the same discharge $Q=0.4$ [l/s], and closed surge tank. At this case the value of pressure height at pressure tunnel is equal to $h=21630.28$ [mm], and pressure height at pressure shaft (water hammer) equal to $h=76136.29$ [mm]. The development of process of pressure inside the pipelines is similar with the previous Load case.

6.2.14 Surge tank, closure of valve opened for 10°



Graph 14: Load case, with discharge $Q=0.25$ [l/s], and closure position of the valve, opened for 10° angle.

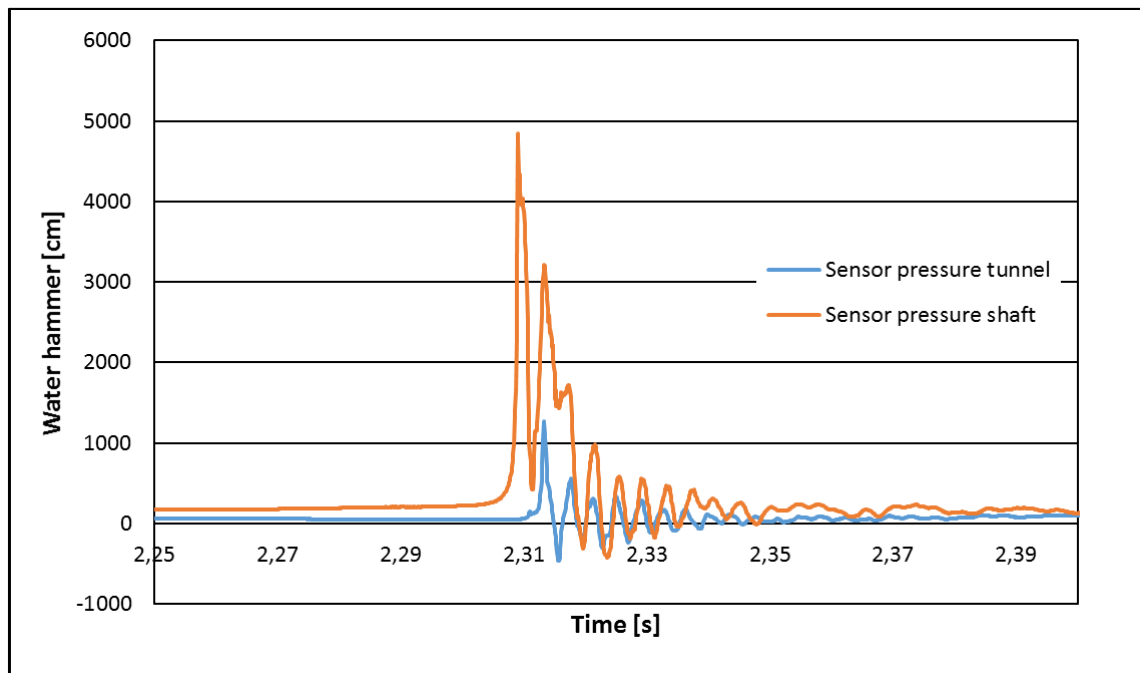
6.2.15 Detail of line graphic, closure of valve opened for 10°



Graph 15: Load case, with discharge $Q=0.25$ [l/s] and closure position of the valve, opened for 10° angle.

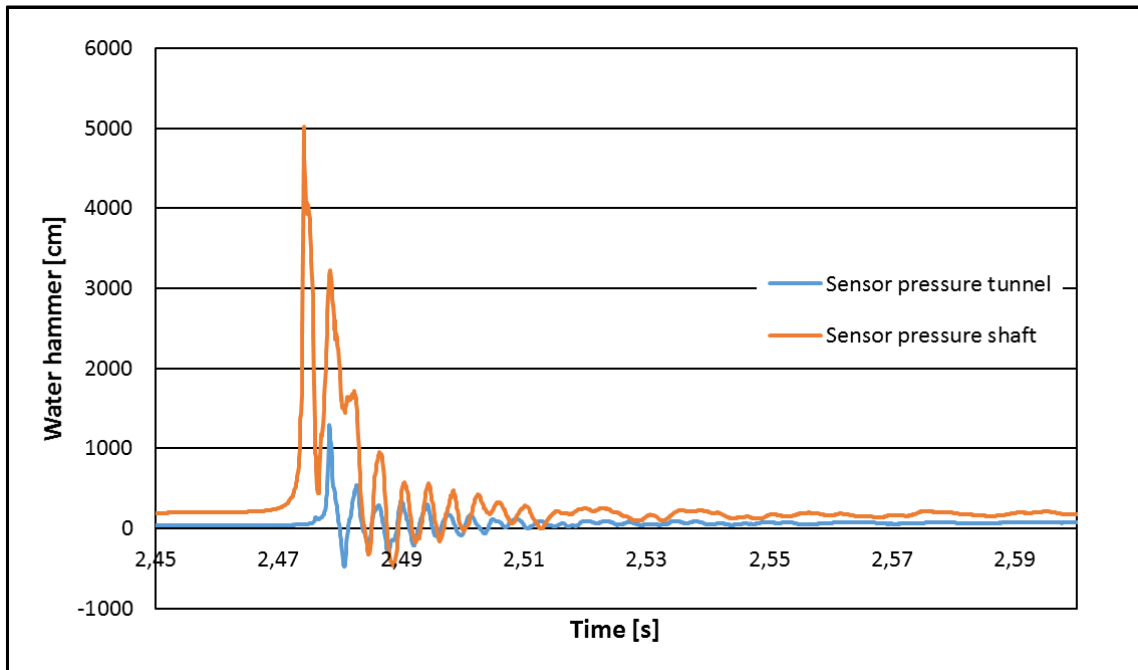
Graph 15 describes the Load case with a discharge equal to $Q=0.25$ [l/s]. This graph indicated the discharge that is lower compared to other Load cases (Graph 1-13), and the closure position (Surge tank opened 10° angle). Pressure height at pressure tunnel is $h=13017.91$ [mm] and water hammer at pressure shaft is $h=49719.48$ [mm]. With a lower discharge inside the pipelines, pressure values decrease inside the pipeline.

6.2.16 2nd detail of line graphic, closure of valve opened for 10°



Graph 16: Load case, with discharge $Q=0.25$ [l/s] and closure position of the valve, opened for 10° angle.

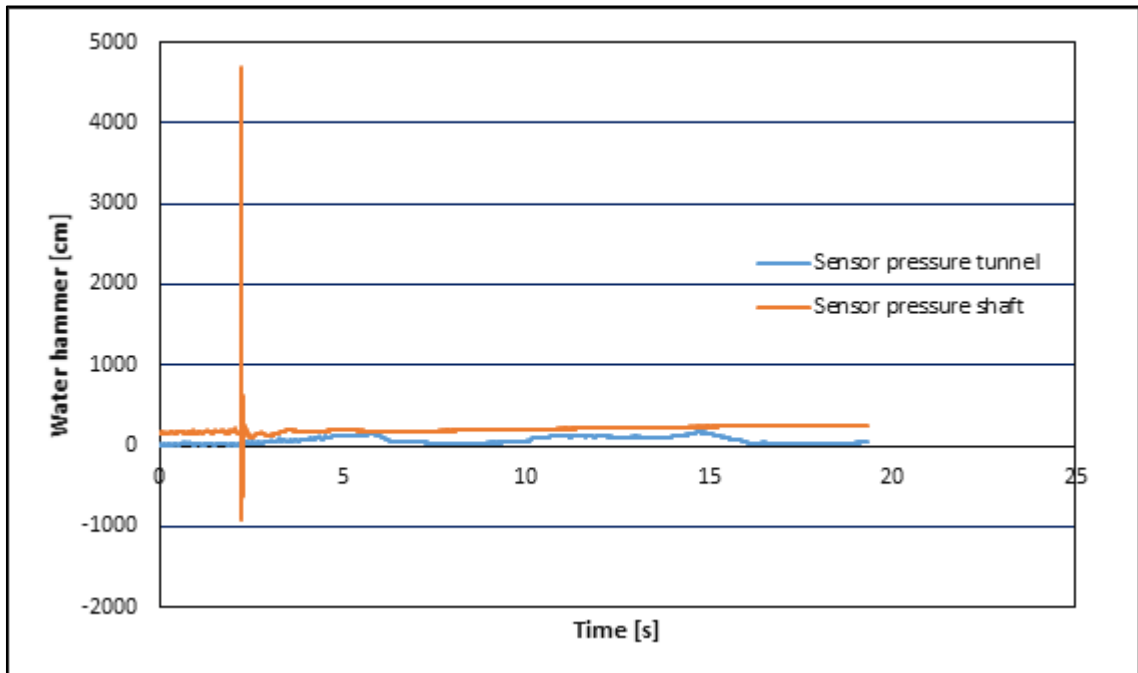
Furthermore, Graph 16 shows the second measurement on the same Load case with same discharge and same closure position (Surge tank opened 10° angle). In this phase the pressure height at pressure tunnel is $h=12742.07$ [mm] while the water hammer at pressure shaft is $h=48467.22$ [mm].

6.2.17 3rd detail of line graph, closure of valve opened for 10°

Graph 17: Load case, with discharge $Q=0.25$ [l/s] and closure position of the valve, opened for 10° angle.

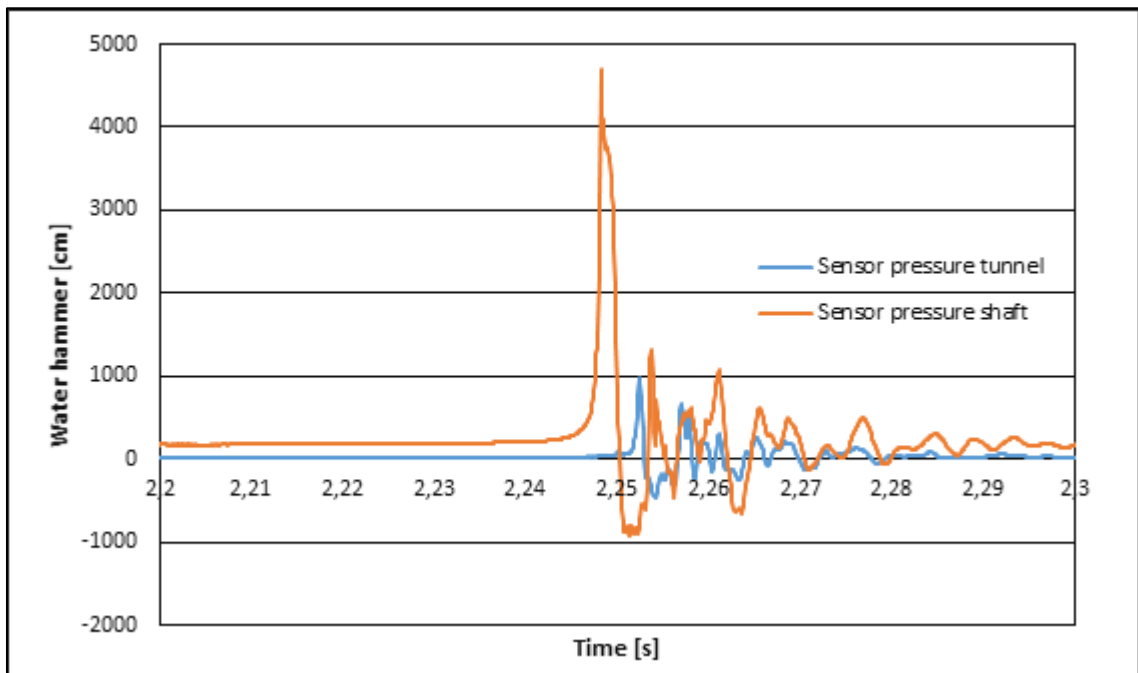
Graph 17 shows the third measurement at the same Load case with same discharge and same closure position (Surge tank opened 10° angle). Pressure height at pressure tunnel is $h=12942.99$ [mm] and water hammer at pressure shaft is $h=50179.12$ [mm].

6.2.18 Surge tank, closure of valve opened for 65°



Graph 18: Load case with discharge $Q=0.25$ [l/s] and closure position of the valve, opened for 65° angle.

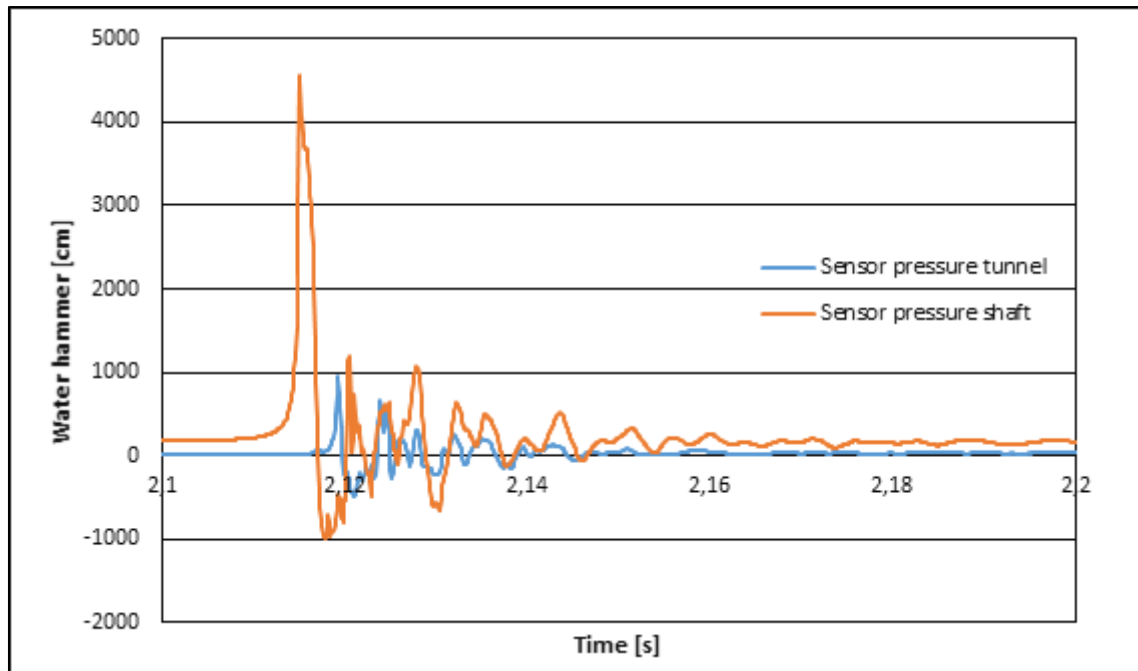
6.2.19 Detail of line graphic, closure of valve opened for 65°



Graph 19: Load case with discharge $Q=0.25$ [l/s] and closure position of the valve, opened for 65° angle.

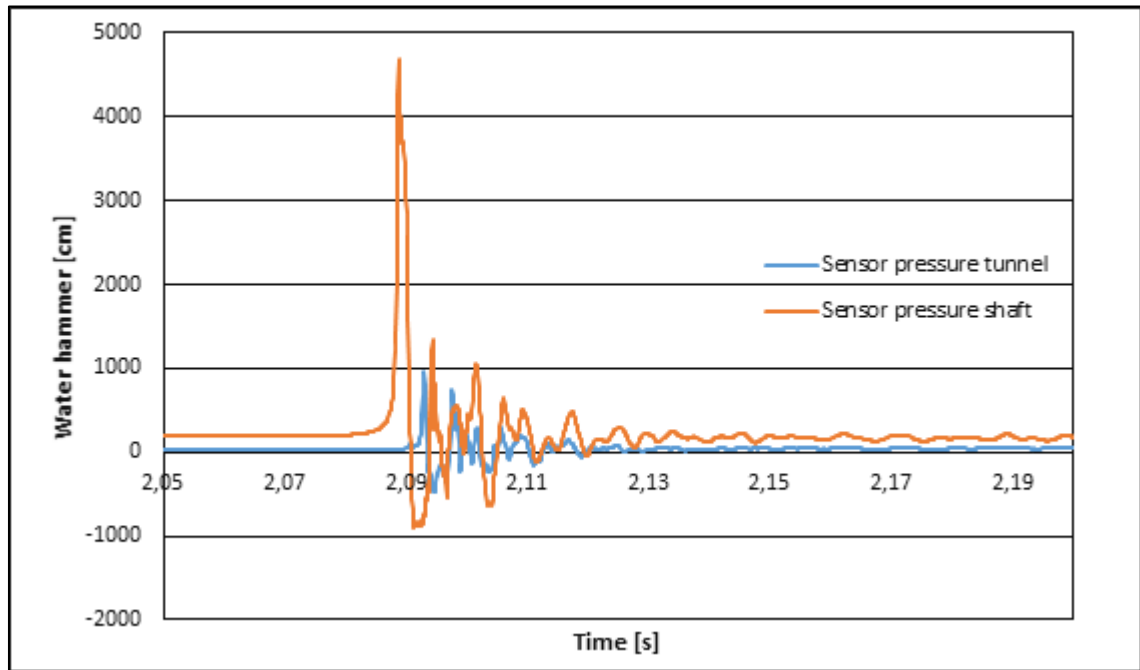
Graph 19 shows the Load case with discharge $Q=0.25$ [l/s] and closure position (Surge tank opened 65° angle). Here the pressure height at pressure tunnel is $h=9908.78$ [mm] and the water hammer at pressure shaft is $h=46910.95$ [mm].

6.2.20 2nd detail of line graphic, closure of valve opened for 65°



Graph 20: Load case with discharge $Q=0.25$ [l/s] and closure position of the valve, opened for 65° angle.

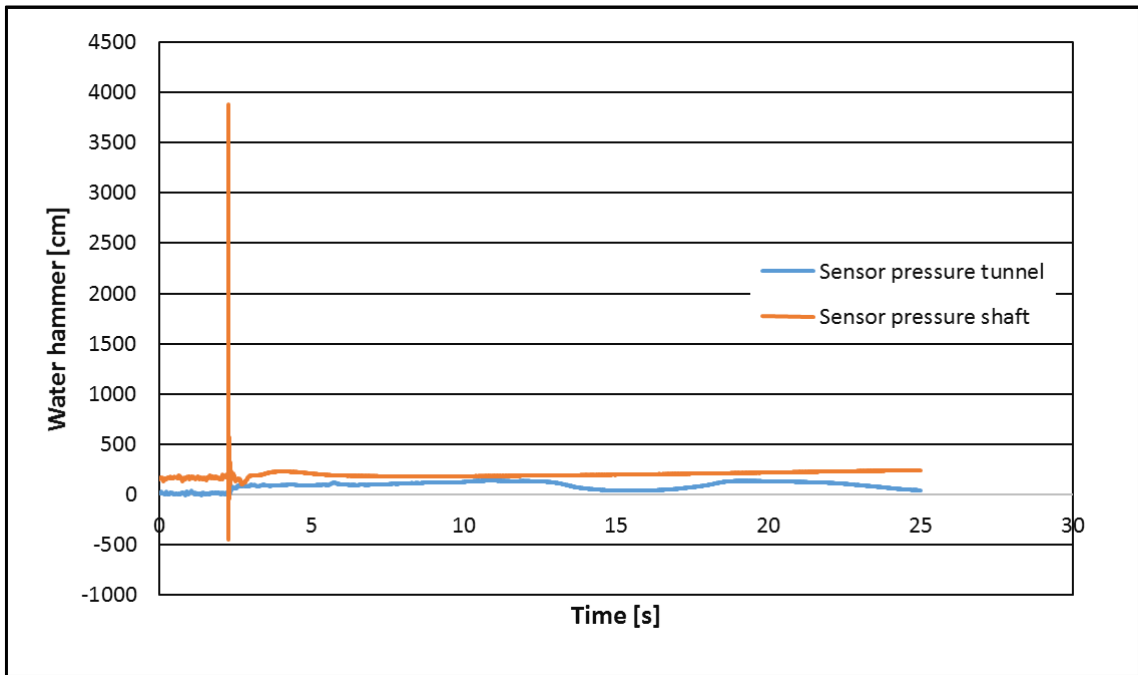
Graph 20 shows the second measurement on the same Load case with same discharge and same closure position (Surge tank opened 65° angle). Pressure height at pressure tunnel is $h=9500.09$ [mm] and water hammer at pressure shaft is $h=45651.46$ [mm].

6.2.21 3rd detail of line graph, closure of valve opened for 65°

Graph 21: Load case with discharge $Q=0.25$ [l/s] and closure position of the valve, opened for 65° angle.

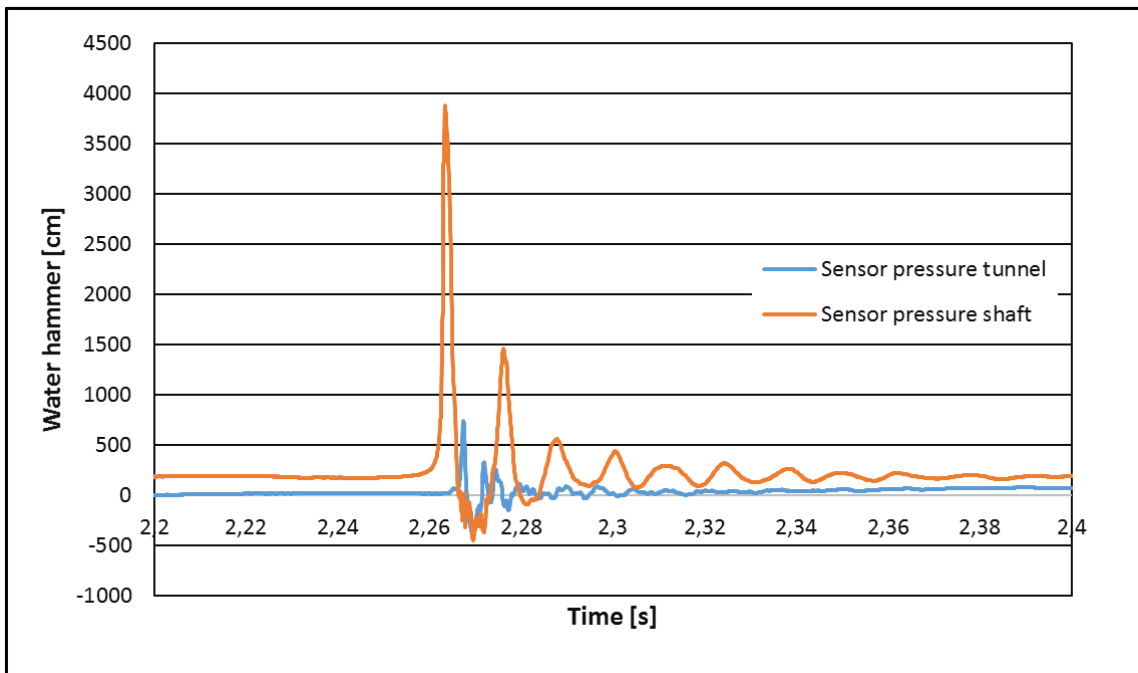
Graph 21 details the third measurement at the same Load case with same discharge and same closure position (Surge tank opened 65° angle). During this case, pressure height at pressure tunnel is $h=9585.23$ [mm] and water hammer at pressure shaft is $h=46787.9$ [mm].

6.2.22 Surge tank, closure of valve opened for 45°



Graph 22: Load of case with discharge $Q=0.25$ [l/s] and closure position of the valve, opened for 45° angle.

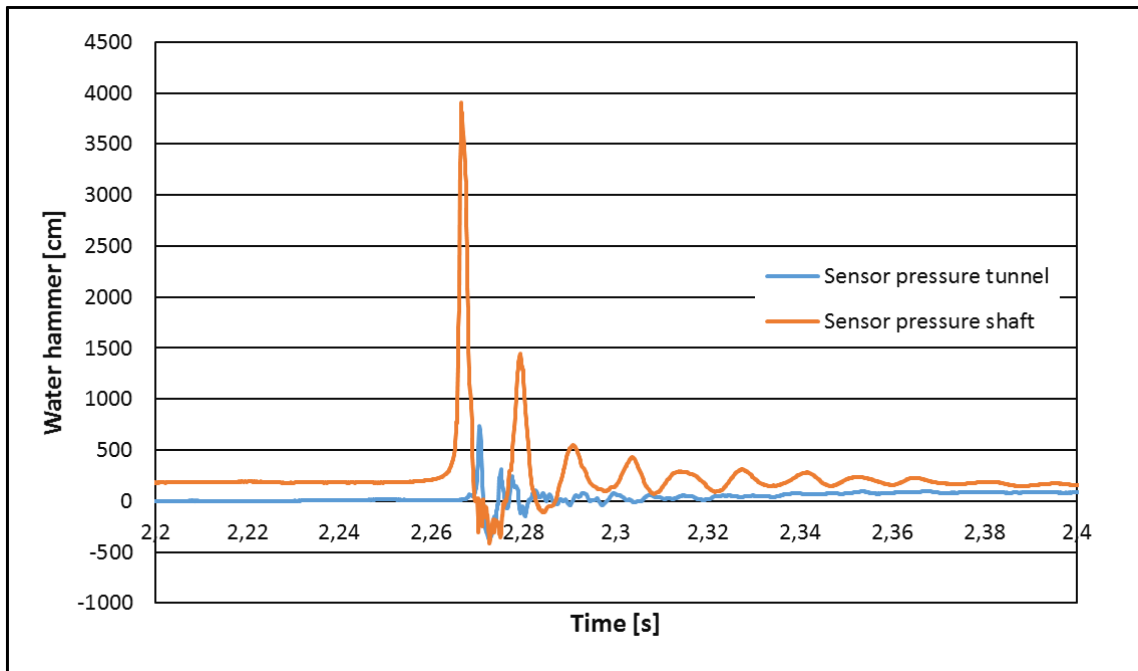
6.2.23 Detail of line graphic, closure of valve opened for 45°



Graph 23: Load of case with discharge $Q=0.25$ [l/s] and closure position of the valve, opened for 45° angle.

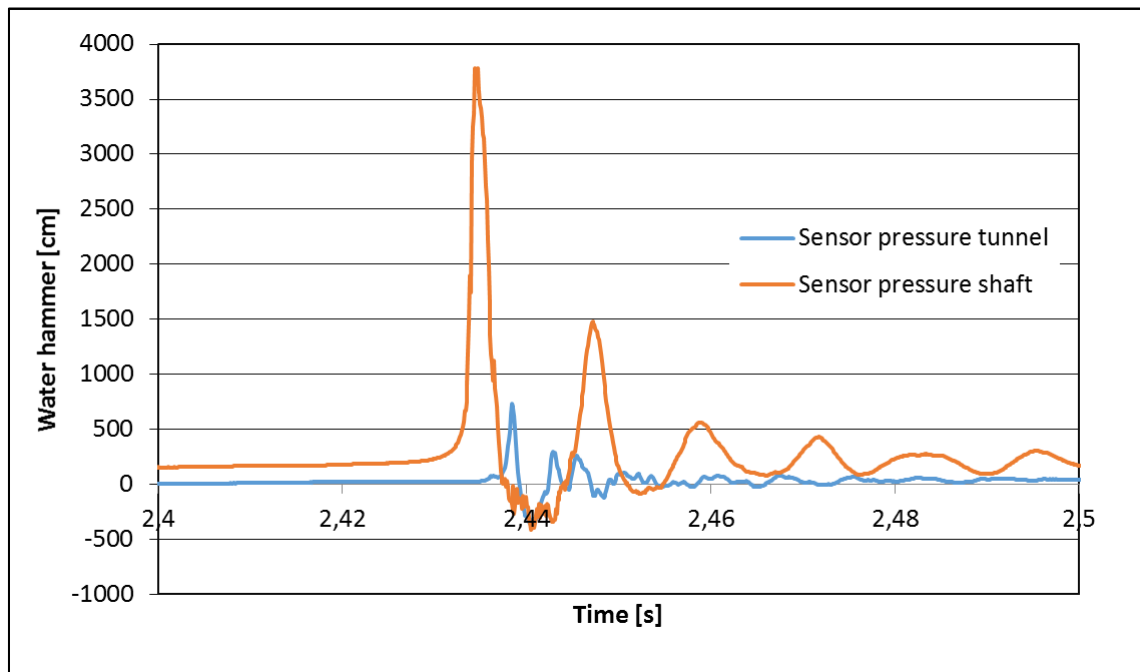
Graph 23 shows the Load case with discharge $Q=0.25$ [l/s] and closure position (Surge tank opened 45° angle). Pressure height at pressure tunnel is $h=7412.55$ [mm] and water hammer at pressure shaft is $h=38829.2$ [mm].

6.2.24 2nd detail of line graphic, closure of valve opened for 45°



Graph 24: Load of case with discharge $Q=0.25$ [l/s] and closure position of the valve, opened for 45° angle.

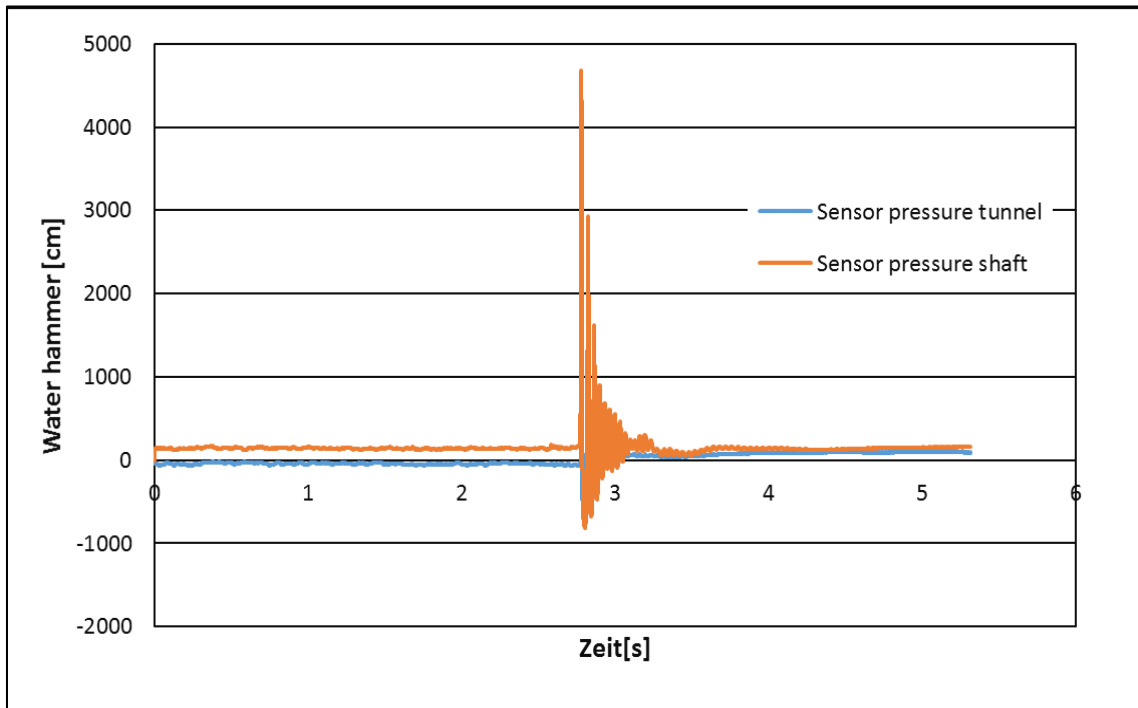
Graph 24 visualizes the second measurement on the same Load case with same discharge and same closure position (Surge tank opened 45° angle): pressure height at pressure tunnel is $h=7585.31$ [mm] and water hammer at pressure shaft is $h=39122.35$ [mm].

6.2.25 3rd detail of line graphic, closure of valve opened for 45°

Graph 25: Load of case with discharge $Q=0.25$ [l/s] and closure position of the valve, opened for 45° angle.

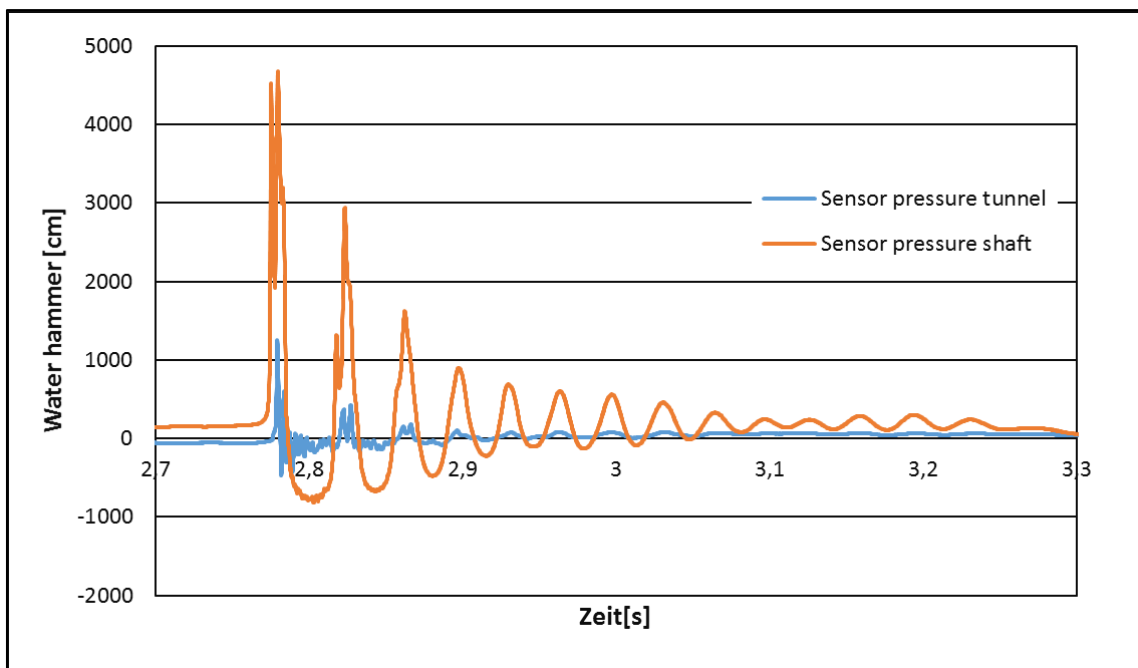
Graph 25 visualizes the third measurement on the same Load case with same discharge and same closure position (Surge tank opened 45° angle): pressure height at pressure tunnel is $h=7347.85$ [mm] and water hammer at pressure shaft is $h=41984.06$ [mm].

6.2.26 Surge tank, closure of valve entirely closed



Graph 26: Load of case with discharge $Q=0.25$ [l/s], closure position of the valve, entirely closed.

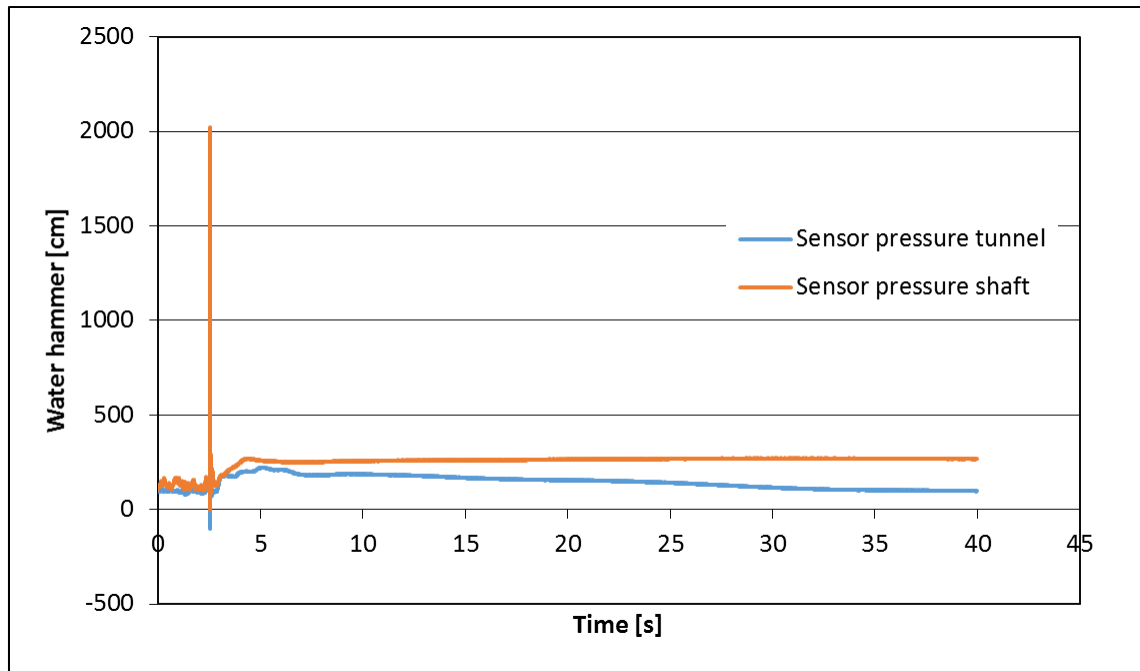
6.2.27 Details of line graphic, closure of valve entirely closed



Graph 27: Load of case with discharge $Q=0.25$ [l/s], closure position of the valve, entirely closed.

Graph 27 shows the Load case with discharge $Q=0.25$ [l/s] and closure position (closed surge tank). In this load case, pressure height at pressure tunnel is $h=12544.56$ [mm] and water hammer at pressure shaft is $h=46777.04$ [mm].

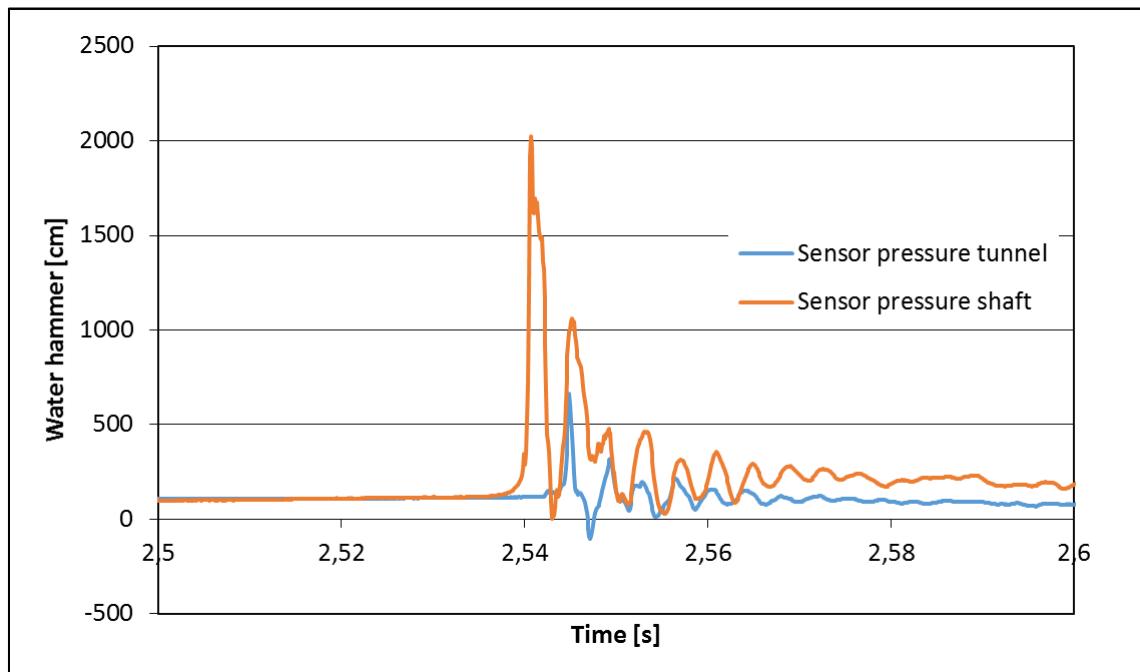
6.2.28 Surge tank, closure of valve opened for 10°



Graph 28: Load case with discharge $Q=0.10$ [l/s] and closure position of the valve, opened for 10° angle.

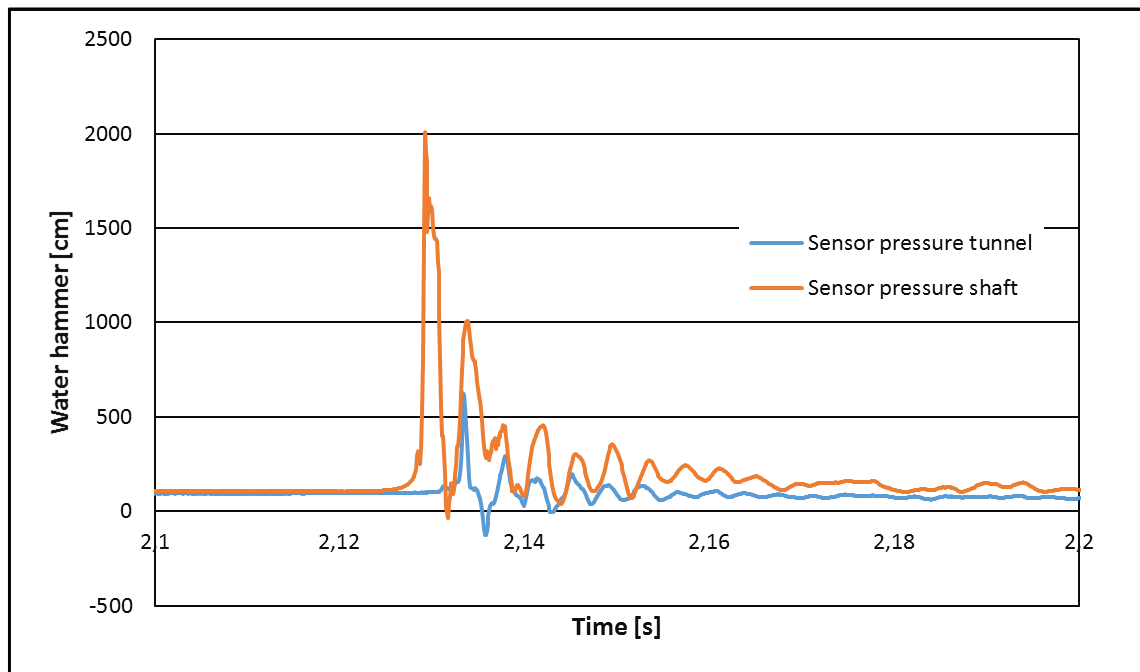
This Load case has the lowest discharge $Q=0.10$ [l/s] and the lowest values of the pressure height inside the pipeline: pressure tunnel and pressure shaft. When discharge of water is smaller, pressure heights inside the pipeline are lower.

6.2.29 Detail of line graphic, closure of valve opened for 10°



Graph 29: Load case with discharge $Q=0.10$ [l/s] and closure position of the valve, opened for 10° angle.

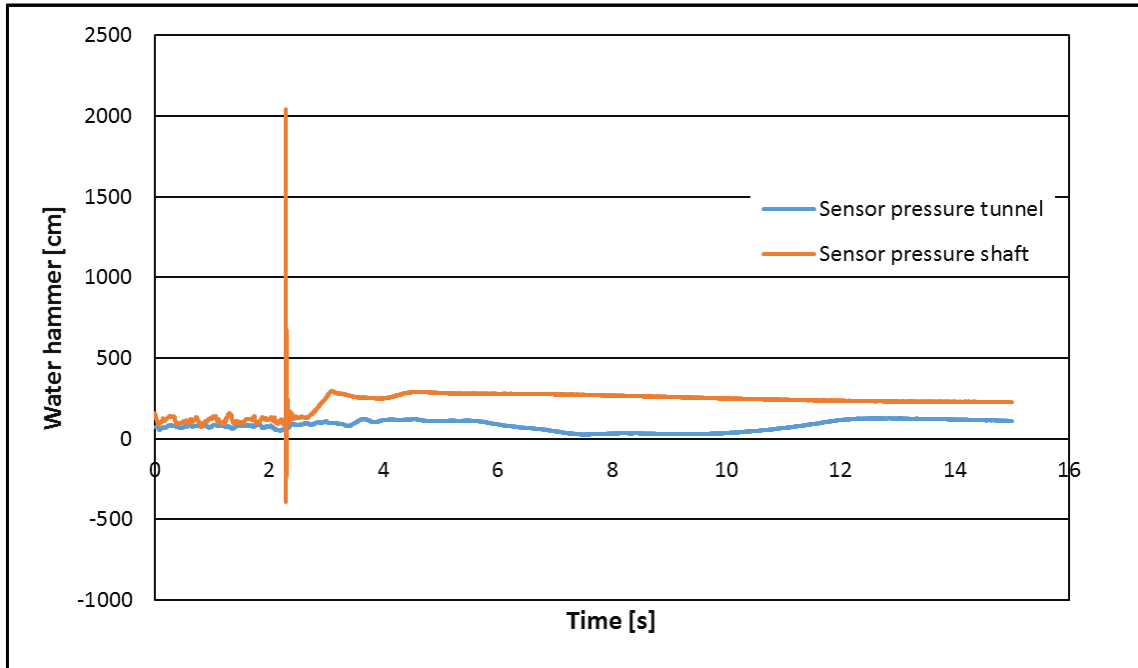
Graph 29 shows a Load case with discharge $Q=0.10$ [l/s] and closure position (Surge tank opened 10° angle). Pressure height at pressure tunnel is $h=6642.92$ [mm] and water hammer at pressure shaft is $h=20237.17$ [mm].

6.2.30 2nd detail of line graphic, closure of valve opened for 10°

Graph 30: Load case with discharge $Q=0.10$ [l/s] and closure position of the valve, opened for 10° angle.

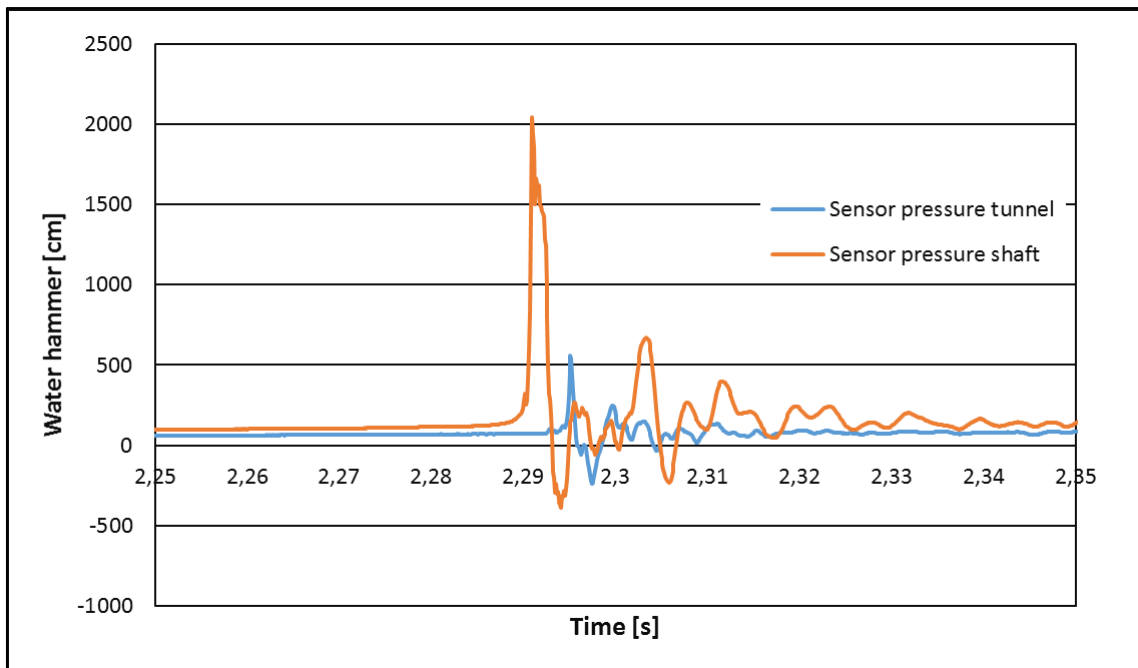
Graph 30, on the second measurement on the same Load case with same discharge and same closure position (Surge tank opened 10° angle) shows that, pressure height at pressure tunnel is $h=6271.73$ [mm] and water hammer at pressure shaft is $h=20063.45$ [mm].

6.2.31 Surge tank, closure of valve opened for 45°



Graph 31: Load case with discharge $Q=0.10$ [l/s] and closure position of the valve, opened for 45° angle.

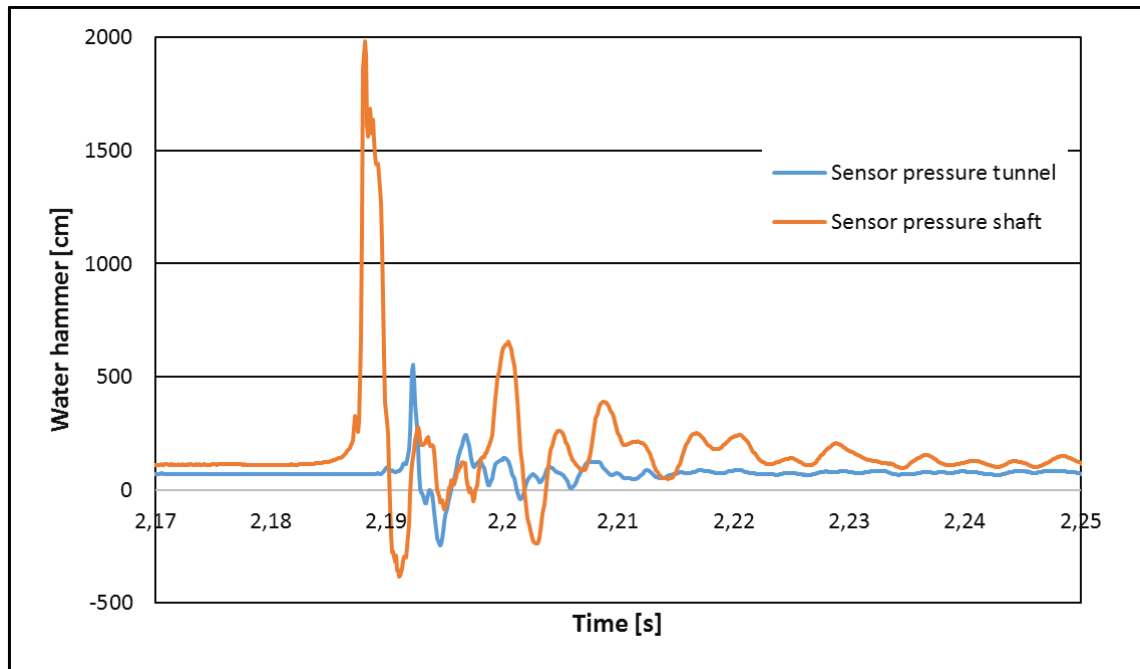
6.2.32 Detail of line graphic, closure of valve opened for 45°



Graph 32: Load case with discharge $Q=0.10$ [l/s], closure position of the valve, opened for 45° angle.

Graph 32 shows a Load case with discharge $Q=0.10$ [l/s] and closure position (Surge tank opened 45° angle): pressure height at pressure tunnel is $h=5594.04$ [mm] and water hammer at pressure shaft is $h=20436.23$ [mm].

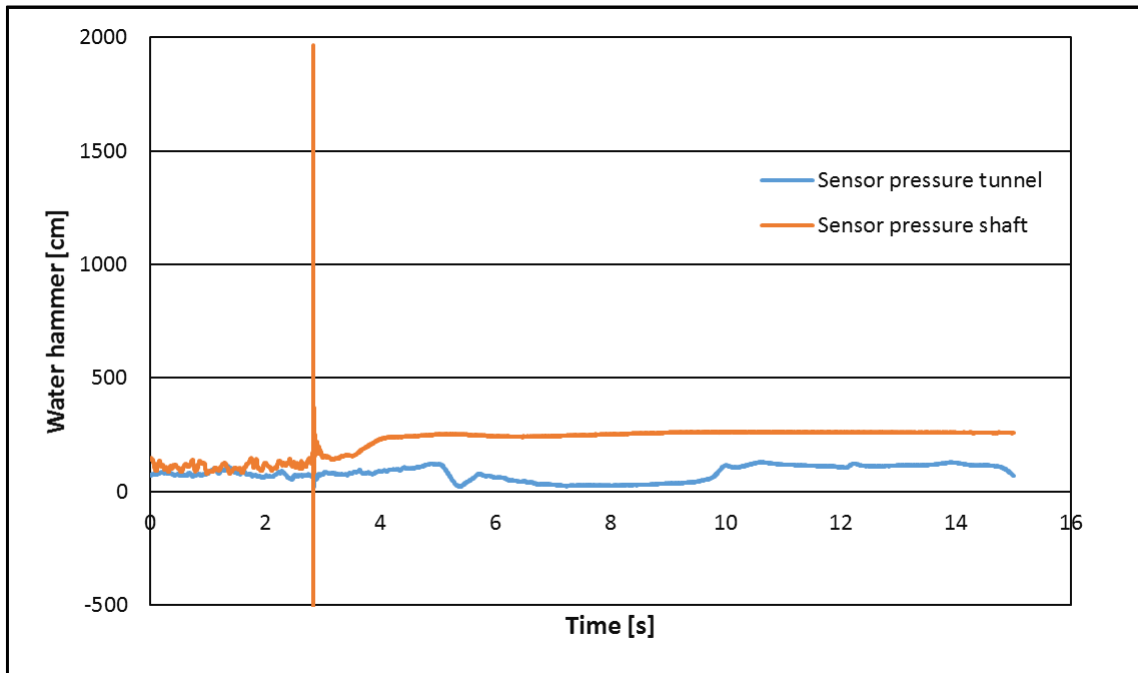
6.2.33 2nd detail of line graphic, closure of valve opened for 45°



Graph 33: Load case with Discharge $Q=0.10$ [l/s], closure position of the valve, opened for 45° angle.

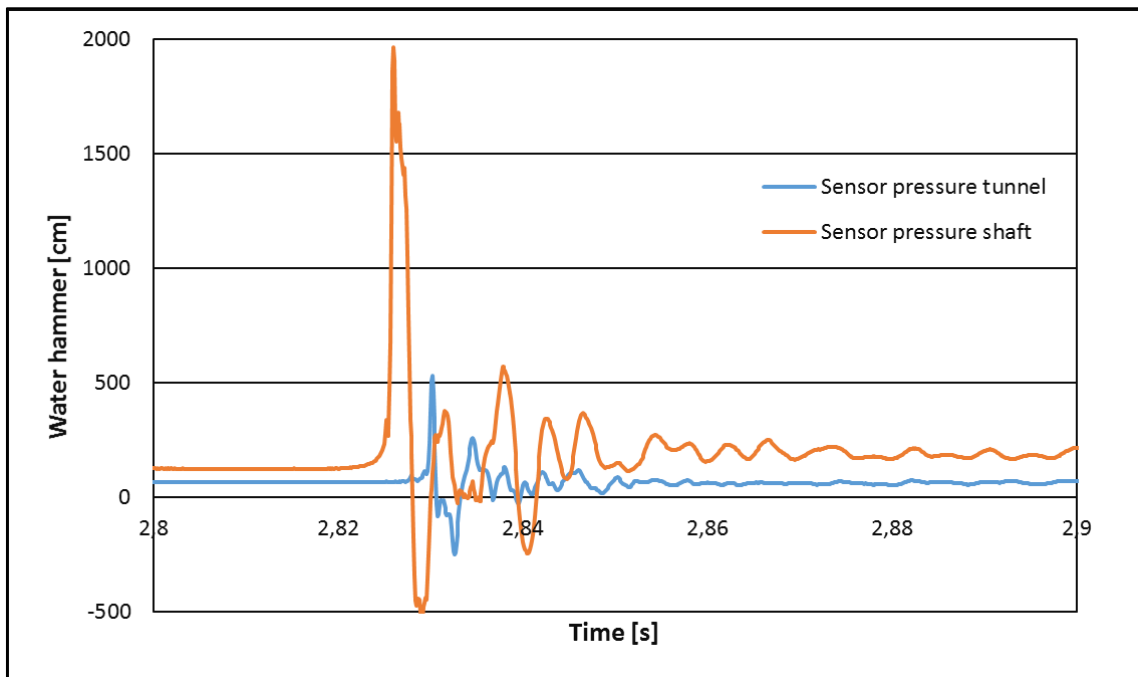
Graph 33 at the second measurement on the same Load case with same discharge and same closure position Surge tank opened 45° angle, shows the values of pressure height at pressure tunnel $h=5546.37$ [mm] and water hammer at pressure shaft $h=19817.34$ [mm].

6.2.34 Surge tank, closure of valve opened for 65°



Graph 34: Load case with discharge $Q=0.10$ [l/s] and closure position of the valve, opened for 65° angle.

6.2.35 Details of line graph, closure of valve opened for 65°



Graph 35: Load case with discharge $Q=0.10$ [l/s], closure position of the valve, opened for 65° angle.

In Graph 35 on Load case with discharge $Q=0.10$ [l/s] and closure position (Surge tank opened 65° angle): pressure height at pressure tunnel is $h=5423.77$ [mm] and water hammer at pressure shaft is $h=19621.9$ [mm].

6.3 Joukowsky pressure

At this chapter, there is calculation of Joukowsky pressure of the model at laboratory. The results are compared with results of pressure head inside the pipeline, which are measured with sensors.

$$\max h_{a,jau} = \pm \frac{a \cdot \Delta v}{g} - [64] \quad (63)$$

$\max h_{a,jau}$ – pressure head change [mwc]

a – wave propagation velocity [m/s]

Δv - flow velocity change [m/s]

g – acceleration due to gravity 9.81 [m/s^2]

- Dimensions of model at laboratory

Calculation of the “Joukowsky” pressure at the small- scale model

The calculation point is the point where the sensors are installed.

Pipe 2, Pressure tunnel

$$L_2 = 2,1[m] \quad Di = 0,020[m] \quad \Delta = 0,0021[m]$$

$$Q = 0,0004 [m^3/s]$$

$$d_i = D - 2 * \Delta = 0,020 m - 2 * 0,0021m = 0,0158m \quad (64)$$

$$A = \frac{\pi \cdot d_i^2}{4} = \frac{3,14 \cdot 0,0158^2}{4} = 0,00034[m^2] \quad (65)$$

$$v = \frac{Q}{A} = \frac{0,0004}{0,00034} = 1,17 \left[\frac{m}{s} \right] \quad (66)$$

$$\Delta h_{jou} = \frac{a * \Delta v_2}{g} = \frac{650 * 1.17}{9.81} = 77.5 \quad (67)$$

Pipe4, pressure shaft

$$L_2 = 0,70 [m] \quad D = 0,035[m] \quad \Delta = 0,0021 [m]$$

$$\begin{aligned} d_i &= D - 2 * \Delta = 0.035m - 2 * 0.0021m \\ &= 0,0308 [m] \end{aligned} \quad (68)$$

$$A = \frac{\pi * d_i^2}{4} = \frac{3,14 * 0,0308^2}{4} = 0.00074 [m^2] \quad (69)$$

$$v = \frac{Q}{A} = \frac{0,0004}{0,00074} = 0.54 \left[\frac{m}{s} \right] \quad (70)$$

$$a = \frac{2,0 + 0,60}{0,004} = 650 \left[\frac{m}{s} \right] \quad (71)$$

$$\Delta h_{jou} = \frac{a * \Delta v_2}{g} = \frac{650 * 0.54}{9.81} = 35.77 [mwc] \quad (72)$$

Joukowsky pressure head change at pressure shaft

When is compared with " Load case with discharge Q=0.4 [l/s], and closed surge tank "

h=75256.82 [mm] = 75.25 [mwc] pressure height at pressure shaft (water hammer) at the model Laboratory

$$\Delta h_{jou} = 77.62 [m] < h=75.25 [m]$$

Pipe 2, Pressure Tunnel			Pipe 4, Pressure Shaft	
L2	2.1	m	0.7	m
Di	0.0209	m	0.035	m
Δ			0.0021	m
Q	0.0004	m^3/s	0.0004	m^3/s
d_i			0.0308	m
A	0.000343		0.000745	m^2
v	1.166535	m/s	0.537142	m/s
a			650	m/s
Δh_{jou}	77.29335	mwc	35.59043	mwc

$$d_i = D_i - 2 * \Delta$$

$$A = \frac{\pi * d_i^2}{4}$$

$$v = \frac{A}{Q}$$

$$\Delta h_{jou} = \frac{A * \Delta v_2}{g}$$

Table 2: Joukowsky calculation 1

When is compared with Load case with discharge $Q=0.5$ [l/s]

$h=90388.85$ [mm] =90.38 [mwc] pressure height at pressure shaft (water hammer) at the model Laboratory

$$\Delta h_{jou} = 96.61 \text{ [m]} \approx h=90.38 \text{ [m]}$$

Pipe 2, Pressure Tunnel			Pipe 4, Pressure Shaft	
L2	2.1	m	0.7	m
Di	0.0209	m	0.035	m
Δ			0.0021	m
Q	0.0005	m^3/s	0.0005	m^3/s
d_i			0.0308	m
A	0.000343		0.000745	m^2
v	1.458169	m/s	0.671427	m/s
a			650	m/s
Δh_{jou}	96.61668	mwc	44.48804	mwc

$$d_i = D_i - 2 * \Delta$$

$$A = \frac{\pi * d_i^2}{4}$$

$$v = \frac{A}{Q}$$

$$\Delta h_{jou} = \frac{A * \Delta v_2}{g}$$

Table 3: Joukowsky calculation 2

When is compared with Load case with discharge $Q=0.25$ [l/s], and closed surge tank

$h=48467.22$ [mm] =48.46 [mwc] pressure height at pressure shaft (water hammer) at the model Laboratory

$$\Delta h_{jou} = 48.30 \text{ [m]} \approx h=48.46 \text{ [m]}$$

Pipe 2, Pressure Tunnel		Pipe 4, Pressure Shaft	
L2	2.1 m	0.7	m
Di	0.0209 m	0.035	m
Δ		0.0021	m
Q	0.00025 m ³ /s	0.00025	m ³ /s
d_i		0.0308	m
A	0.000343	0.000745	m ²
v	0.729084 m/s	0.335714	m/s
a		650	m/s
Δh_{jou}	48.30834 mwc	22.24402	mwc

$$d_i = D_i - 2 * \Delta$$

$$A = \frac{\pi * d_i^2}{4}$$

$$v = \frac{A}{Q}$$

$$\Delta h_{jou} = \frac{A * \Delta v_2}{g}$$

Table 4: Joukowsky calculation 3

When is compared with Load case with discharge $Q=0.25$ [l/s],

$h=19621.9$ [mm] =19.62 [mwc] pressure height at pressure shaft (water hammer) at the model Laboratory

$$\Delta h_{jou} = 19.32 \text{ [m]} \approx h=19.62 \text{ [m]}$$

Pipe 2, Pressure Tunnel		Pipe 4, Pressure Shaft	
L2	2.1 m	0.7	m
Di	0.0209 m	0.035	m
Δ		0.0021	m
Q	0.0001 m ³ /s	0.0001	m ³ /s
d_i		0.0308	m
A	0.000343	0.000745	m ²
v	0.291634 m/s	0.134285	m/s
a		650	m/s
Δh_{jou}	19.32334 mwc	8.897608	mwc

$$d_i = D_i - 2 * \Delta$$

$$A = \frac{\pi * d_i^2}{4}$$

$$v = \frac{A}{Q}$$

$$\Delta h_{jou} = \frac{A * \Delta v_2}{g}$$

Table 5: Joukowsky calculation 4

Assumption: In this chapter there are compared the results of Joukowsky pressure at pressure tunnel of the model, and results of water hammer measured with sensor at pressure shaft of the model.

Bibliography

- A.Bergant, A. A. (2005). *Water hammer with column separation: A historical review*.
- Giesecke , & Mosonyi. (2009). *Wasserkraftanlagen*. Springer.
- Horace.W.King. (1996). *Handbook of Hydraulics*. Michigan.
- Idelchik. (2005). *Handbook of hydraulics and resistance*. Jaico publishing house.
- Jirka, G. H. (2007). *Einführung in die Hydromechanik*. Universty of Klastruhe.
- Johnson. (1908). *The surge tank at water plants*.
- Kay, M. (2008). *Practical Hydraulics*. Taylor & Francis Group.
- Mosonyi, E. (1960). *WATER POWER DEVELOPMENT* . Budapest: House of the Hungarian Academy of Sciences.
- R.E.Featherstone, C.Nalluri. (2001). *Civil engineering and hydraulics*. Wiley.
- Reclamation, B. o. (1977). *Welded steel Penstock, Engineering Monograph*. United States.Bureau of reclamation.
- Xylem. (2015). *Engineering and Expertise, Transient analysis*.
- Zaruba, J. (1993). *Water hammer in pipe-line systems*. Elsevier.

Tables

Table 1: Results from small-scale investigation at the laboratory.....	55
Table 2: Joukowsky calculation 1	87
Table 3: Joukowsky calculation 2.....	87
Table 4: Joukowsky calculation 3.....	88
Table 5: Joukowsky calculation 4.....	88

Figures

Figure 1: Tower intake at Hoover dam, Colorado River	5
Figure 2: Head above the soffit of the tunnel.....	6
Figure 3: Concrete-lined pressure tunnel.....	8
Figure 4: Penstocks, Ohakuri Dam New Zealand [3]	9
Figure 5: Outer and inner Diameter.....	14
Figure 6: Joukowsky pressure and reflections time.....	27
Figure 7: Report between closing time and reflection time.....	29
Figure 8: Graphical representation of the formulas	32
. Figure 9: High-head hydropower plant, longitudinal section surge tank.....	34
Figure 10: Surge tank types	36
Figure 11: Sample of the investigated prototype model	38
Figure 12: Description for each part of the example, elements as used for TUG Hammer.....	39
Figure 13: TUG_hammer GUI interface	40
Figure 14: TUG_hammer GUI interface	41
Figure 15: TUG_hammer – part connections	42
Figure 16: Notepad- values of discharge inside the pipeline.....	43
Figure 17: Evaluation of mass oscillation (a).....	44
Figure 18: Evaluation mass oscillation (b).....	46
Figure 19: Working lab where experiment is processed in the hydraulic laboratory	49
Figure 20: Scheme of the surge tank model	50
Figure 21: Sensor.....	50

Graphs

Graph 1: Load case with discharge $Q=0.5$ [l/s] and closure position of the valve, opened for 10° angle.....	56
Graph 2: Load case with discharge $Q=0.5$ [l/s] and closure position of the valve, opened for 10° angle.....	57
Graph 3: Load case with discharge $Q=0.5$ [l/s] and closure position of the valve, opened for 10° angle.....	58
Graph 4: Load case, with discharge $Q=0.5$ [l/s] and closure position of the valve, opened for 45° angle.....	59
Graph 5: Load case, with discharge $Q=0.5$ [l/s] and closure position of the valve, opened for 45° angle.....	60
Graph 6: Load case, with discharge $Q=0.5$ [l/s] and closure position of the valve, opened for 45° angle.....	61
Graph 7: Load case, with discharge $Q=0.5$ [l/s] and closure position of the valve, opened for 45° angle.....	62
Graph 8: Load case, with discharge $Q=0.5$ [l/s] and closure position of the valve, opened for 65° angle.....	63
Graph 9: Load case, with discharge $Q=0.5$ [l/s] and closure position of the valve, opened for 65° angle.....	64
Graph 10: Load case, with discharge $Q=0.5$ [l/s] and closure position of the valve, opened for 65° angle.....	65
Graph 11: Load case, with discharge $Q=0.4$ [l/s], closure position of the valve, entirely closed.....	66
Graph 12: Load case, with discharge $Q=0.4$ [l/s], closure position of the valve, entirely closed.....	67
Graph 13: Load case, with discharge $Q=0.4$ [l/s], closure position of the valve, entirely closed.....	68
Graph 14: Load case, with discharge $Q=0.25$ [l/s], and closure position of the valve, opened for 10° angle.	69

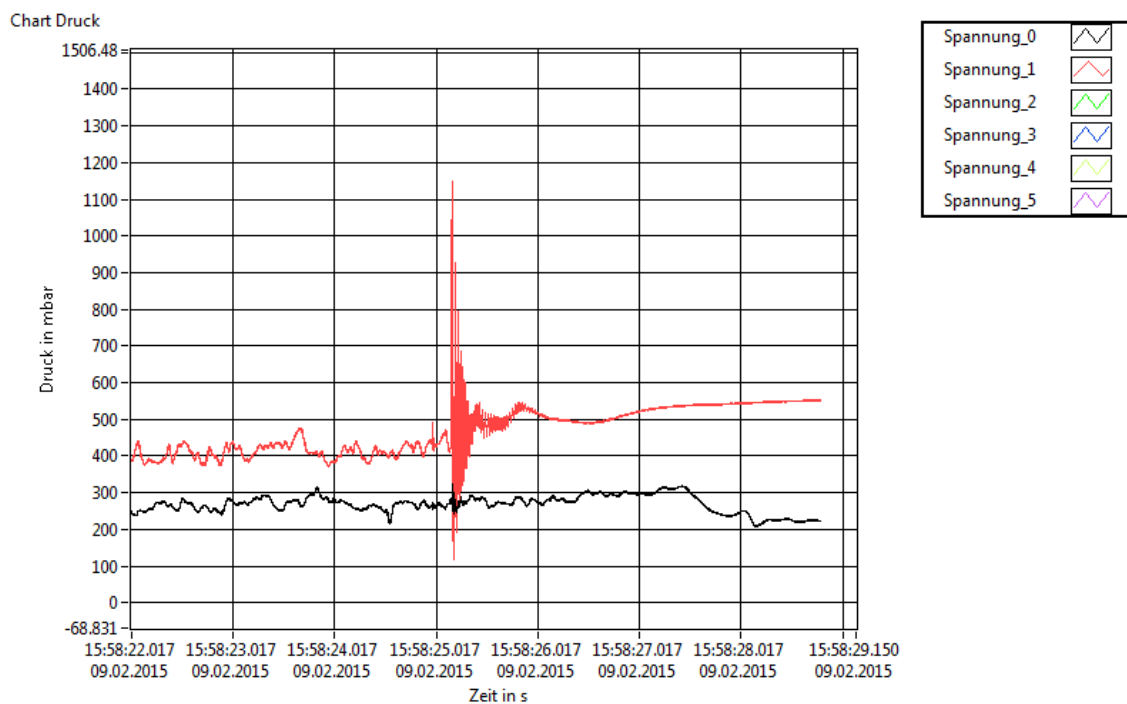
Graph 15: Load case, with discharge $Q=0.25$ [l/s] and closure position of the valve, opened for 10° angle.	69
Graph 16: Load case, with discharge $Q=0.25$ [l/s] and closure position of the valve, opened for 10° angle.	70
Graph 17: Load case, with discharge $Q=0.25$ [l/s] and closure position of the valve, opened for 10° angle.	71
Graph 18: Load case with discharge $Q=0.25$ [l/s] and closure position of the valve, opened for 65° angle.	72
Graph 19: Load case with discharge $Q=0.25$ [l/s] and closure position of the valve, opened for 65° angle.	72
Graph 20: Load case with discharge $Q=0.25$ [l/s] and closure position of the valve, opened for 65° angle.	73
Graph 21: Load case with discharge $Q=0.25$ [l/s] and closure position of the valve, opened for 65° angle.	74
Graph 22: Load of case with discharge $Q=0.25$ [l/s] and closure position of the valve, opened for 45° angle.	75
Graph 23: Load of case with discharge $Q=0.25$ [l/s] and closure position of the valve, opened for 45° angle.	75
Graph 24: Load of case with discharge $Q=0.25$ [l/s] and closure position of the valve, opened for 45° angle.	76
Graph 25: Load of case with discharge $Q=0.25$ [l/s] and closure position of the valve, opened for 45° angle.	77
Graph 26: Load of case with discharge $Q=0.25$ [l/s], closure position of the valve, entirely closed.....	78
Graph 27: Load of case with discharge $Q=0.25$ [l/s], closure position of the valve, entirely closed.....	78
Graph 28: Load case with discharge $Q=0.10$ [l/s] and closure position of the valve, opened for 10° angle.	79
Graph 29: Load case with discharge $Q=0.10$ [l/s] and closure position of the valve, opened for 10° angle.	80

Graph 30: Load case with discharge $Q=0.10$ [l/s] and closure position of the valve, opened for 10° angle.	81
Graph 31: Load case with discharge $Q=0.10$ [l/s] and closure position of the valve, opened for 45° angle.	82
Graph 32: Load case with discharge $Q=0, 10$ [l/s], closure position of the valve, opened for 45° angle.....	82
Graph 33: Load case with Discharge $Q=0.10$ [l/s], closure position of the valve, opened for 45° angle.....	83
Graph 34: Load case with discharge $Q=0.10$ [l/s] and closure position of the valve, opened for 65° angle.	84
Graph 35: Load case with discharge $Q=0.10$ [l/s], closure position of the valve, opened for 65° angle.....	84
Graph 36: Load case with Discharge $Q=0.10$ [l/s] with closure position of the valve, opened for 65° angle.	91
Graph 37: Load case with discharge $Q=0.2$ [l/s] with surge tank entirely opened	92
Graph 38: Load case with discharge $Q=0.2$ [l/s] with surge tank entirely closed.	92
Graph 39: Load case with discharge $Q=0.3$ [l/s] with surge tank entirely opened.	94
Graph 40: Load case with Discharge $Q=0.3$ [l/s] with surge tan entirely closed.	95
Graph 41: Load case with Discharge $Q=0.5$ [l/s] with surge tank entirely opened.	95
Graph 42: Load case with discharge $Q=0.5$ [l/s] with surge tank entirely closed.	96
Graph 43: Cavitation Graph	96
Graph 44: Cavitation Detail 1.Discharge $Q=0.4$ [l/s].....	97
Graph 45: Cavitation Detail 2.	98
Graph 46: Cavitation Detail 3.Discharge $Q=0.4$ [l/s].....	98

APPENDIX

7. APPENDIX - Laboratory software (Lab view)

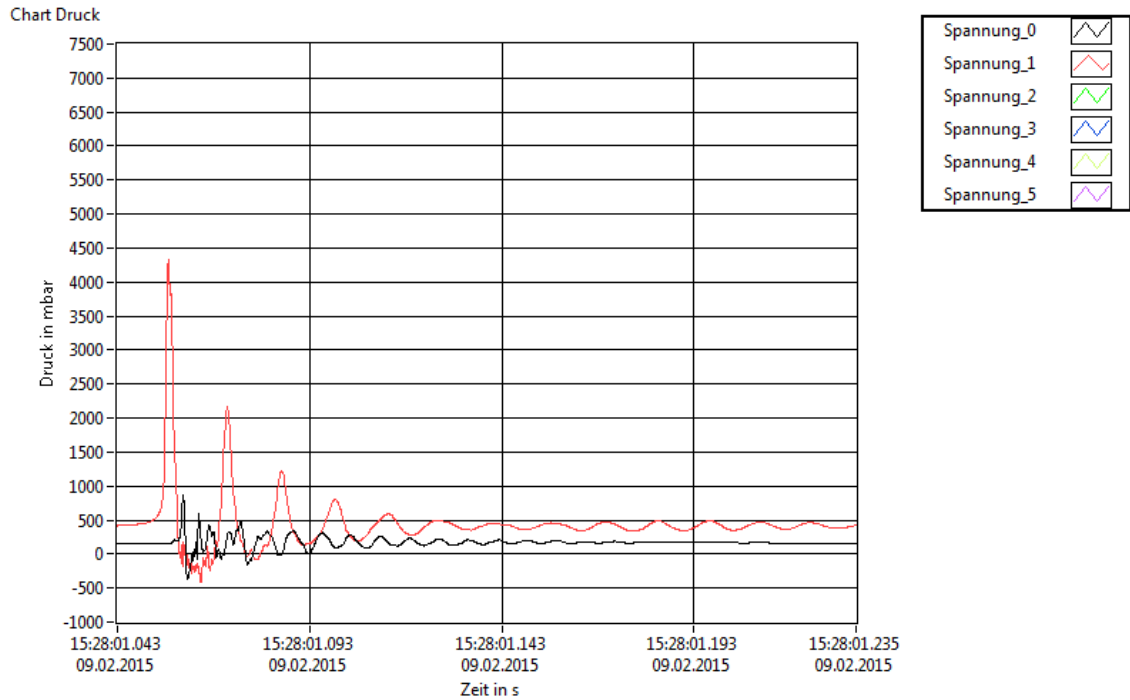
Evaluations of the results from different “Load cases”, from the software at computer in Laboratory .These are the results from model in Laboratory. The excel data below, were taken from software. The results compare with those from the excel results are the same.



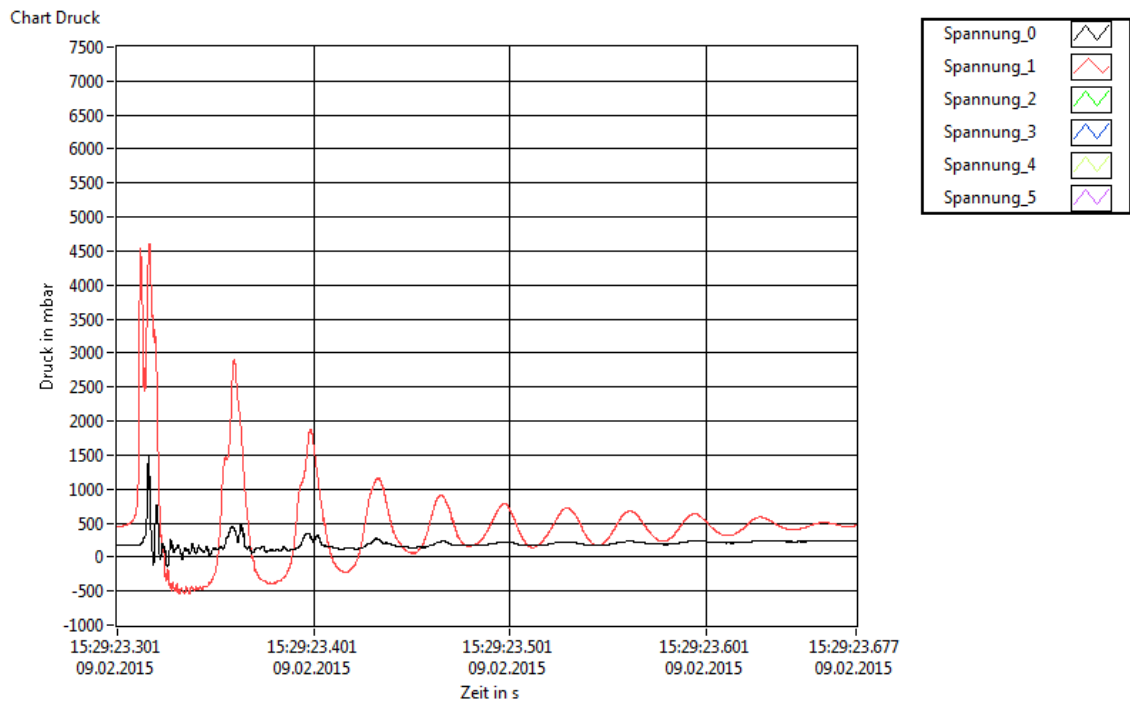
Graph 36: Load case with Discharge $Q=0.10$ [l/s] with closure position of the valve, opened for 65° angle.

- Red line, evaluation of the pressure height (water hammer) at the pressure shaft.
- Black line, evaluation of the pressure height at the pressure tunnel.

Coordinates which measures the pressure height are different. On the vertical coordinate (y) pressure height it's measured with [mbar] and on the horizontal coordinate "time" has more details than diagram in the excel.



Graph 37: Load case with discharge $Q=0.2[l/s]$ with surge tank entirely opened



Graph 38: Load case with discharge $Q=0.2[l/s]$ with surge tank entirely closed.

These files from “*Lab view*” were taken, in order to compare the results with data that were evaluated in excel format. That is why there are no details as those have to be noted in excel. But in this “Load case”, where discharge is $Q=0.2$ [l/s], pressure head at the pressure shaft is more the 4500mbar, if we convert it in [cm] it is exactly the same value, and the pressure head at the pressure tunnel is lower than 1500mbar.

Attention: The results from “*Lab view*” measurement are not exactly the same with data from excel. They have the same discharge but different closing time of valves. But they are compared to be assure that results are near each other.

Load case with discharge $Q= 0,25$ [l/s], from first measurement: (excel data)

Pressure height at pressure tunnel $h=1254.456$ [cm].

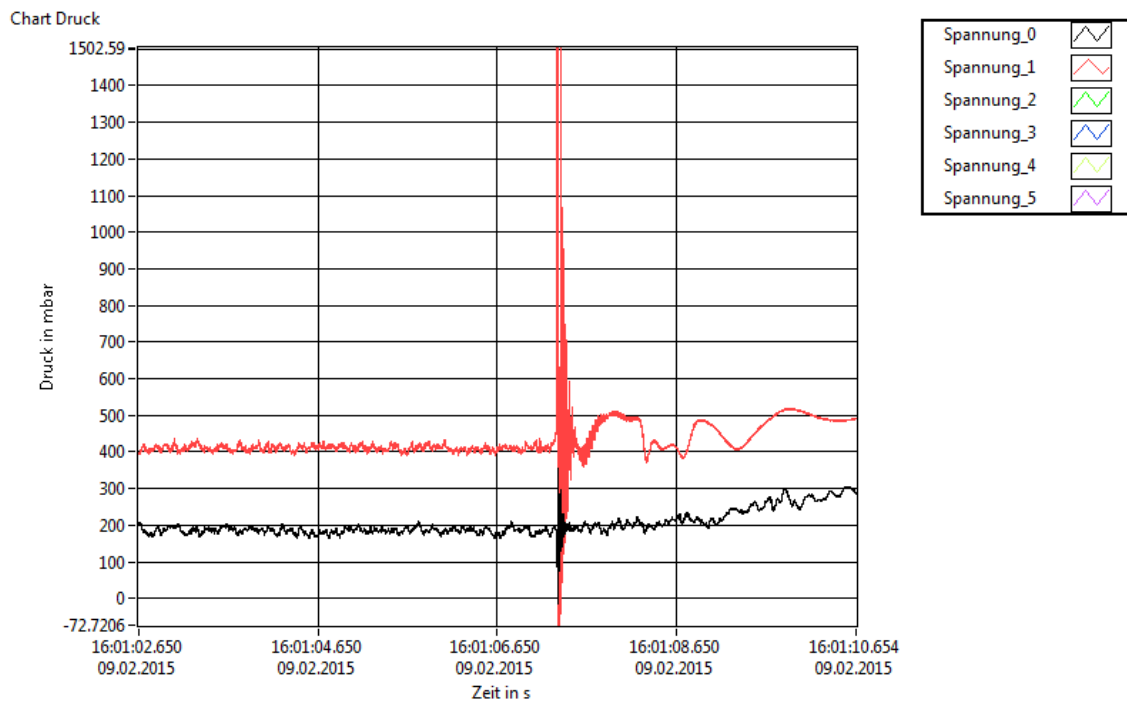
Pressure height (water hammer) at pressure shaft $h= 4677.704$ [cm].

Compared with “*Lab view diagram*”

Load case with discharge $Q= 0,25$ [l/s], from first measurement: (Lab view data)

Pressure height at pressure tunnel under $h=1500$ [mbar].

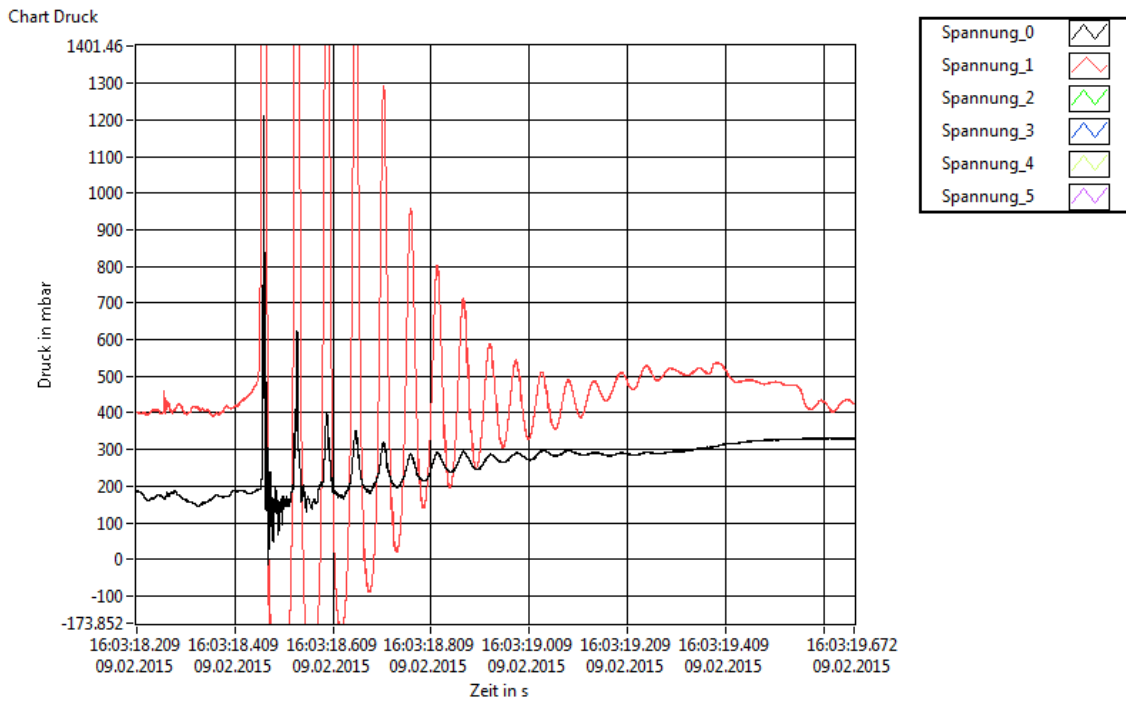
Pressure height (water hammer) at pressure shaft above $h= 4500$ [mbar].



Graph 39: Load case with discharge $Q=0.3[l/s]$ with surge tank entirely opened.

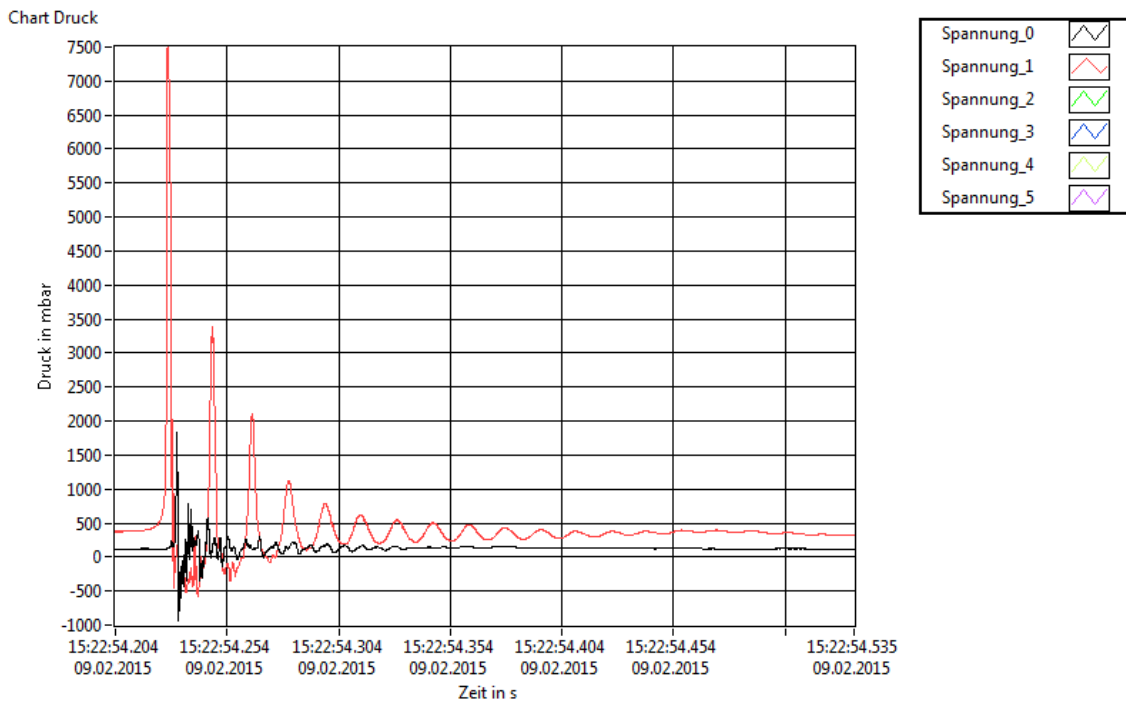
Load cases with discharge $Q=0.2[l/s]$ and $Q=0.3[l/s]$ has almost the same results. That is why the diagram in this case is zoomed in, in order to note the evaluation of the line graphic from near.

At pipe4 line graphic has bigger movements in comparison with the line graphic at the pressure tunnel (pipe2)

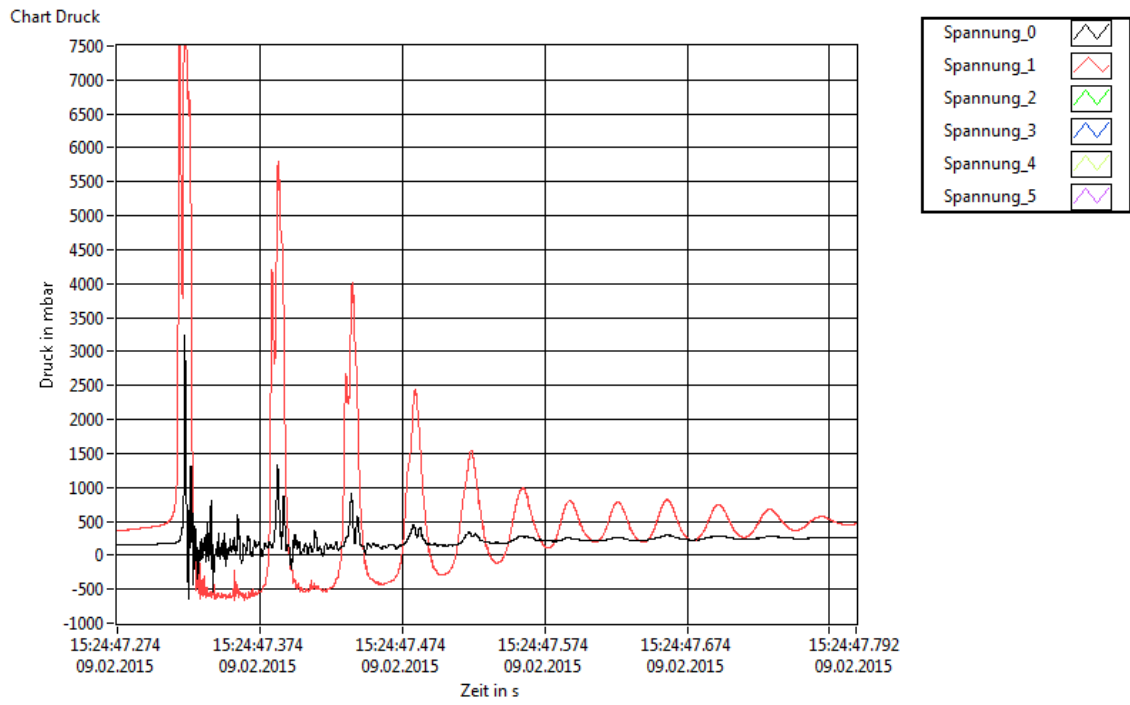


Graph 40: Load case with Discharge $Q=0.3[l/s]$ with surge tank entirely closed.

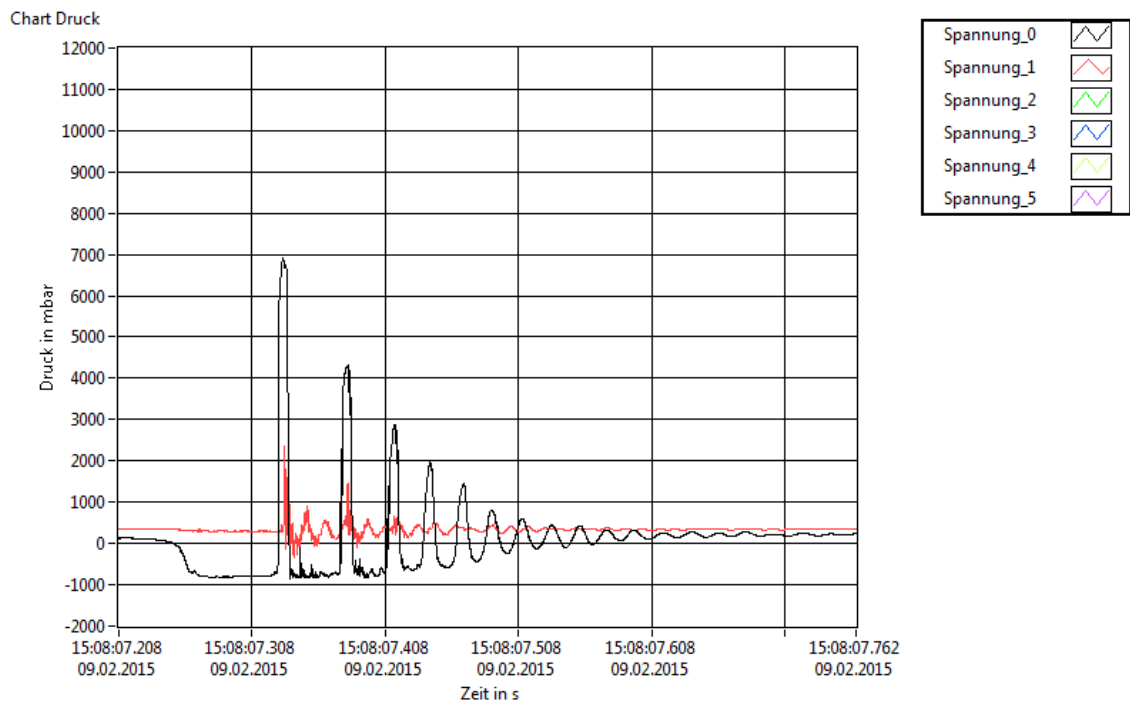
At this case where “Load case” is with closed surge tank, ups and downs from the line graph are more visible, and the water hammer occurs in a very short time.



Graph 41: Load case with Discharge $Q=0.5[l/s]$ with surge tank entirely opened.

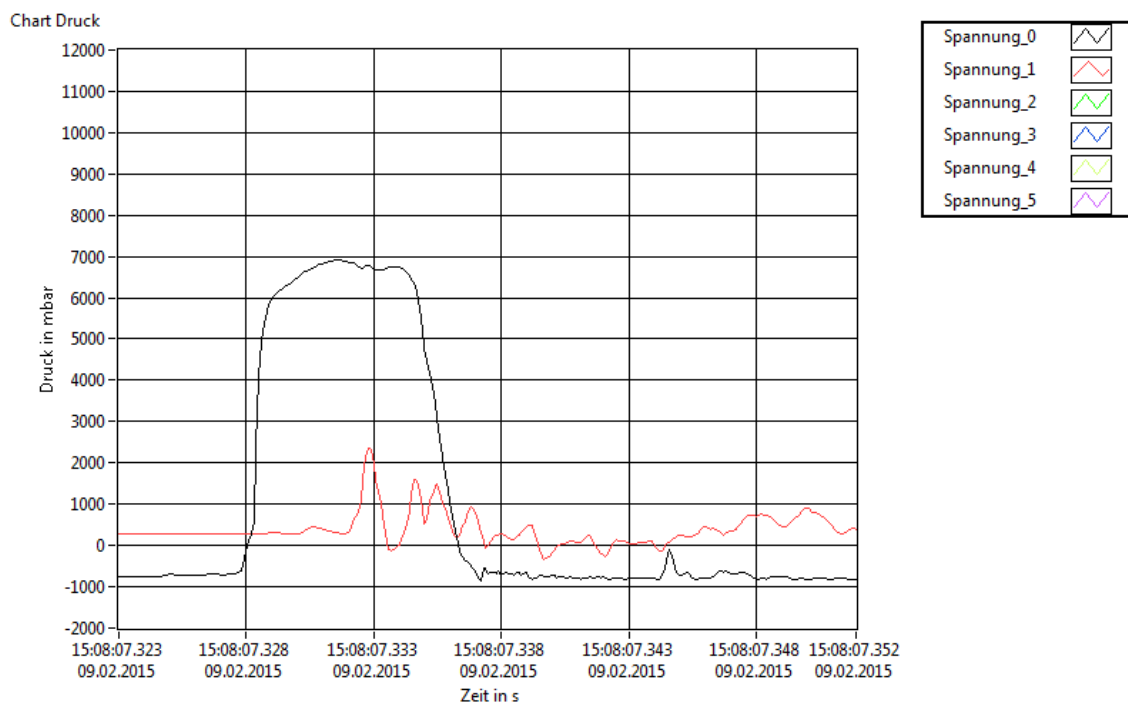


Graph 42: Load case with discharge $Q=0.5[l/s]$ with surge tank entirely closed.



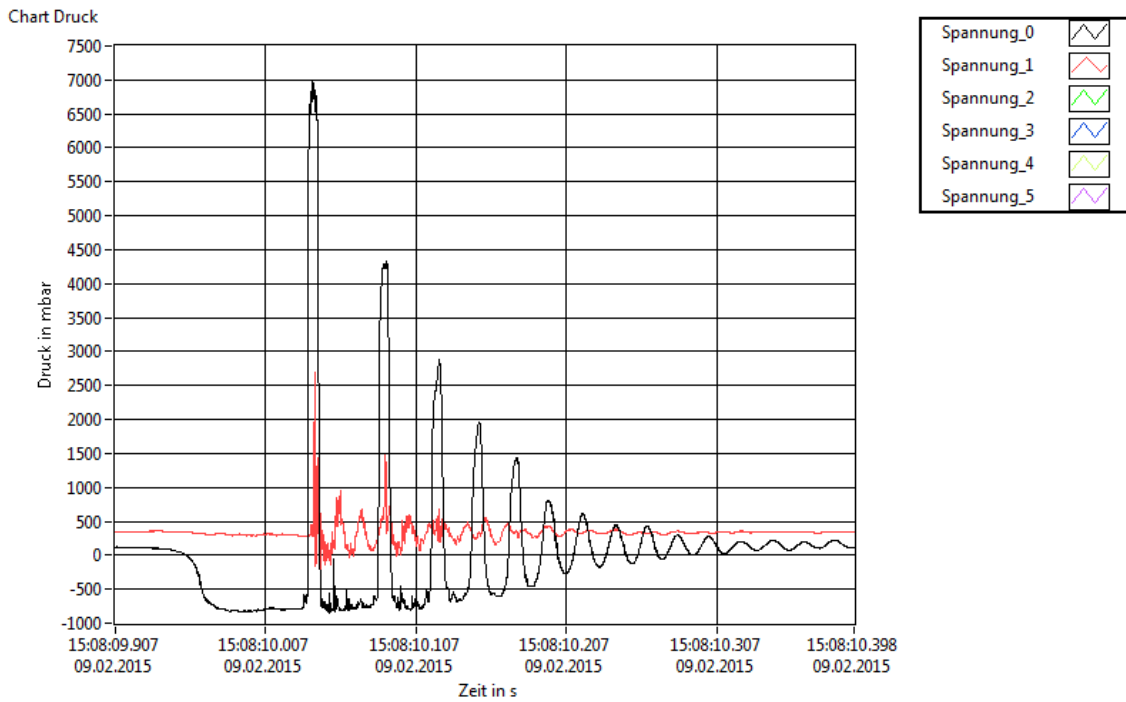
Graph 43: Cavitation Graph

This line graphic describes pressure that is occurring from *cavitation process* inside the model. The closure at the beginning of pressure tunnel (pipe 2), at the model of laboratory, has the main role for this process: at the exact moment when the closure of pipe 2 is fully closed. This is the result of the pressure height at pressure tunnel and pressure shaft at pipe2 and pipe4. But in this case pressure height at pipe2 is higher than pipe4. Because of the closure or the valves are close to the pipe2.



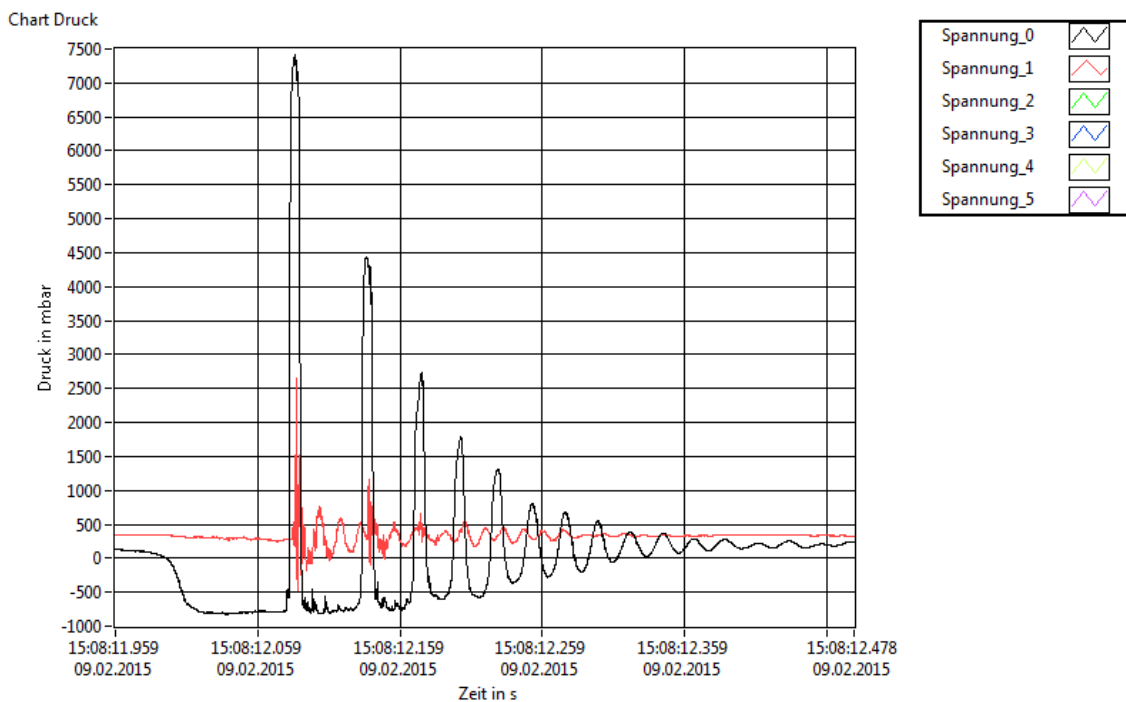
Graph 44: Cavitation Detail 1. Discharge $Q=0.4[l/s]$.

“Graph 47”: Following the black line, which is pressure height at pressure tunnel. The pressure height at pressure tunnel is $h=7000[mbar]$. Following the red line, which is pressure height at pressure shaft, pressure height is $h=2000-3000 [mbar]$.



Graph 45: Cavitation Detail 2.

“Graph 48”: Following the black line, which is pressure height at pressure tunnel. The pressure height at pressure tunnel is $h=7000$ [mbar]. Following the red line, which is pressure height at pressure shaft, pressure height is $h=2000-3000$ [mbar].



Graph 46: Cavitation Detail 3. Discharge $Q=0.4$ [l/s].

Cavitation at the pipes is also dependent on the discharge inside them. Cavitation is higher when the discharge of the water is bigger